

DETERMINATION OF OPTIMUM OVERALL SLOPE ANGLE FOR AN OPEN
PIT IRON MINE

A THESIS SUBMITTED TO
THE GRADUATE SCHOOL OF APPLIED AND NATURAL SCIENCES
OF
MIDDLE EAST TECHNICAL UNIVERSITY

BY

SELAHATTİN AKDAĞ

IN PARTIAL FULFILLMENT OF THE REQUIREMENTS
FOR
THE DEGREE OF MASTER OF SCIENCE
IN
MINING ENGINEERING

SEPTEMBER 2015

Approval of the thesis:

**DETERMINATION OF OPTIMUM OVERALL SLOPE ANGLE FOR AN
OPEN PIT IRON MINE**

submitted by **SELAHATTİN AKDAĞ** in partial fulfillment of the requirements for
the degree of **Master of Science in Mining Engineering Department, Middle East
Technical University** by,

Prof. Dr. Gülbin Dural Ünver
Dean, Graduate School of **Natural and Applied Science**

Prof. Dr. Ali İhsan Arol
Head of Department, **Mining Engineering**

Assoc. Prof. Dr. Hakan Başarır
Supervisor, **Mining Engineering Dept., METU**

Examining Committee Members:

Prof. Dr. Celal Karpuz
Mining Engineering Dept., METU

Assoc. Prof. Dr. Hakan Başarır
Mining Engineering Dept., METU

Prof. Dr. Levend Tutluoğlu
Mining Engineering Dept., METU

Assoc. Prof. Dr. Hasan Öztürk
Mining Engineering Dept., METU

Assoc. Prof. Dr. Mehmet Ali Hindistan
Mining Engineering Dept., HU

Date: 07.09.2015

I hereby declare that all information in this document has been obtained and presented in accordance with academic rules and ethical conduct. I also declare that, as required by these rules and conduct, I have fully cited and referenced all material and results that are not original to this work.

Name, Last Name: Selahattin Akdağ

Signature:

ABSTRACT

DETERMINATION OF OPTIMUM OVERALL SLOPE ANGLE FOR AN OPEN PIT IRON MINE

Akdağ, Selahattin

M.S., Department of Mining Engineering

Supervisor: Assoc. Prof. Dr. Hakan Başarır

September 2015, 127 pages

Currently, vast majority of the mineral extraction is conducted by open pit mining operations. With the improvements in mining industry, mines have become progressively deeper leading to slope stability problems. Therefore, slope stability assessment has gained more significance for geotechnical engineering. Moreover, deepening the open pit mines has revealed the necessity of designing optimized slopes with regard to the economic viability. Steepening the ultimate slope of an open pit as much as possible minimizes the amount of waste rock which results in reduced production cost under a prerequisite of ensuring the mining safety conditions. Hence, slope stability evaluation is important to keep the balance between safety of slopes and economic efficiency. In this study, optimum overall slope angle for open pit mines in Bizmişen region by conducting slope stability analyses is aimed to be determined. Additionally, the study presents the slope design chart constituted for iron ore mines in Bizmişen region to contribute the further designs of open pits. Within the scope of this research, geotechnical fieldwork was carried out to gain geotechnical relevant data about the rock mass characteristics around the mine sites. Q-system, Rock Mass Rating (RMR) method and Geological Strength Index (GSI) system were used to characterize the dominating lithological units observed in the field. Besides, GSI ratings were assigned directly by field observations for the lithological layers within the mine sites. Moreover, mechanical properties of the rock mass around the region was obtained by

laboratory experiments conducted on the cored samples taken from the exploration drillings and rock blocks taken from the mine site. Afterwards, according to the mining plans, the most critical cross-section within the mine site was determined by considering the instability conditions and for the deepest part of the open pit. Slope stability analyses were performed for various overall slope angle schemes with the combined use of limit equilibrium methods and numerical modeling which increases the reliability and accuracy of the stability analyses. Due to the topography and the orebody orientation, mining depth differs around the open pit. Therefore, optimum overall slope angle for varying mining depths were also determined by considering the results of slope stability analyses. These analyses were carried out to determine the factor of safety (FOS) and strength reduction factor (SRF) values that are the indicators of slope stability. The results from the limit equilibrium methods and numerical modeling were compared, and optimized safe overall slope angles, that satisfy minimum FOS and SRF values of 1.2, were estimated for different mining depths. Additionally, slope performance chart has been created for the region by considering the overall slope angles and corresponding mining depth. The developed chart can also be applicable for the iron ore mines in Turkey showing the same geotechnical characteristics with Bizmişen region.

Keywords: Open-pit Mining, Rock Slope Stability, Overall Slope Angle, Limit Equilibrium Method, Numerical Modeling, Factor of Safety

ÖZ

BİR AÇIK OCAK DEMİR MADENİ İÇİN GENEL OCAK EĞİM AÇISI TAYİNİ

Akdağ, Selahattin

Yüksek Lisans, Department of Mining Engineering

Tez Yöneticisi: Doç. Dr. Hakan Başarır

Eylül 2014, 127 sayfa

Günümüzde, maden üretiminin büyük çoğunluğu, açık ocak madencilik faaliyetleri ile yürütülmektedir. Madencilik endüstrisindeki gelişmelerle, madenler gittikçe daha derin olmaya başlamış ve bu durum şev duraylılığı problemlerine yol açmaktadır. Bu yüzden, geoteknik mühendisliği için, şev duraylılık değerlendirmesi daha fazla önem kazanmıştır. Ayrıca, ekonomik uygulanabilirlik bakımından, açık ocak madenlerini derinleştirmek, optimize edilmiş şev tasarımının gereksinimini ortaya çıkarmıştır. Maden güvenliği şartlarını sağlamak önkoşulunda, bir açık ocağın nihai şevini mümkün olduğunca dikleştirmek, pasa miktarını minimize eder ve bu durum üretim maliyetinde azalmayla sonuçlanmaktadır. Dolayısıyla, şev duraylılık değerlendirmesi, şev güvenliği ve ekonomik verimlilik arasındaki dengeyi korumak için önemlidir. Bu araştırma çalışmasında, şev duraylılık analizleri yürütülerek, Bizmişen bölgesindeki açık ocaklar için, ideal genel ocak eğim açısının belirlenmesi amaçlanmaktadır. Buna ek olarak, çalışma, ileride yapılacak olan açık ocak maden tasarımlarına katkıda bulunmak amacıyla Bizmişen bölgesindeki demir madenleri için oluşturulmuş şev tasarımı çizelgesini sunmaktadır. Bu bilimsel araştırma kapsamında, maden sahası etrafındaki kaya kütleleri özellikleri ile ilgili geoteknik veri elde etmek amacıyla geoteknik saha çalışması gerçekleştirilmiştir. Sahada gözlemlenen hakim litolojik birimlerini sınıflandırmak için Q sistemi, kaya kütleleri puanlama sistemi (RMR) ve jeolojik dayanım indeksi (GSI) sistemi kullanılmıştır. Bunun yanında,

maden sahalarındaki litolojik katmanlar için GSI derecelendirmeleri doğrudan saha gözlemleri ile atanmıştır. Ayrıca, araştırma sondajlarından alınan karot numuneleri ve maden sahasından alınan kaya blokları üzerinde gerçekleştirilen laboratuvar deneyleri ile saha etrafındaki kaya kütlelerinin mekanik özellikleri elde edilmiştir. Devamında, maden tasarımlarına göre, duraysızlık durumları ve açık ocağın en derin kısmı dikkate alınarak maden sahasındaki en kritik kesit tespit edilmiştir. Limit denge yöntemlerinin ve numerik modellemenin birlikte kullanımı ile çeşitli genel ocak eğim açısı planları için şev duraylılık analizleri gerçekleştirilmiştir ve bu durum duraylılık analizlerinin güvenilirliğini ve doğruluğunu arttırmaktadır. Topografya ve cevher kütlelerinin yöneliminden dolayı, açık ocak etrafında maden derinliği değişiklik göstermektedir. Bu nedenle, şev duraylılık analiz sonuçları dikkate alınarak değişken maden derinlikleri için ideal genel ocak eğim açıları tespit edilmiştir. Bu analizler şev duraylılığının göstergesi olan güvenlik katsayısını (FOS) ve dayanım indirgeme faktörünü (SRF) hesaplamak amacıyla yürütülmüştür. Limit denge yöntemleri ve numerik modelleme sonuçları karşılaştırılmış ve farklı maden derinlikleri için ideal güvenli şev açıları, FOS ve SRF değerleri en az 1.2 olacak şekilde, tespit edilmiştir. Buna ek olarak, maden derinliğine karşılık gelen genel ocak eğim açıları düşünülerek bölge için şev performans çizelgesi oluşturulmuştur. Bu çizelge aynı zamanda Türkiye’de, Bizmişen bölgesiyle aynı geoteknik özellikler gösteren demir madenleri için de uygulanabilir.

Anahtar Kelimeler: Açık Ocak Madenciliği, Kaya Şev Duraylılığı, Genel Ocak Eğim Açısı, Limit Denge Yöntemi, Sayısal Modelleme, Güvenlik Katsayısı

To My Dear Family and Friends,

ACKNOWLEDGEMENTS

First of all, I would like to express my great sincere gratitude and appreciation to my supervisor, Assoc. Prof. Dr. Hakan Bařarır for his invaluable supervision, kind support, continuous guidance, encouragements and insight throughout the preparation of this thesis. I also present my special thanks to the examining committee members, Prof. Dr. Celal Karpuz, Prof. Dr. Levend Tutluođlu, Assoc. Prof. Dr. Hasan Öztürk and Assoc. Prof. Dr. Mehmet Ali Hindistan for their valuable contributions and for serving on the M.Sc. thesis committee.

I specially want to thank the project team of “Erzincan Bizmiřen Demir Cevheri Maden İřletme Projesi”; Prof. Dr. Celal Karpuz, Prof. Dr. Levend Tutluođlu, Assoc. Prof. Dr. Hakan Bařarır, Assoc. Prof. Dr. Nuray Demirel, and Res. Asst. Ahmet Güneř Yardımcı.

I would like to thank the BİLFER Mining Inc. for valuable supports. I also express my gratitude to the company for the permission to use and publish the data.

I must express my special thanks to my friends and colleagues; Onur Gölbařı, Ahmet Güneř Yardımcı, Dođukan Güner, Deniz Tuncay, and Uđur Alkan, for their continuous support and motivation.

Finally, I owe my loving thanks to my family for their encouragement, great passion and understanding during the preparation of this study. Most of all, I would like to express my sincere gratitude to my mother Serpil Akdađ who has always been supportive and encouraging with love and great passion throughout the period of my studies.

TABLE OF CONTENTS

ABSTRACT	v
ÖZ	vii
ACKNOWLEDGEMENTS	x
TABLE OF CONTENTS	xi
LIST OF TABLES	xiii
LIST OF FIGURES	xv
LIST OF ABBREVIATIONS	xix
CHAPTERS	
1. INTRODUCTION	1
1.1 Background	1
1.2 Statement of the Problem	2
1.3 Objectives and Scope of Study	3
1.4 Research Methodology	4
1.5 Thesis Outline	4
2. LITERATURE SURVEY	7
2.1 Open Pit Mining and Slope Stability	7
2.1.1 Introduction	7
2.1.2 Basic Terms and Definitions in Open Pit Slope Design	7
2.2 Slope Failure Mechanisms	9
2.2.1 Structurally Controlled Failure Mechanisms	9
2.2.2 Rock mass (Circular) Failure Mechanisms	15
2.3 Rock Slope Design Methods	16
2.3.1 Kinematical Analysis	17
2.3.2 Empirical Design Methods	18
2.3.3 Limit Equilibrium Methods	25
2.3.4 Numerical Modeling	35
2.3.5 Comparison of Limit Equilibrium Methods and Numerical Modeling	50

2.4	Summary of Literature Review	52
3.	GENERAL INFORMATION ABOUT THE STUDY AREA AND GEOTECHNICAL STUDIES.....	55
3.1	Research Area.....	55
3.2	General Geology of the Area.....	56
3.3	Geotechnical Site Characterization	58
3.3.1	Geotechnical Survey	59
3.3.2	Laboratory Studies	67
3.4	Rock Mass Design Parameters for Stability Analyses	72
4.	SLOPE STABILITY ANALYSES.....	79
4.1	Introduction	79
4.2	Selection of Critical Cross-section for Stability Analyses	79
4.3	Model Generation.....	81
4.4	Limit Equilibrium Analysis.....	85
4.4.1	Model Input Parameters	86
4.5	Numerical Modeling.....	88
4.5.1	Model Input Parameters	89
5.	STABILITY ANALYSES RESULTS AND DISCUSSION	93
5.1	Assessment of Factor of Safety (FOS) as Design Criterion	93
5.2	Results of Analyses with Limit Equilibrium Methods	95
5.3	Results of Analyses with Numerical Modeling.....	99
5.4	Discussion on the Analysis Results	106
5.5	Development of Slope Performance Chart.....	109
6.	CONCLUSIONS AND RECOMMENDATIONS	111
	REFERENCES.....	113
	APPENDIX A	121

LIST OF TABLES

TABLES

Table 2.1 Parameters used for slope design by McMahon (1976).....	20
Table 2.2 Comparison of Methods of Slices (Anon, Slope stability engineering manual, 2003).....	27
Table 2.3 Static equilibrium conditions satisfied by each method of slices	34
Table 2.4 Summary of methods used for limit equilibrium analysis (Duncan, Wright, and Brandon, 2014).....	34
Table 2.5 Comparison of continuum and discontinuum modeling techniques with advantages and limitations (Coggan <i>et al.</i> , 1998).....	47
Table 2.6 Summary of differences of numerical modeling and limit equilibrium methods (Wyllie and Mah, 2004).....	50
Table 3.1 Estimated GSI ratings for the lithological units in Bizmişen sectors (Karpuz, et al., 2014).....	61
Table 3.2 Estimated rock mass properties for the lithological units in Bizmişen region.....	65
Table 3.3 Number and type of laboratory tests	67
Table 3.4 Percentage distribution of laboratory tests for each lithological unit	68
Table 3.5 Rock material properties of dominating lithological units.....	69
Table 3.6 Rock mass strength and deformation properties for the host rock of model based on Section #A-A'	77
Table 4.1 Overall slope angles for various mining depths.....	81
Table 4.2 Model inputs of most critical section, Section #A-A', in Bizmişen region	88
Table 4.3 Model inputs of most critical section, Section #A-A'	92
Table 5.1 Allowable FOS guideline (Priest and Brown, 1983)	94
Table 5.2 Design factors of safety for pit slope design (Sullivan, 2006).....	94
Table 5.3 Allowable FOS and POF criteria values (Read and Stacey, 2009).....	95
Table 5.4 FOS computation results by limit equilibrium analysis for the most critical section, Section #A-A' with various overall slope angle scenarios	96

Table 5.5 Estimated FOS values for various mining depths with corresponding overall slope angle.....	98
Table 5.6 SRF results by SSR method for Section #A-A' with several schemes of overall slope angle.....	101
Table 5.7 Computed SRF results by SSR technique for different mining depths and corresponding overall slope angle.....	104
Table 5.8 FOS and SRF results of analyses for different mining depth and corresponding overall slope angle.....	108

LIST OF FIGURES

FIGURES

Figure 2.1 Open pit wall terminology (Read & Stacey, 2009)	9
Figure 2.2 (a) Plane failure with tension crack (b) Required lateral-release surfaces (c) Stereographic analysis for kinematic condition of plane failure (Wyllie & Mah, 2004)	11
Figure 2.3 (a) Wedge failure geometry (b) Stereoplot of wedge failure (c) Section view of kinematical condition of wedge failure (d) Stereonet illustration of the limit range with respect to orientation (Wyllie & Mah, 2004)	12
Figure 2.4 Common types of toppling failures (a) Block toppling (b) Flexural toppling (c) Block-Flexural toppling (d) Secondary toppling (e) Stereonet representation of the kinematical condition required for toppling failure (Wyllie & Mah, 2004)	14
Figure 2.5 Typical circular failure (a) without tension crack (b) with tension crack (c) three dimensional geometry of circular shear failure (Hoek and Bray, 1981).....	16
Figure 2.6 Example of preliminary evaluation of slope stability of an open pit mine by kinematic analysis (Hoek and Bray, 1981)	18
Figure 2.7 Slope performance chart of slope height vs. slope angle created by Hoek & Bray (1981)	19
Figure 2.8 Slope angle vs. slope height curves by McMahon (1976).....	21
Figure 2.9 Slope height vs. slope angle graph for MRMR (Haines & Terbrugge, 1991)	22
Figure 2.10 Slope angle vs. slope height chart with respect to Haines and Terbrugge (1991) slope data	23
Figure 2.11 Comparison of slope performance curves proposed by Robertson, Bieniawski and Douglas (Douglas, 2002).....	24
Figure 2.12 Simple example illustration of the limit equilibrium analysis (Wyllie & Mah, 2004)	26
Figure 2.13 Illustration of a slice and force condition for Ordinary Method of Slices (Anon, 2003)	28
Figure 2.14 Illustration of slice and forces for Bishop's Simplified Method (Anon, 2003)	30

Figure 2.15 Forces on a slice by Janbu’s method (Chowdhury <i>et al.</i> , 2010).....	31
Figure 2.16 Forces on a slice for Spencer’s method (Duncan, Wright and Brandon, 2014).....	32
Figure 2.17 Forces on a slice for Morgenstern and Price method (Chowdhury <i>et al.</i> , 2010).....	33
Figure 2.18 Graphical illustrations of differential and integral continuum methods (Hoek <i>et al.</i> , 1990).....	37
Figure 2.19 Explicit calculation cycle used in finite difference method (Itasca, 2011)	39
Figure 2.20 Three-dimensional finite difference model of FLAC3D showing the typical computational mesh and rock materials (He <i>et al.</i> , 2008).....	40
Figure 2.21 Terms used in finite element method and mesh generation using 9-noded elements (Eberhardt, 2003)	41
Figure 2.22 SSR conducted in finite difference analysis considering the unbalanced forces as stability indicator (Dawson <i>et al.</i> , 1999).....	43
Figure 2.23 Convergence approach of SSR analysis for finite element method (Dawson <i>et al.</i> , 1999)	44
Figure 2.24 Influence of plan geometry for stability of a slope	49
Figure 3.1 Location map of Bizmişen (Erzincan) region (Google Earth, 2015).....	55
Figure 3.2 Plan view of the location of drilling operations in Bizmişen region	56
Figure 3.3 Tectonic units of Turkey (Durand <i>et al.</i> , 1999)	57
Figure 3.4 Generalized tectonostratigraphic column cross-section of the Bizmişen region (Yıldırım and Hamarat, 1985).....	58
Figure 3.5 Satellite view of Dönentaş and Taştepe sectors and the drillhole locations (Karpuz, et al., 2014).....	59
Figure 3.6 Satellite view of Ayşe Ocağı and Orta Ocak sectors and the drillhole locations (Karpuz, et al., 2014)	60
Figure 3.7 Investigation area in Taştepe sector (Karpuz, et al., 2014).....	61
Figure 3.8 Investigation area in Ayşe Ocağı sector (Karpuz, et al., 2014)	62
Figure 3.9 Investigation area in Orta Ocak sector (Karpuz, et al., 2014)	62
Figure 3.10 GSI ranges for the lithological units in Bizmişen sectors (Karpuz, et al., 2014).....	63
Figure 3.11 An example of drillhole core in Bizmişen region (Karpuz, et al., 2014)	64

Figure 3.12 An example of compiled results of core logging with evaluated parameters and lithological units in Dönentaş sector.....	66
Figure 3.13 Percentage distribution of laboratory tests	68
Figure 3.14 Illustration of UCS test	70
Figure 3.15 Illustration of Static Deformability Test.....	70
Figure 3.16 Illustration of indirect tensile strength test	71
Figure 3.17 Illustration of triaxial compression test	72
Figure 3.18 Schematic representation of rock mass and material condition (Hoek <i>et al.</i> , 1995)	74
Figure 3.19 Hoek-Brown and Mohr-Coulomb failure envelopes	78
Figure 4.1 Cross sections for different mining depths	80
Figure 4.2 Illustration of model geometry based on cross section, Section # A-A' ..	83
Figure 4.3 Illustration of model geometry based on cross section, Section #E-E'	84
Figure 4.4 Lithological illustration of Dönentaş region based on Section #A-A' (Micromine Pty, 2014)	85
Figure 4.5 Slope search option for circular failure surface in Slide v6.0 (Rocscience Inc., 2014)	87
Figure 4.6 Finite element mesh type used in Phase ² software (Rocscience Inc., 2014)	91
Figure 5.1 Results of analyses with limit equilibrium methods for Section #A-A' with overall slope angle of 36°	97
Figure 5.2 Typical mesh dimensions and boundary conditions of the model based on Section #A-A' with overall slope angle of 36°	100
Figure 5.3 SSR analysis of Section #A-A' with overall slope angle of 36° showing the progress of failure surface by maximum shear strain and deformation vectors.	102
Figure 5.4 SSR analyses with SRF results and corresponding displacement for the west slope of Dönentaş open pit.....	103
Figure 5.5 SSR solution for the west slope of Dönentaş open pit for model Section #A-A' with overall slope angle of 36° at SRF: 1.20 indicating the total displacement	103
Figure 5.6 SSR analyses with SRF results and corresponding displacement for the analyses of different mining depths and corresponding overall slope angle	105

Figure 5.7 FOS and SRF results of overall slope angle optimization analyses for the west slope of Dönentaş open pit with varying angle between 32° and 42°	106
Figure 5.8 Overall Slope Angle, FOS and Amount of Overburden Stripping relation	107
Figure 5.9 Slope performance chart created based on Bizmişen geotechnical characteristics	110
Figure A.1 General Chart for GSI Estimates with respect to Geological Observations (Hoek <i>et al.</i> , 2005).....	121
Figure A.2 Geotechnical Core Logging Sheet	122
Figure A.3 Rock Mass Rating System (Bieniawski, 1989).....	123
Figure A.4 Classification of Individual Parameters used in Q-system (Barton <i>et al.</i> , 1974).....	124
Figure A.5 Guidelines for Estimating Disturbance Factor D.....	127

LIST OF ABBREVIATIONS

ASTM	American Society for Testing and Materials
BEM	Boundary Element Method
CSRF	Critical Strength Reduction Factor
DDA	Discontinuous Deformation Analysis
DEM	Discrete Element Method
FDM	Finite Difference Method
FEM	Finite Element Method
FOS	Factor of Safety
GSI	Geological Strength Index
MRMR	Mining Rock Mass Rating
POF	Possibility of Failure
RMR	Rock Mass Rating
RQD	Rock Quality Designation
SRF	Strength Reduction Factor
SSR	Shear Strength Reduction
UCS	Uniaxial Compression Strength

CHAPTER 1

INTRODUCTION

1.1 Background

In mining engineering, huge amount of the minerals are exploited from the ground by open pit mining methods. With an increase in mining operations, the depth of open pit mines are getting deeper instead of small surface scratching. While increasing the mining depth, the slope height of the mine is continuously getting deeper which leads worse situation for the stability and the safety of the slope. Therefore, for a large scale surface mining operation, slope stability is very important for long term sustainability. Besides, it is necessary to optimize the slope angle for deep open pit mines by increasing the slope angle as high as possible providing that mining operations are carried out under safety conditions. Considering from the economic point of view, making the overall slope angle as high as possible is a crucial way to minimize the amount of stripped waste rock and reduce the production cost for deep open pit mines. A case in point, Bizmişen iron ore mines which owned and will be operated by Bilfer Mining Corporation are located in the Eastern Turkey. The deepest part of one of the open pits has been planned to be around 400 m which will be one of the deepest open pit mines in Turkey. For this deep open pit, increasing the overall slope angle of the west side wall by 1° may reduce approximately 3 million m^3 stripping of waste rock. Therefore, it is important to keep the balance between slope stability and economic efficiency.

In the preliminary methodology for designing overall slope angles in open pits, some approaches were performed. Slope performance charts has been prepared by means of using the recorded stable and unstable case studies. However, the applicability of the charts is restricted since they are composed of worldwide general cases and give rough estimates. Therefore, the requirement of slope performance charts based on local variables has risen. Additionally, those conventional design performance charts would be enhanced with the help of more case studies.

There are some more available approaches in use to assess the slope stability. Limit equilibrium method, one of the traditional methods, is an adequate approach providing information about the potential for slope failure and deriving the factor of safety (FOS) which can be defined as the ratio of the resisting forces (strength) and the driving forces (loading) along the potential failure surface. Numerical modeling is another slope stability method which may assist further analysis of a more complex mechanism by determining both the displacement and stress using the theoretical system of stress-strain conditions. However, combined use of limit equilibrium method and numerical modeling increases the reliability and accuracy of the slope stability analysis and optimum slope design can be achieved. Therefore, overall stability of an open pit and optimized overall slope angle can be obtained by re-examining and comparing the results of 2D numerical modeling and limit equilibrium methods.

1.2 Statement of the Problem

The slope performance charts can be used as a practical preliminary guidelines for the design of open pit slopes. Despite their usage is limited, learning from past experience based on empirical data is a significant part of the slope design study. Therefore, verification of the slope design by using such additional techniques can enhance the reliability of the analysis.

For the determination of optimum overall slope angle, preparation of slope design chart for a specific region or regions showing same formation characteristics could be

a practical tool for long term planning and slope stability assessment. In this research, a slope design chart for iron ore mines in Bizmişen region has been created. Optimum overall slope angle for open pits with different mining depths can be determined by using this chart.

Using the relationship between open pit mining depth and overall slope angle, a slope design and performance chart has been constituted for Erzincan Bizmişen region. The described chart can be used as a convenient design tool to reduce the time frame of mining design. Using this chart to determine optimum safe overall slope angle makes a decrease in the production cost under a prerequisite condition to ensure the safety of mining. Besides, the chart may also be used for the other iron ore bodies with similar geotechnical characteristics.

1.3 Objectives and Scope of Study

In Bizmişen region, it has been planned to design multiple open pit mines. Mining depths of the open pits differ due to the topography and the orientation of the ore bodies. The scope of this research is to determine the optimum overall slope angle of open pits by considering the relation mining depth and overall slope angle for Bizmişen region. In fact, the study makes a practical pre-estimation about the optimum safe slope angle for further production practice of open pit mining activities around the region. Considering the geotechnical structures, obtained relation between overall slope angle and ultimate mining depth can be applicable to other iron ore open pit mines.

In addition, the study aims to improve the local based slope performance charts by increasing the reliability and accuracy. Combined use of limit equilibrium method and numerical modeling has made an effective way to optimize the slope design and strengthen the concept of site specific slope design charts.

1.4 Research Methodology

The main components of the research methodology of this study are listed below:

- i. Carrying out geotechnical investigations in Bizmişen region,
- ii. Conducting laboratory tests on cored samples taken from exploration drillings and rock blocks directly from the mine site,
- iii. Determination of rock mass and material properties,
- iv. Assignments of bench geometry and hydrogeological conditions,
- v. Stability analyses by conventional limit equilibrium methods and numerical modeling,
- vi. Verification and comparison of the 2D stability analysis results from limit equilibrium methods and numerical modeling in terms of instability in Bizmişen.
- vii. Analysis of the results, and improvement of slope design and performance chart composed of mining depth and overall slope angle.

1.5 Thesis Outline

This dissertation is composed of six chapters and contents included in each chapter are briefly presented as follows.

Chapter 1 introduces the background and the problem statement of the study and also objectives are included. The scope of this research are shortly mentioned with the methodology pursued.

Chapter 2 reviews the literature survey related to terms and definitions used in open pit slope design, slope failure mechanisms and rock slope design methods regarding the stability analyses.

In Chapter 3, general information about the study area and geotechnical studies conducted during the fieldwork applications are covered. Moreover, geotechnical characterization of the slope rock mass are presented.

Chapter 4 describes selection of the most critical cross-section and model generation for stability analyses. Moreover, stability analyses conducted by using limit equilibrium method and numerical modeling are included in this chapter.

In Chapter 5, factor of safety assessment obtained from both limit equilibrium and numerical methods is evaluated and the locations of critical failure surfaces are criticized. Additionally, extensive comparison of the analysis results are presented with the discussion and the improvement of the slope design chart is mentioned.

Chapter 6 summarizes the conclusions about the conducted study. Suggestions or recommendations for further studies are presented in this chapter.

CHAPTER 2

LITERATURE SURVEY

2.1 Open Pit Mining and Slope Stability

2.1.1 Introduction

Open pit mining can be defined as the process of excavating any near-surface ore deposit by means of an excavation or cut made at the surface, using one or more horizontal benches to extract the ore while dumping overburden and tailings at a dedicated disposal site outside the final pit boundary (Hartman, 1992). Open pits account for the major part of the world's mineral production due to being large scale, high productivity and high effectiveness. The occupied areas of open pits differ between a few hectares and hundreds of hectares with respect to the grade of ore deposits and mining depths. Along with an increase in mining operations, the depth of open pit mines is getting deeper causing slope stability problems and safety issues. Therefore, open pit slope stability has become significant for long term sustainability. On the other hand, designing optimum overall slope angle such that the mining operations are carried out under safe conditions is a crucial work to minimize the amount of stripped waste rock and to reduce the production cost. Thus, technical, economic, environmental and safety conditions must be considered for conducting open pit slope design.

2.1.2 Basic Terms and Definitions in Open Pit Slope Design

Proper terminology used in open pit mining slope design study can be summarized as followed. Several components such as ramps, benches, bench stacks (inter-ramp),

berms, etc. constitute an overall slope or wall of an open pit. The standard terminology used for the geometric arrangement of an open pit wall is illustrated in Figure 2.1. Their meaning differs with respect to the geographic regions (Africa, Australia or North America). The descriptions of the main terms related to slope components for various regions include as the following.

- ✓ Bench face (North America) = batter (Australia).
- ✓ Bench (North America) = berm (Australia): The flat area between bench faces used for rock fall catchment. The adjective ‘catch’ or ‘safety’ is often in front of the term in either area.
- ✓ Berm (North America) = windrow (Australia): Rock piles placed along the toe of a bench face to increase rock fall catchment and along the crest of benches to prevent personnel and equipment falling over the face below. Note the potential confusion with the use of the term ‘berm’ for a flat surface.
- ✓ Bench stack or Inter-ramp: A group of benches between wider horizontal areas, e.g. ramps or wider berms left for geotechnical purposes.

The stack or inter-ramp slope is defined as the slope between the ramps and also the crest or toe of the excavation and intermediate ramp in an open pit. The inter-ramp slope angle depends upon bench face angle, bench height and width and it is measured from crest to crest or toe to toe as shown in Figure 2.1. On the other hand, overall slope angle which considers all ramps and inter-ramps is measured from toe to crest of the open pit (Figure 2.1).

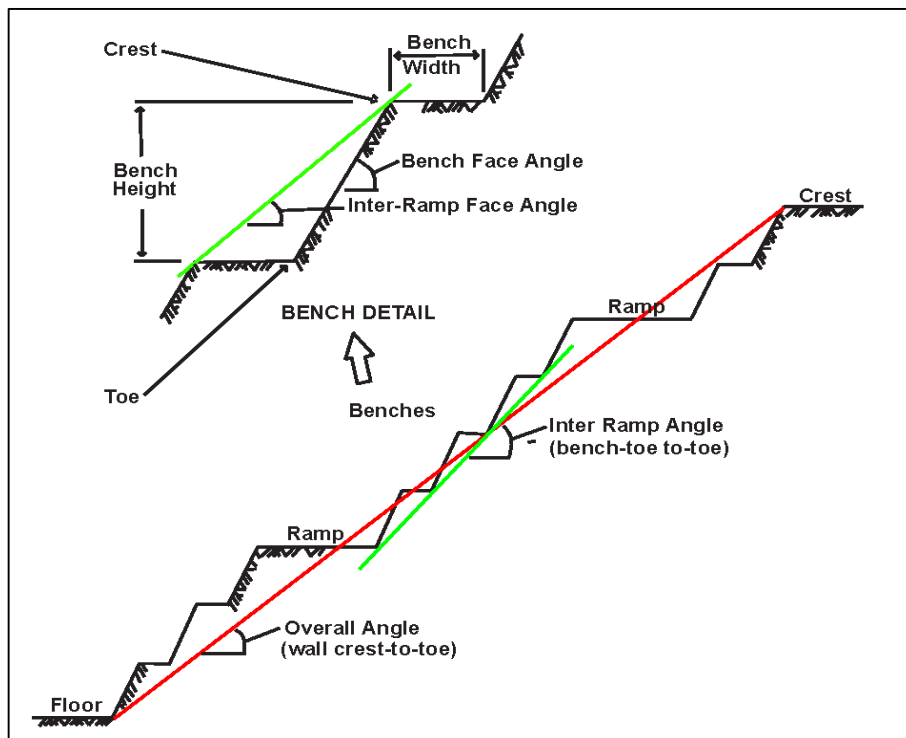


Figure 2.1 Open pit wall terminology (Read & Stacey, 2009)

2.2 Slope Failure Mechanisms

In large scale slopes, various modes of slope failure occur depending on geological structure and the stress conditions of the rock mass. Field data and the failure surface are significant features to gain more and exact failure mechanism. Since determination of complete mode of slope failure is difficult, successive field observations are required to predict the appropriate failure mechanism for slope stability analysis. In the following, commonly governing failure mechanisms are described in detail.

2.2.1 Structurally Controlled Failure Mechanisms

Failures primarily rely on the orientation, shear strength and water pressure conditions of the discontinuities in the rock mass and can be accurately determined by means of proper site investigations and relevant field data. Therefore, it is recommended to gain adequate information about the kinematic constraints. Planar failure, wedge failure and

toppling failure are the most widely observed structural failure modes (Simmons & Simpson, 2006).

Planar Failure

Planar failure occurs when a rock block slides along a discontinuity plane which dips out of the slope face. Most of the failure take place by the tension crack formed at the slope crest. General conditions for plane failure are;

- The plane on which sliding occurs must strike within approximately $\pm 20^\circ$ of the slope face,
- The failure plane must “daylight” in the slope face which means that its dip must be less than the dip of the slope face, expressed as $\Psi_p < \Psi_f$, shown in Figure 2.2 (a),
- The dip of the failure plane must be greater than the angle of friction of this plane, expressed as $\Psi_p > \varphi$, illustrated in Figure 2.2 (a),
- Failure surface intersects the slope with tension crack in slope face or the slope with tension crack in upper slope surface,
- Release surfaces which provide negligible resistance to sliding must present in the rock mass to define the lateral boundaries of the slide. Alternatively failure can occur on a failure plane passing through the convex portion of a slope (Wyllie & Mah, 2004), presented in Figure 2.2 (b).

where,

Ψ_p = Dip of the sliding plane,

Ψ_f = Slope face angle,

φ = Angle of friction of the sliding plane.

Typical planar failure conditions and stereographical illustration can be seen in Figure 2.2.

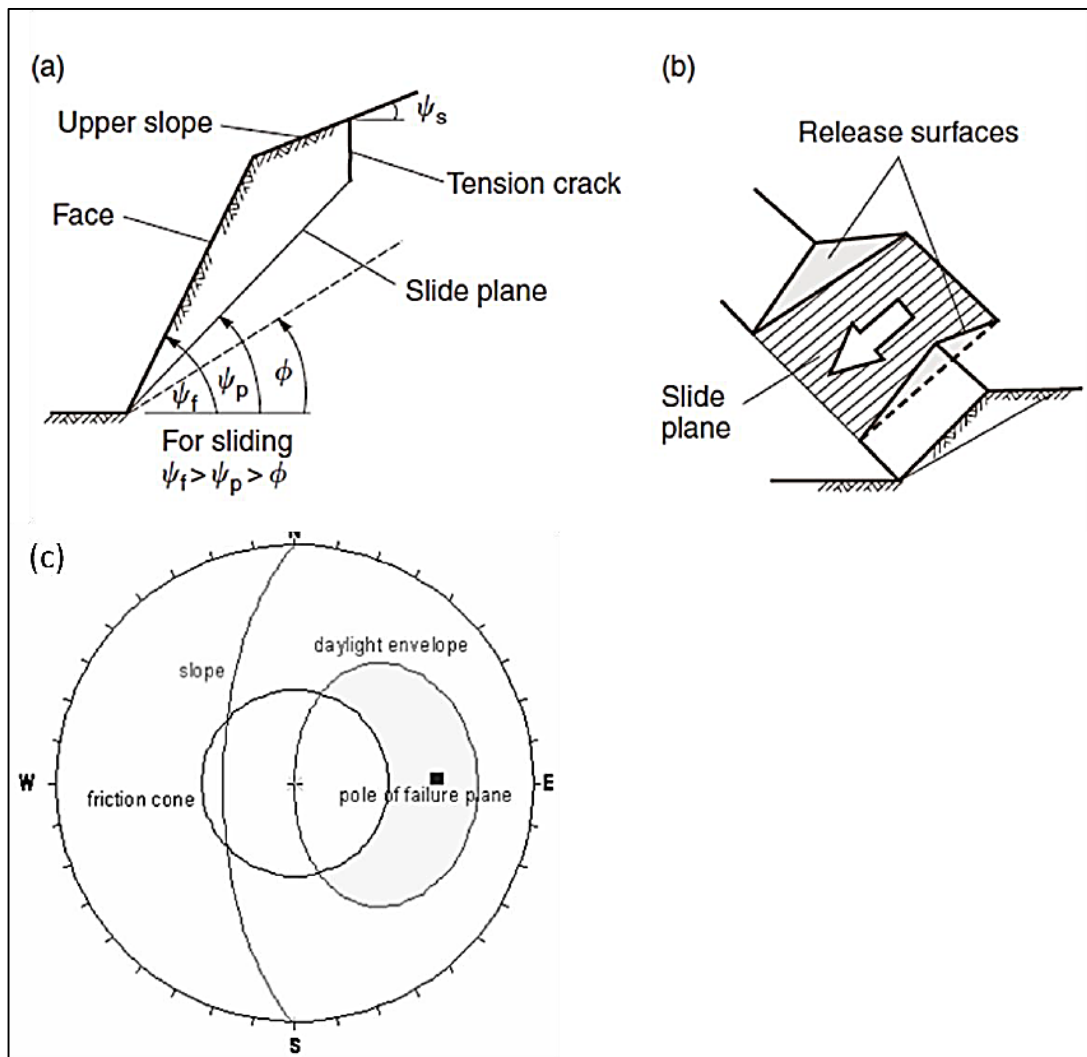


Figure 2.2 (a) Plane failure with tension crack (b) Required lateral-release surfaces (c) Stereographic analysis for kinematic condition of plane failure (Wyllie & Mah, 2004)

Wedge Failure

Wedge failure occurs in which at least two discontinuities intersecting each other and daylight in the slope face. Due to the geological and geometrical aspects, wedge failure is more frequently seen than planar failures in rock slopes. Kinematic conditions for the occurrence of wedge failure are:

- The line of intersection (ψ_i) must be less than the dip of the slope face (ψ_{fi}) but also steeper than the average friction angle (ϕ) of the two sliding planes, which can be presented as, $\psi_{fi} > \psi_i > \phi$ (Wyllie & Mah, 2004),
- For kinematical analysis, discontinuities must strike at angles greater than 20° to the strike of the slope face (Read & Stacey, 2009).

Geometrical and stereographical conditions related to wedge failure are presented in Figure 2.3.

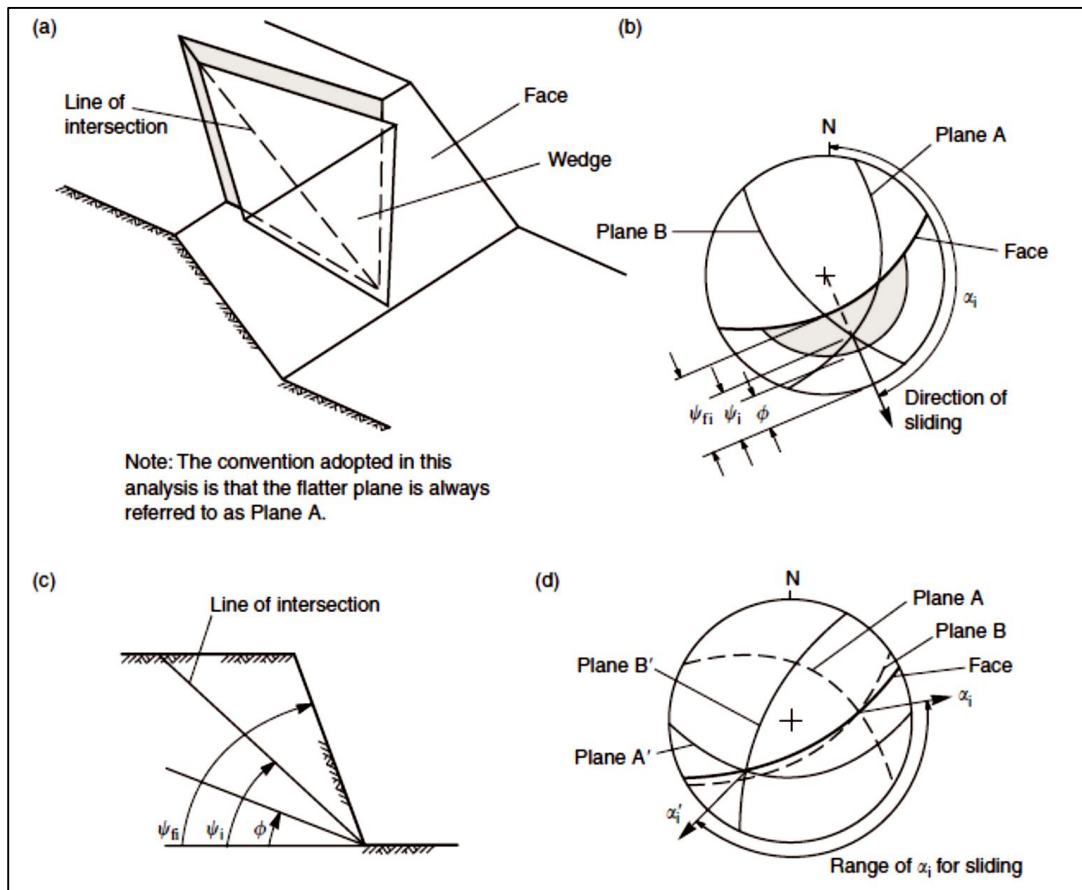


Figure 2.3 (a) Wedge failure geometry (b) Stereoplot of wedge failure (c) Section view of kinematical condition of wedge failure (d) Stereonet illustration of the limit range with respect to orientation (Wyllie & Mah, 2004)

Toppling Failure

Toppling failure can be described as the failure mode of overturning the rock columns formed by steeply dipping and sub horizontal discontinuities. Several kinds of toppling failures were described by Goodman and Bray (1976).

- i. **Block Toppling:** Block toppling occurs in which individual columns are divided by a set of discontinuities. Load caused by the longer overturning columns pushes forward the short columns which compose the toe of the slope and eventually the sliding of the toe leads the toppling progress through the higher up the slope. Existence of bedded sandstone and columnar basalt with orthogonal jointing make possible to occur this type of failure.
- ii. **Flexural Toppling:** This type of failure occurs in slopes with a steeply dipping discontinuity set. Bedded shale and slate with not well developed orthogonal jointing are the triggering geological conditions to occur flexural toppling failure.
- iii. **Block-Flexural Toppling:** Pseudo-continuous flexure along long columns divided by sets of cross joints characterize this type of failure. Accumulated displacements on the cross-joints causes the toppling of columns.
- iv. **Secondary toppling modes:** Unlike the primary toppling modes which occur under the action of gravity and in situ stresses, secondary toppling is caused by natural mechanisms such as weathering or by human activities. Undercutting of the toe of the slope by these independent events initiates this type of toppling failure mode. Horizontally bedded sandstone and shale are examples of geological conditions to occur the failure type.

Common types of toppling failures and stereographic representation of the kinematic conditions for toppling failure are presented in Figure 2.4.

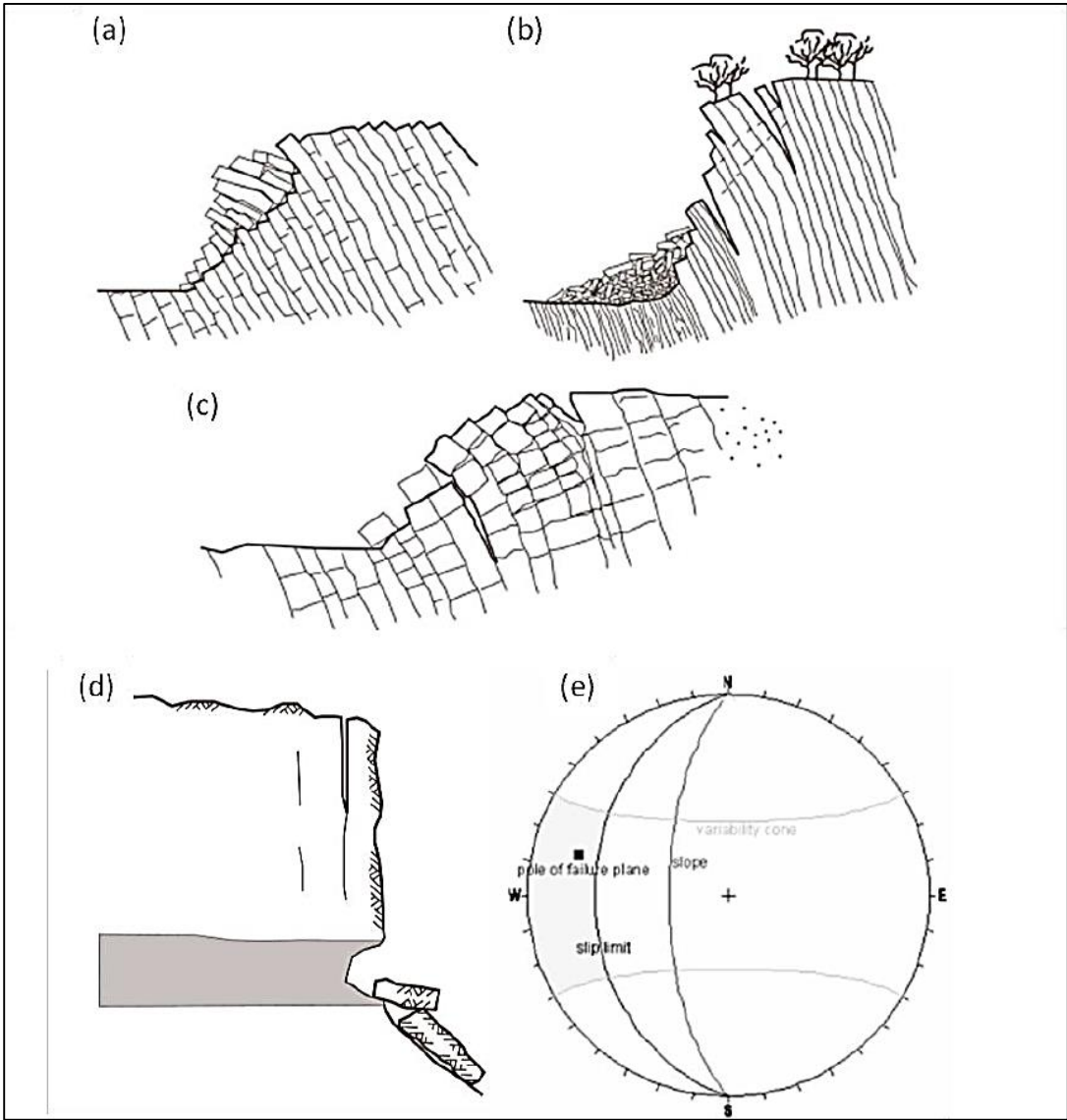


Figure 2.4 Common types of toppling failures (a) Block toppling (b) Flexural toppling (c) Block-Flexural toppling (d) Secondary toppling (e) Stereonet representation of the kinematical condition required for toppling failure (Wyllie & Mah, 2004)

According to Goodman and Bray (1976) toppling failure occur in case such conditions are fulfilled;

- If

$$(90 - \Psi_f) + \varphi_d \leq \Psi_d \quad (2.1)$$

Ψ_f = Dip of slope face

φ_d = Internal friction angle of plane/joint (discontinuity)

Ψ_d = Dip of plane/joint (discontinuity)

- If discontinuity dips into the slope face and strikes within 30° of the face, toppling failure is possible to occur.

2.2.2 Rock mass (Circular) Failure Mechanisms

Circular failure generally occur in highly weathered or closely jointed rock masses. The failure surface is mostly in the form of circular shape by developing the line of least resistance path through the slope. This type of failure is not controlled by structural geology for stability and takes place when the individual particles in a rock mass are very small compared with the size of the slope (Wyllie and Mah, 2004). Moreover, formation of tension crack behind the slope crest is commonly possible in which the sliding surface extends to the toe of the slope. In Figure 2.5, two and three dimensional illustrations of circular failure are presented. Limit equilibrium method is a commonly used analysis method for circular shear failure by applying the method of slice in which a circular failure surface is assumed. Additionally, finite element, finite difference and distinct element method are frequently preferred numerical modeling tools for analysis of rock mass failure.

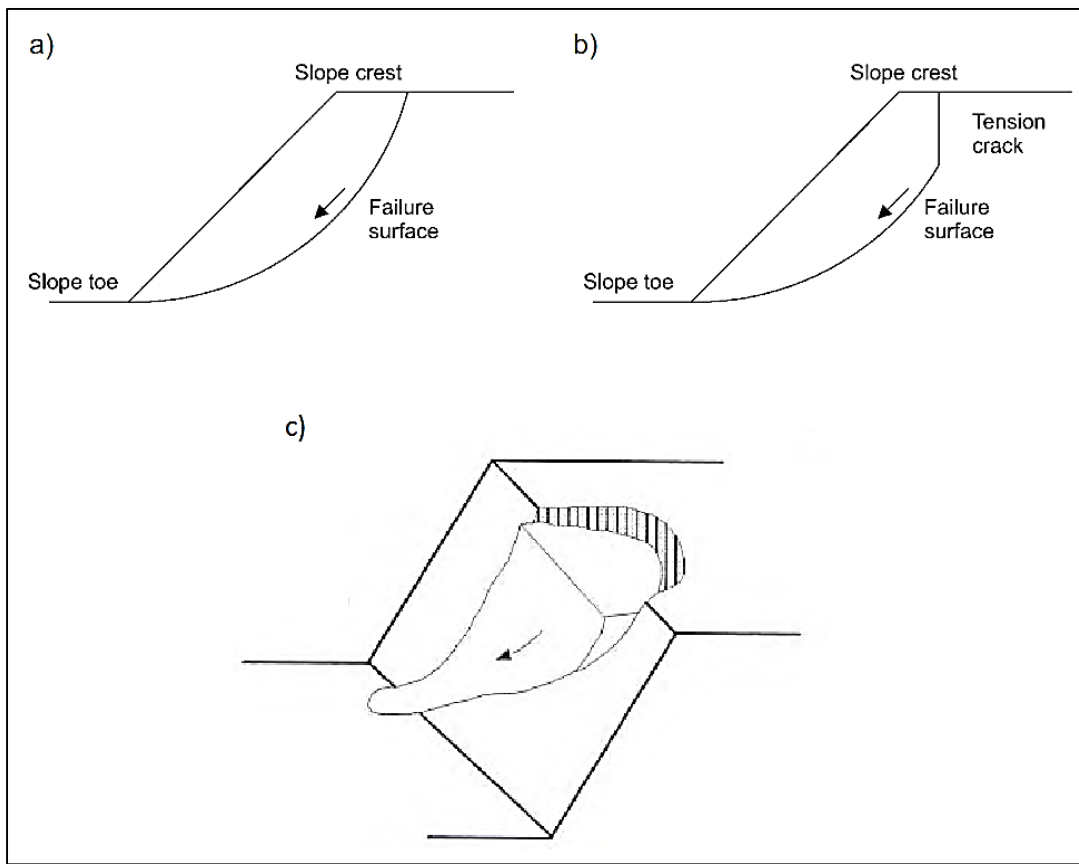


Figure 2.5 Typical circular failure (a) without tension crack (b) with tension crack (c) three dimensional geometry of circular shear failure (Hoek and Bray, 1981)

2.3 Rock Slope Design Methods

The purpose of design methods for rock slopes is basically to determine and predict whether or not failure occurs. In fact, they are intended to determine when the acting stress on a slope exceed the strength of the rock mass. Various methods were proposed for the design analyses, including kinematic analysis and empirical design methodology, limit equilibrium methods and numerical modeling analysis.

2.3.1 Kinematical Analysis

Kinematic analysis is a useful method to investigate the possible structurally controlled slope failure modes examining the sliding direction by stereographic projection. Kinematic is described as the motion of bodies without reference to the forces that cause them to move (Goodman, 1989). Maximum safe slope angle can be estimated based on the basic failure modes such as planar failure, wedge failure and toppling failure. The analysis is conducted by using the orientation of discontinuities and the slope generally in terms of dip and dip direction. However, strength conditions, bench geometry, external forces, seismic or groundwater conditions are not considered in this technique. Stereonet plots are used to determine the failure type and the direction of the slide which gives data about the stability conditions. A preliminary slope stability evaluation of a mine by conducting kinematic analysis associated with susceptible failure mode is presented in Figure 2.6. Although kinematic analysis is a relatively simple to use, it just gives an initial indication of failure potential. Therefore, kinematic analysis is only utilized for preliminary design purposes by eliminating stable slopes for further detailed analyses.

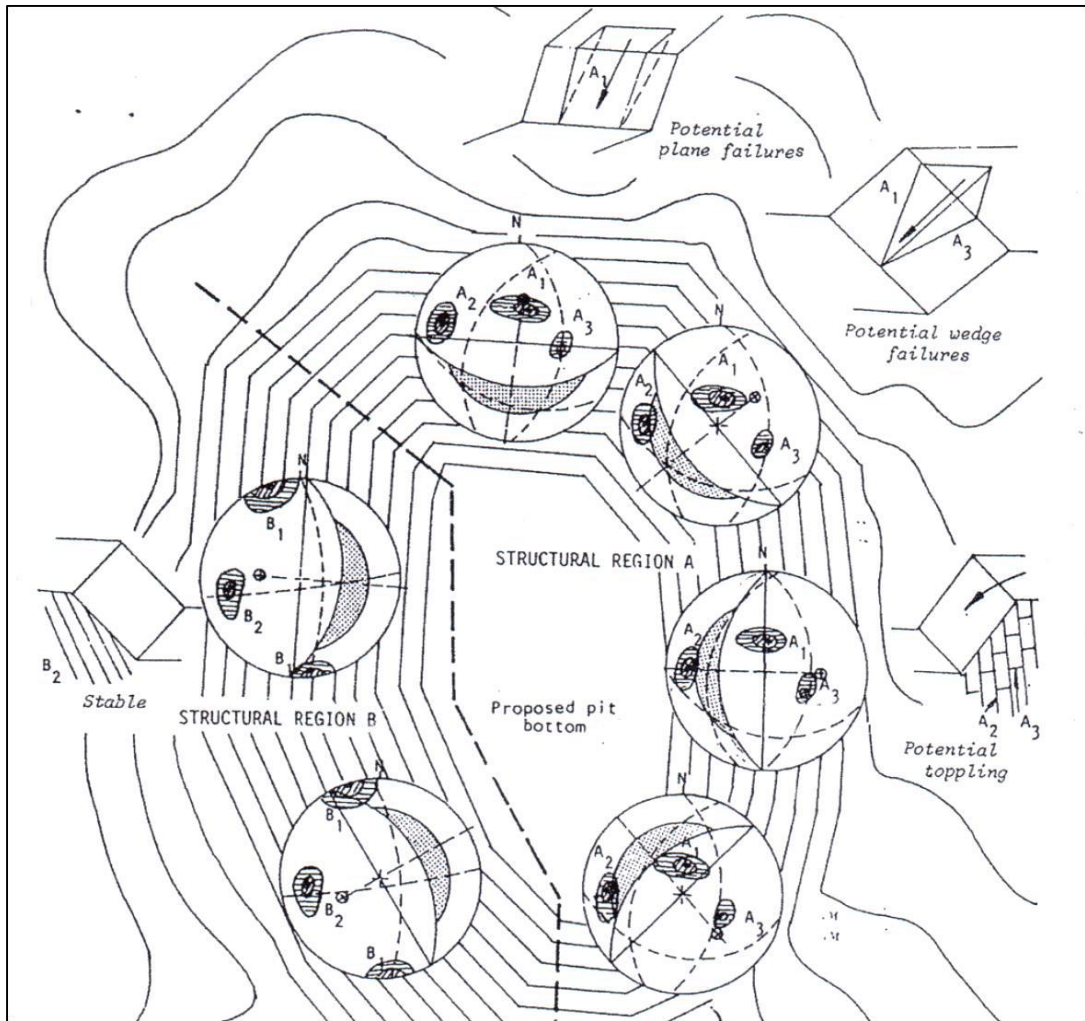


Figure 2.6 Example of preliminary evaluation of slope stability of an open pit mine by kinematic analysis (Hoek and Bray, 1981)

2.3.2 Empirical Design Methods

In the preliminary design of slopes, use of the database constituted with the recorded slope stability behavior is a practical approach and has a significant role in the slope stability. An initial attempt was presented by Lutton (1970) by gathering data from several mines with steepest and highest slopes. The most commonly used chart, shown in Figure 2.7, was developed for global design purposes using the stable and unstable hard rock slopes data obtained from mines, quarries, dam foundation excavations and highway cuts by Hoek and Bray (1981). Although the plot is mostly composed of

slopes in hard rock with various height and angle, most of the flatter slopes have failure. Accordingly, for higher and steeper slopes, the line can be considered as a guideline for the slope design purposes (Douglas, 2002).

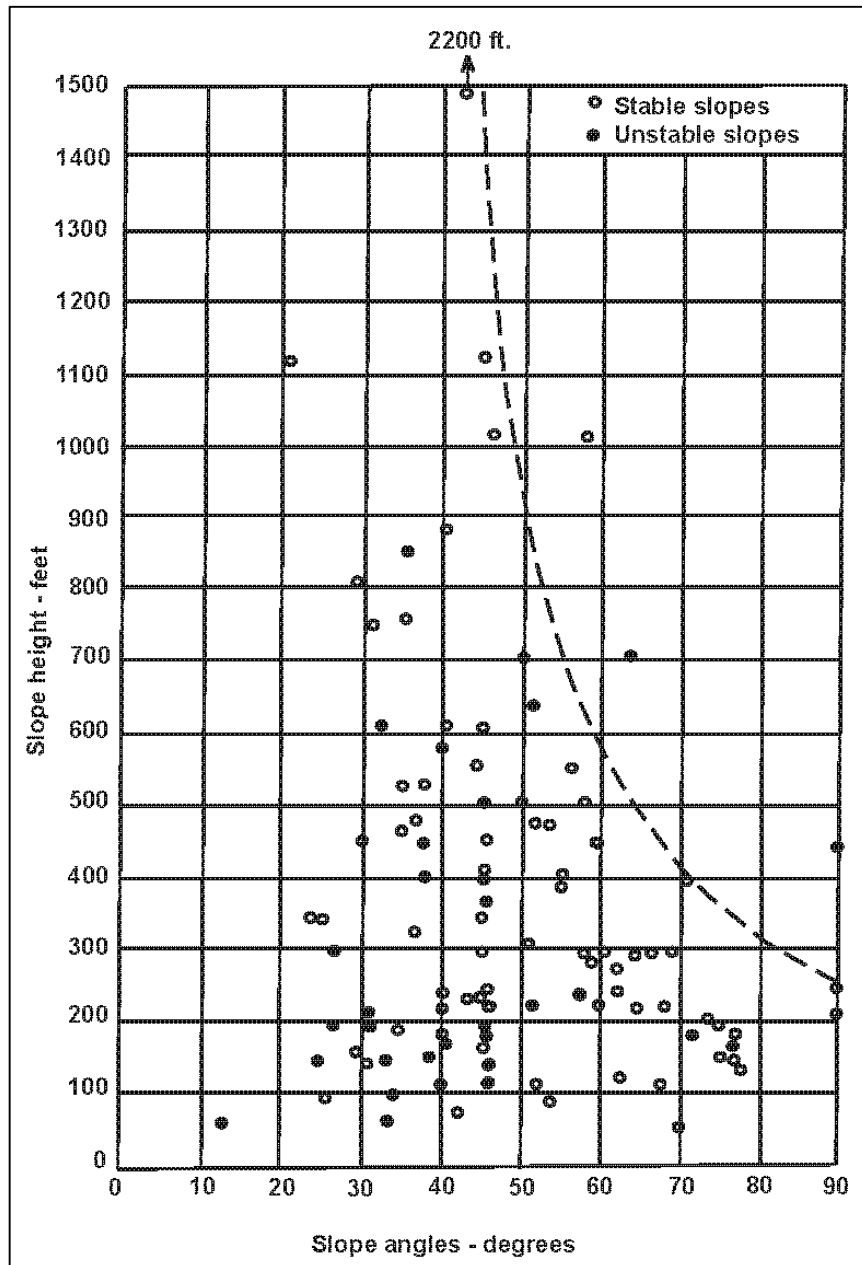


Figure 2.7 Slope performance chart of slope height vs. slope angle created by Hoek & Bray (1981)

By gathering the similar rock mass types, McMahon (1976) studied on the determination of the slope length (L) and slope height (H) by using the correlation between them. The researcher obtained a relation and using the parameters of different rock masses given in Table 2.1 and slope height versus slope angle curve was created (Figure 2.8). However, as seen in the Figure 2.8, the relation does not fit for the stronger rock masses.

$$H = aL^b \tag{2.2}$$

$$L = H/\tan(\text{slope angle}) \tag{2.3}$$

In the equation, a and b are constants changing depending on the type of rock mass as shown in Table 2.1.

Table 2.1 Parameters used for slope design by McMahon (1976)

Rock mass type	a	b
Massive granite with few joints	139	0.28
Horizontally layered sandstone	85	0.42
Strong but jointed granite and gneiss	45	0.47
Jointed partially altered crystalline rocks	16	0.58
Stable shales	8.5	0.62
Swelling shales	2.4	0.75

McMahon’s slope design technique was developed by Haines and Terbrugge (1991) by correlating slope design curves with further rock mass ratings. The design methodology of this technique depends upon the Mining Rock Mass Rating (MRMR) which is rock mass classification system proposed by Laubscher (1977 and 1990). The researchers plotted a graph of slope angle versus slope height with MRMR contours, shown in Figure 2.9. The graph is composed of three design zones conditions for which are classification alone may be sufficient, marginal on classification alone, additional analysis is required for slopes respectively. Moreover, Haines and Terbrugge (1991)

conducted case studies of excavated slopes with paired different MRMR values in order to assess the design curves (Figure 2.10). However, this attempt does not seem appropriate for design purposes since all cases were selected from stable slopes and the curves are almost linear for slopes up to 100 m height (Douglas, 2002).

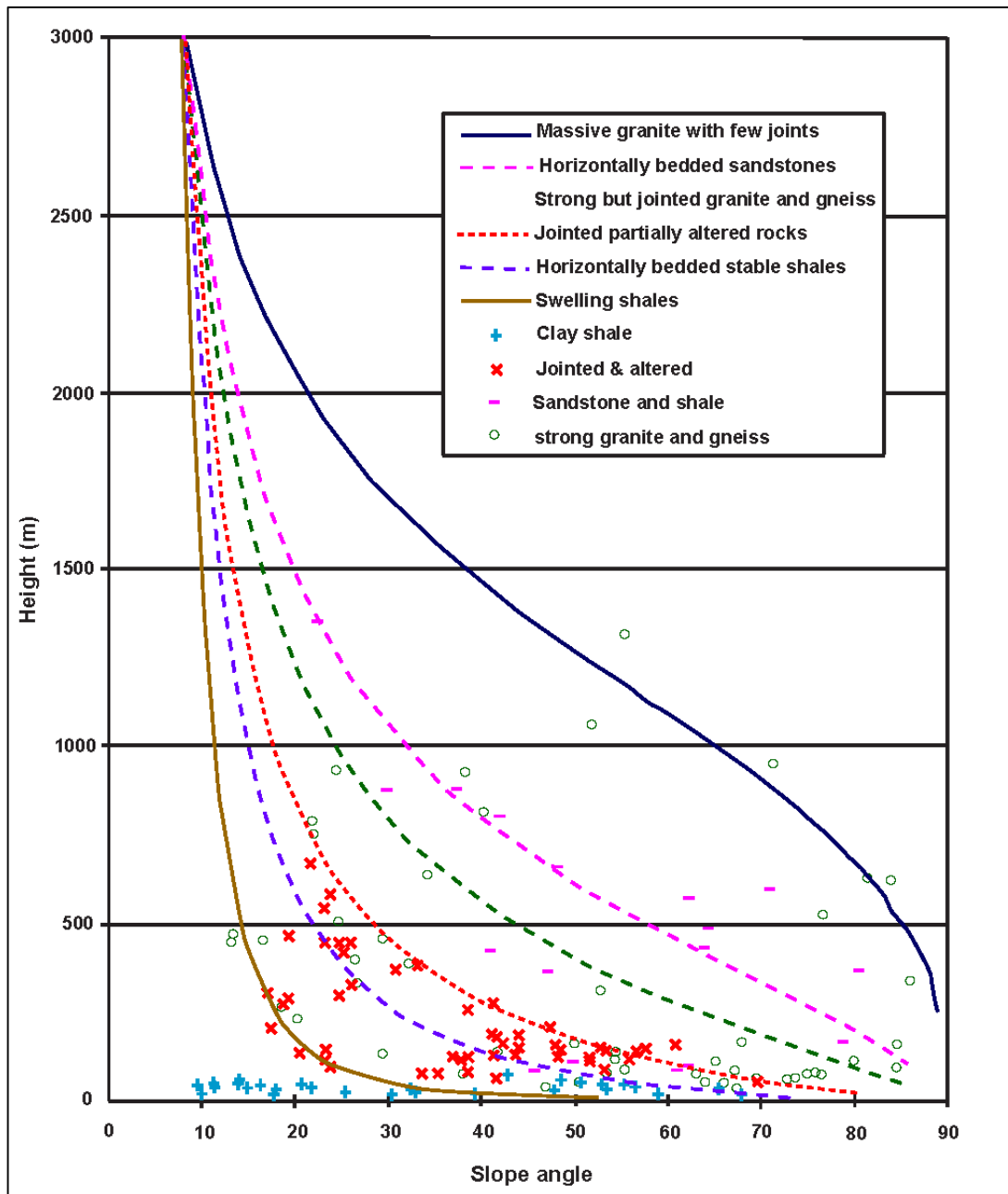


Figure 2.8 Slope angle vs. slope height curves by McMahon (1976)

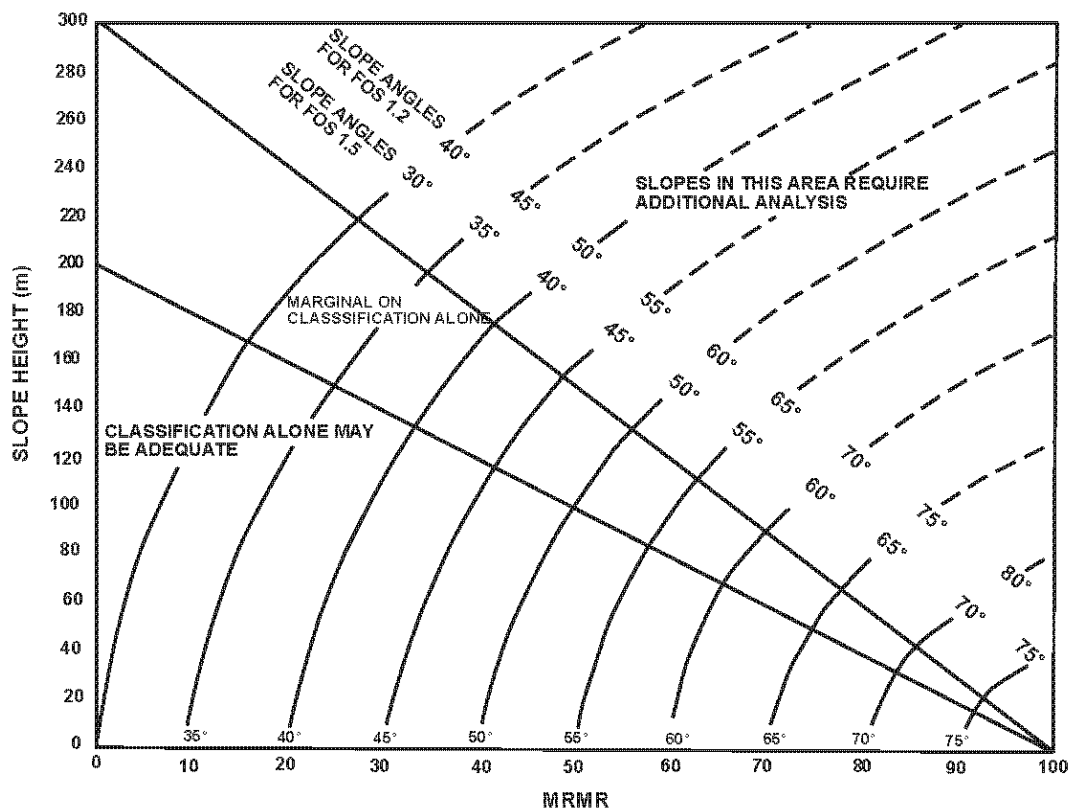


Figure 2.9 Slope height vs. slope angle graph for MRMR (Haines & Terbrugge, 1991)

Slope performance curves for Rock Mass Rating (RMR_{76}) were generated by Bieniawski (1976) by assuming a factor of safety as one and no adjustment was made for the orientation. Unlike slope performance curves proposed by Bieniawski, Robertson's and Douglas's curves are used for weaker rock mass types (Figure 2.11). Robertson (1988) and Douglas (2002) made estimates on slope performance curves with respect to various Geological Strength Index (GSI) values and the trends shown by the curves are compatible for slope heights greater than 150 m under moderate water pressure conditions.

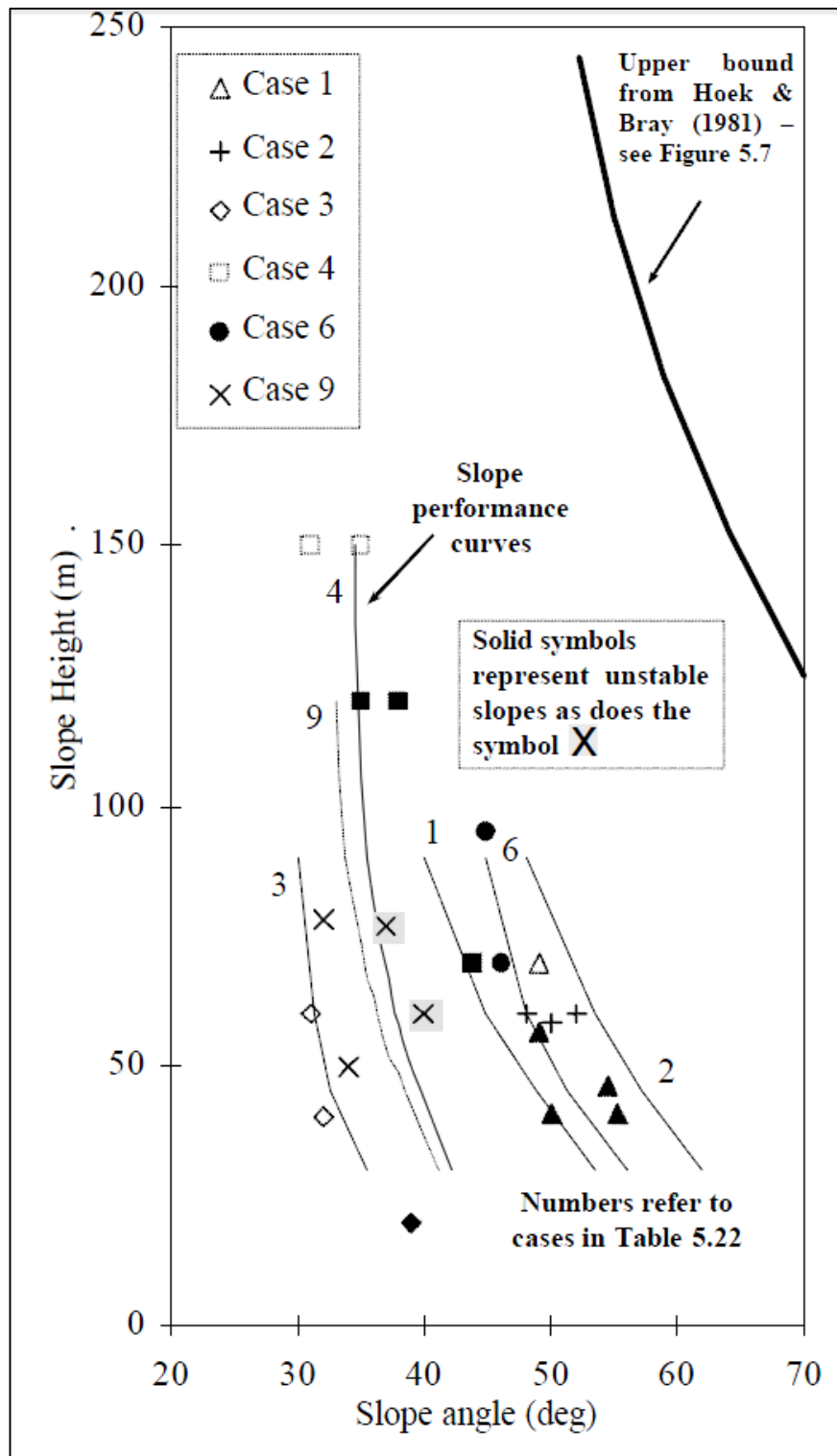


Figure 2.10 Slope angle vs. slope height chart with respect to Haines and Terbrugge (1991) slope data

As a conclusion, empirical design methods may be a practical preliminary guide for the slope design in open pits. In case detailed data analysis about the slope is not available, past experience of the stable and unstable slopes can lead during the design work and be applicable by extending the database with various stability conditions.

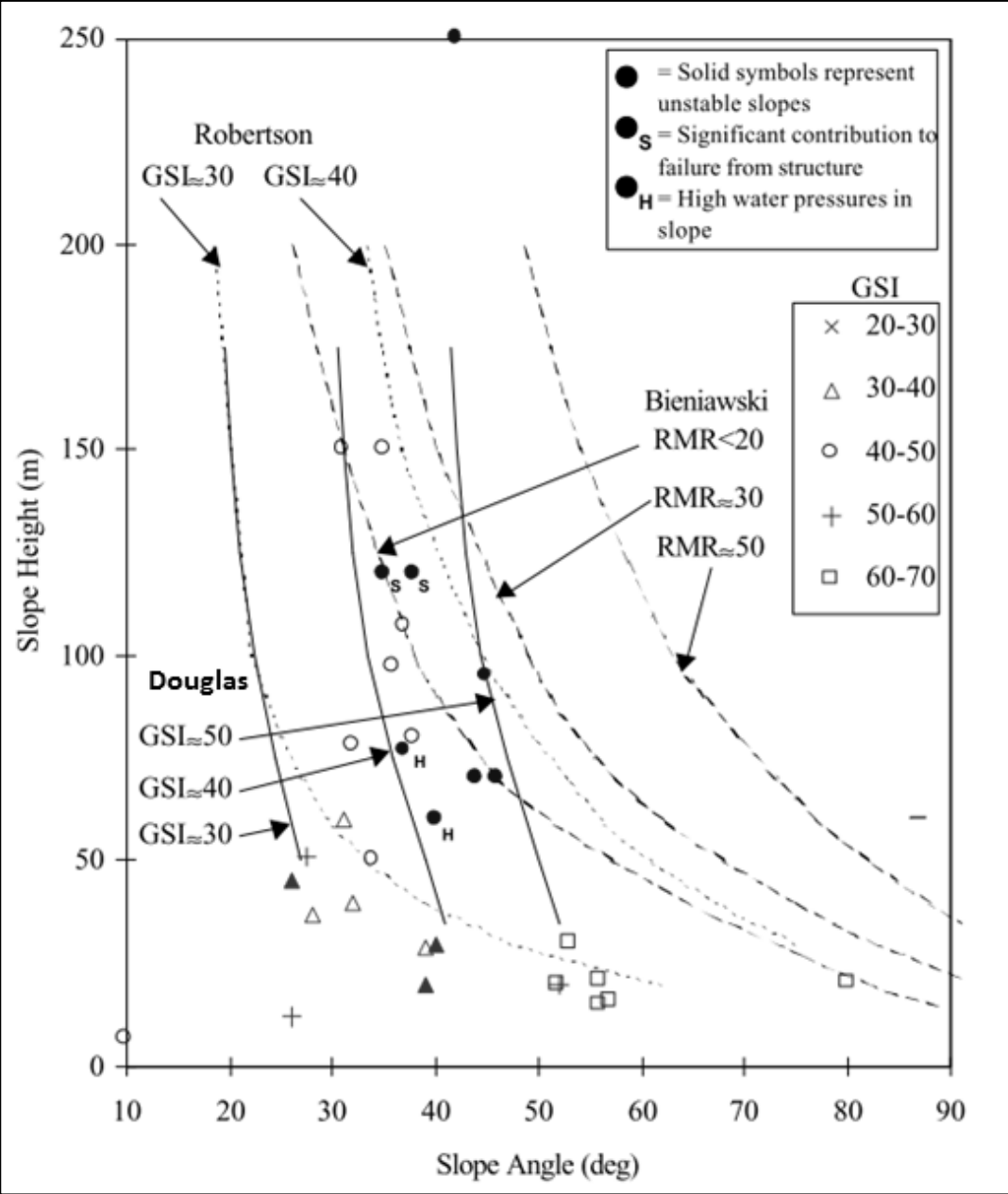


Figure 2.11 Comparison of slope performance curves proposed by Robertson, Bieniawski and Douglas (Douglas, 2002)

2.3.3 Limit Equilibrium Methods

Limit equilibrium methods are the most commonly used conventional slope stability analysis technique, depends upon the force and moment equilibrium. In the method, rock mass is assumed as a rigid body considering the principle of static equilibrium. Failure surface must be assumed and the stability of the rock mass is investigated with respect to force-moment relation. The shear strength of the rock mass is governed by Mohr-Coulomb criterion in which material properties are expressed in terms of cohesion (c) and friction angle, (ϕ) (Wyllie & Mah, 2004). The method enables the calculation of minimum factor of safety (FOS) value which is an indicator of instability. FOS can be simply stated as the ratio of resisting forces to driving forces along the assumed failure surface. FOS is obtained from the comparison between the forces and moments of causing instability and resisting failure. In fact, FOS is determined by ensuring that the rock mass can maintain the stability on the assumed possible failure surface. The rock mass is considered as in limiting equilibrium condition in case the driving and resisting forces exactly equal to each other which states that FOS is equal to 1.0. The sketch illustration of the limit equilibrium analysis is shown in Figure 2.12 and the expression is shown in the equation as below:

$$\text{Factor of Safety (FOS)} = \frac{\sum \text{Resisting Forces}}{\sum \text{Driving forces}} \quad (2.4)$$

If the shear resistance of the rock mass is not sufficient which states that magnitude of the driving forces exceeds the resisting forces, the failure takes place along the assumed slip surface and slope is considered as unstable with FOS less than 1.0 or else, the slope is considered as stable with FOS greater than 1.0. At the point of limit equilibrium condition, FOS equals to 1.0, the resisting and driving forces are in balance on the slope in which slope is considered in a threshold position between being stable and unstable.

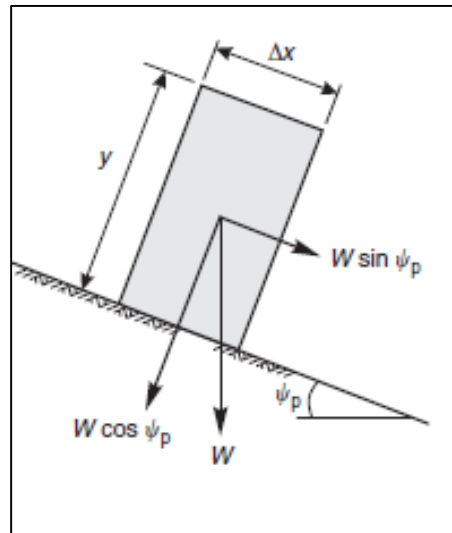


Figure 2.12 Simple example illustration of the limit equilibrium analysis (Wyllie & Mah, 2004)

Analytical solutions considered in limit equilibrium methods rely on;

- Weight of the sliding mass (W)
- Cohesion and internal friction angle
- Pore water pressure
- Geometry of the slope
- Seismic acceleration
- Tension crack position
- External loads

for design purposes and determination of the appropriate remedial measure.

Method of slices is the mostly used in limit equilibrium method which are composed of various assumptions and equilibrium conditions. Methods are based on;

- The rock mass above the failure plane is divided usually into a finite vertical slices,
- In order to reach the sliding mass into a limit state, the strength of the failure surface is mobilized,
- Considering the inter-slice forces, assumptions are employed,

- FOS value is determined by means of force and moment equilibrium equations (Cheng & Lau, 2008).

There are several types of methods of slices have been developed and FOS results may differ due to the different assumptions made and conditions of equilibrium. An early attempt which is the ordinary method of slices based on a rigorous mechanics principle was done by Fellenius (1936). The method is the simplest and amenable to hand calculations. Developments have occurred on the method of slices by Bishop (1955), Janbu (1954), Lowe and Karafiath (1960), Morgenstern and Price (1965) and Spencer (1967). Basic features of the methods are compared in Table 2.2.

Table 2.2 Comparison of Methods of Slices (Anon, Slope stability engineering manual, 2003)

Comparison of Features of Limit Equilibrium Methods						
Feature	Ordinary Method of Slices	Simplified Bishop	Spencer	Modified Swedish	Wedge	Infinite Slope
Accuracy		X	X			X
Plane slip surfaces parallel to slope face						X
Circular slip surfaces	X	X	X	X		
Wedge failure mechanism			X	X	X	
Non-circular slip surfaces-any shape			X	X		
Suitable for hand calculations	X	X		X	X	X

Ordinary Method (Swedish or Fellenius Method)

The ordinary method of slices is the simplest method. All inter-slice forces are neglected and it only satisfies moment equilibrium around the center of the sliding surface to determine FOS (Fellenius, 1936). The method is suitable to calculate FOS

by hand since unlike the other methods, iterative solutions is not required. The slice and the condition of the forces are shown in the Figure 2.13 and the FOS is determined with the equation below;

$$F = \frac{\sum [c' \Delta l + (W \cos^2 \alpha - u \Delta l \cos^2 \alpha) \tan \phi']}{\sum W \sin \alpha} \tag{2.5}$$

Where

- c' and ϕ' Shear strength parameters for the center of the base of the slice
- W Weight of the slice
- α Inclination of the bottom of the slice
- u Pore water pressure at the center of the base of the slice
- Δl Length of the bottom of the slice

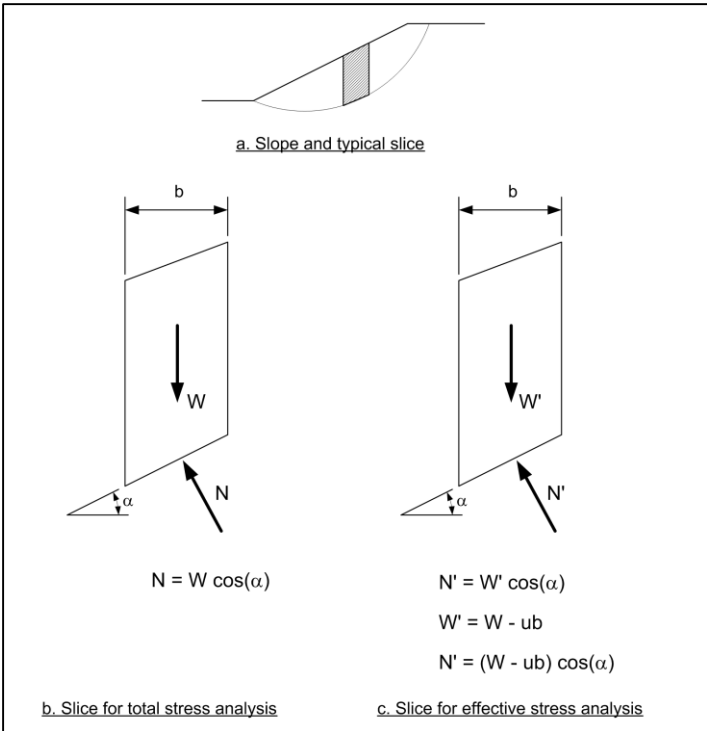


Figure 2.13 Illustration of a slice and force condition for Ordinary Method of Slices (Anon, 2003)

in which

W = Weight of slice,

W' = Effective slice weight,

N = Normal force on the base of slice,

N' = Effective normal force on the base of slice,

α = Inclination of the bottom of the slice,

u = Pore water pressure on the slip surface,

b = Width of slice.

The method does not satisfy either horizontal or vertical force equilibrium and moment equilibrium is not considered for individual slices. Moreover, it cannot be used for effective stress analyses with high pore water pressures since the error in the value of FOS may be as much 50-60% which could lead to uneconomical designs (Whitman & Bailey, 1967).

Bishop's Simplified Method

Bishop's Simplified method is the most widely used method of slices for limit equilibrium analysis. In the method, inter-slice forces are assumed as horizontal which means that inter-slice shear forces are ignored and can be used for only circular failures (Bishop, 1955) (Figure 2.14).

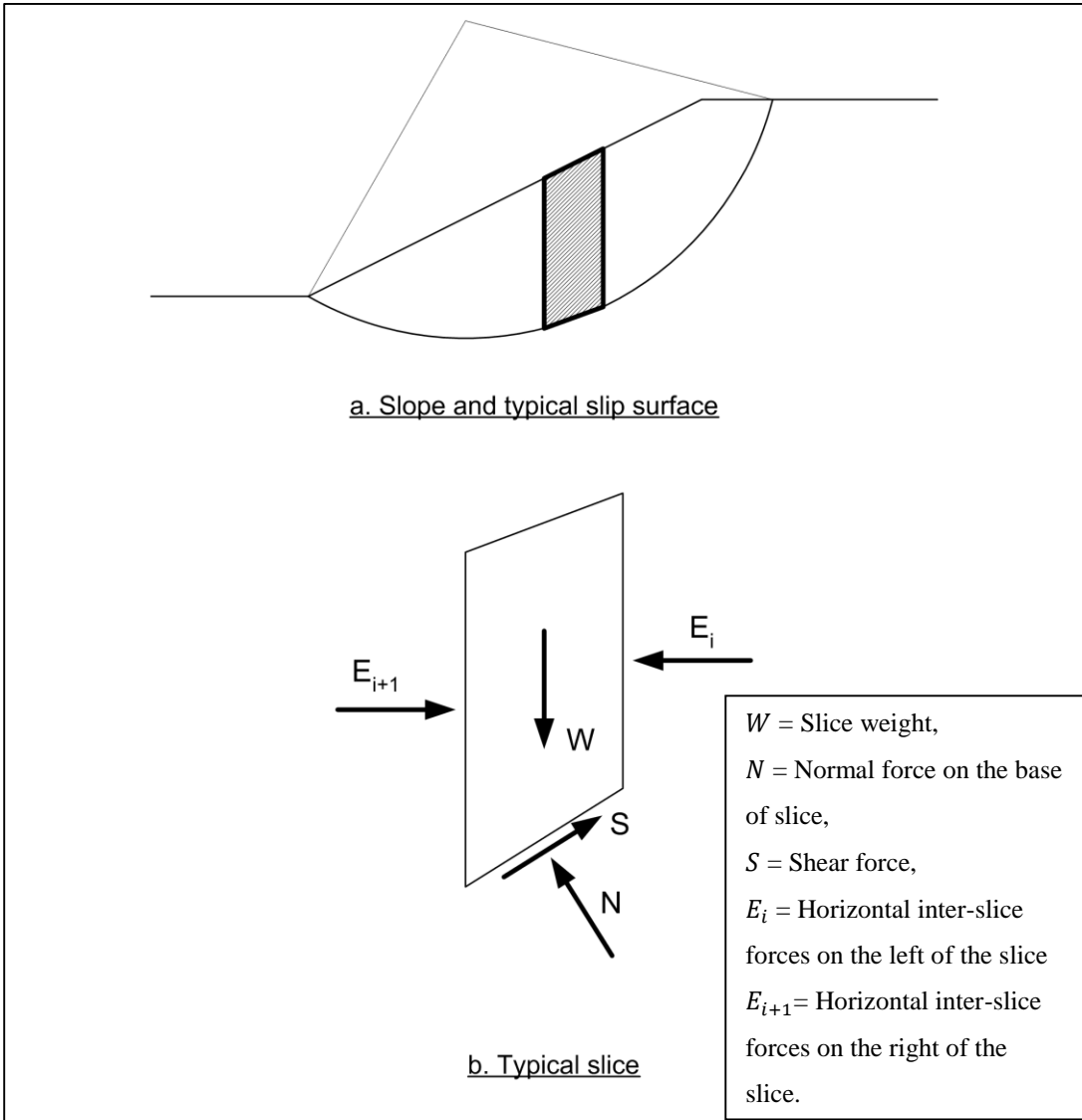


Figure 2.14 Illustration of slice and forces for Bishop's Simplified Method (Anon, 2003)

The method does not satisfy horizontal force equilibrium which causes a restriction for pseudo-static earthquake analyses. The FOS is determined by using the equation below;

$$F = \frac{\sum \frac{c + (\gamma h - p) \tan \phi}{\cos \alpha \left(1 + \frac{\tan \alpha \tan \phi}{F}\right)}}{\sum \gamma h \sin \alpha} \quad (2.6)$$

where

p Pore water pressure

α Angle of the slip surface of the slice with slip center

Since F appears on both sides of the Bishop's equation, it is most conventional to solve F iteratively. In terms of mechanics, Bishop's Simplified method gives more accurate results than Ordinary method for effective stress analyses.

Simplified Janbu Method

This method is used for the analysis of both circular and non-circular failure surfaces. It is assumed that the inter-slice forces are horizontal and shear forces are neglected which gives underestimated FOS values than the rigorous methods (Janbu, 1954). To improve the FOS values correction factor is used based on case studies (Abramson *et al.*, 2002). Moment equilibrium condition is not satisfied for the method. Forces acting on a slice by the method is presented in Figure 2.15.

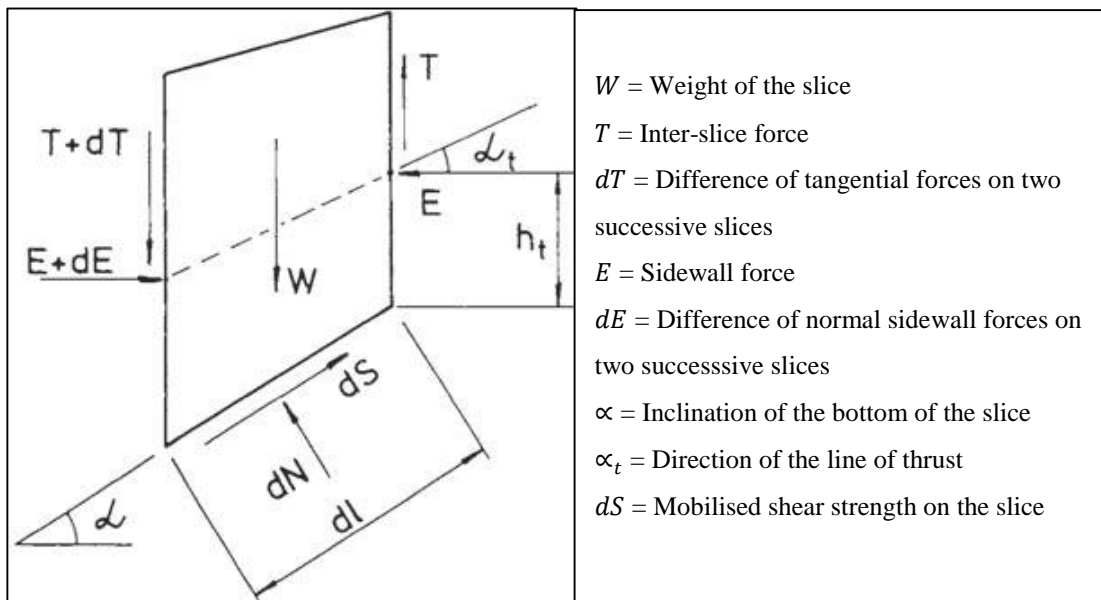
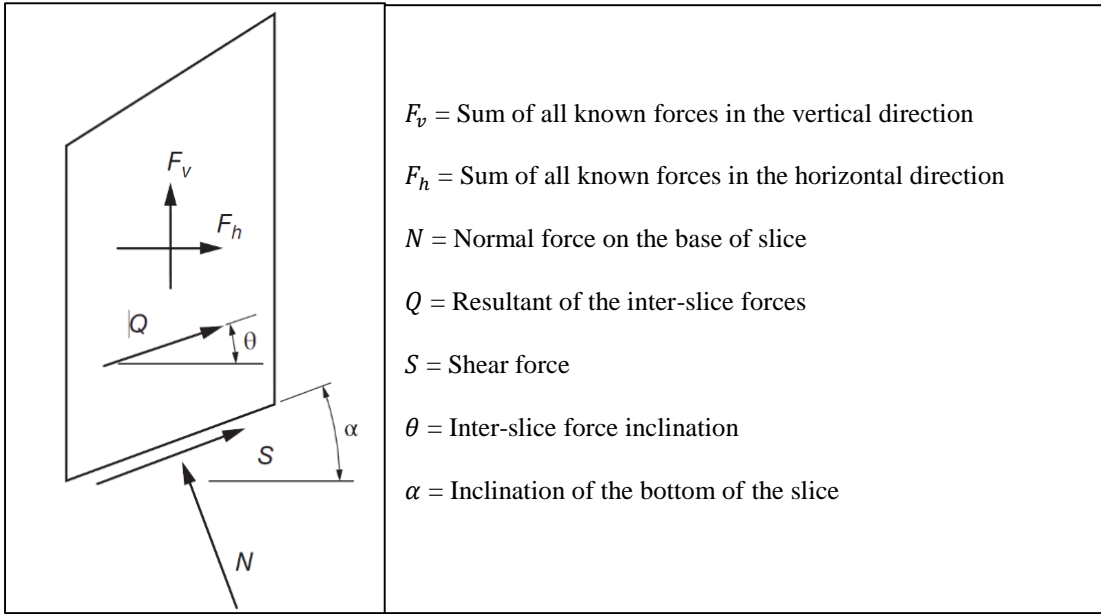


Figure 2.15 Forces on a slice by Janbu's method (Chowdhury *et al.*, 2010)

Spencer’s Method

The method is originally proposed for circular sliding surfaces by Spencer (1967). However, it was proven that the application of the method can be extended to be applied for non-circular failure surfaces (Wright, 1970). It is assumed that all inter-slice forces are inclined at a constant angle. In the method, force and moment equilibrium requirements are fully satisfied. As a result of the iterative procedure until the force and moment equilibrium conditions are satisfied for each slice, two factor of safety equations are derived which are based on the summation of moments and summation of forces in a direction parallel to inter-slice forces (Spencer, 1967). The forces on a slice for Spencer’s method are shown in Figure 2.16.



- F_v = Sum of all known forces in the vertical direction
- F_h = Sum of all known forces in the horizontal direction
- N = Normal force on the base of slice
- Q = Resultant of the inter-slice forces
- S = Shear force
- θ = Inter-slice force inclination
- α = Inclination of the bottom of the slice

Figure 2.16 Forces on a slice for Spencer’s method (Duncan, Wright and Brandon, 2014)

Morgenstern – Price Method

The method is convenient to be applied for both circular and non-circular failure sliding surfaces. In the method all static equilibrium conditions are satisfied and a relation between shear forces and normal forces by a mathematical function as;

$$X/E = \lambda f(x) \quad (2.7)$$

where $f(x)$ is a function varying continuously across the slip with respect to x and λ is a scaling factor (Morgenstern and Price, 1965).

Typical slice with forces for this rigorous method is presented in Figure 2.17.

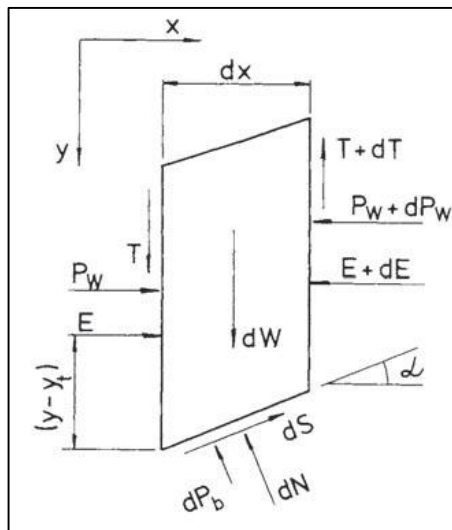


Figure 2.17 Forces on a slice for Morgenstern and Price method (Chowdhury *et al.*, 2010)

As mentioned, to calculate FOS, all limit equilibrium methods utilize the equations of static equilibrium. In Table 2.3, static equilibrium conditions satisfied by each method of slices are summarized. Moreover, the limitations, assumptions and equilibrium conditions of all methods are briefly summarized in Table 2.4.

Table 2.3 Static equilibrium conditions satisfied by each method of slices

Method	Force equilibrium		Moment equilibrium
	x	y	
Fellenius OMS	No	No	Yes
Bishop's simplified	Yes	No	Yes
Janbu's simplified	Yes	Yes	No
US Corps of Engineers	Yes	Yes	No
Lowe&Karafiath	Yes	Yes	No
Morgenstern&Price	Yes	Yes	Yes
Spencer	Yes	Yes	Yes
Sarma	Yes	Yes	Yes

Table 2.4 Summary of methods used for limit equilibrium analysis (Duncan, Wright, and Brandon, 2014)

Procedure	Use
Infinite Slope	Homogeneous cohesionless slopes and slopes where the stratigraphy restricts the slip surface to shallow depths and parallel to the slope face. Very accurate where applicable.
Logarithmic Spiral	Applicable to homogeneous slopes; accurate. Potentially useful for developing slope stability charts and used in software for design of reinforced slopes.
Swedish Circle; $\phi=0$ method	Applicable to slopes where $\phi=0$ (i.e., undrained analyses of slopes in saturated clays). Relatively thick zones of weaker materials where the slip surface can be approximated by a circle.
Ordinary Method of Slices	Applicable to nonhomogeneous slopes and $c-\phi$ soils where slip surface can be approximated by a circle. Very convenient for hand calculations. Inaccurate for effective stress analyses with high pore water pressures.
Simplified Bishop procedure	Applicable to nonhomogeneous slopes and $c-\phi$ soils where slip surface can be approximated by a circle. More accurate than Ordinary Method of Slices, especially for analyses with high pore water pressures. Calculations feasible by hand or spreadsheet.
Force Equilibrium procedures (Lowe and Karafiath's side force assumption recommended)	Applicable to virtually all slope geometries and soil profiles. The only procedures suitable for hand calculations with noncircular slip surfaces. Less accurate than complete equilibrium procedures and results are sensitive to assumed inclinations for inter-slice forces.
Spencer's procedure	An accurate procedure applicable to virtually all slope geometries and soil profiles. The simplest complete equilibrium procedure for computing the factor of safety
Morgenstern and Price's procedure	An accurate procedure applicable to virtually all slope geometries and soil profiles. Rigorous, well-established complete equilibrium procedure.
Chen and Morgenstern's procedure	Essentially an updated Morgenstern and Price procedure. A rigorous and accurate procedure applicable to any shape of slip surface and slope geometry, loads, etc.
Sarma's procedure	An accurate procedure applicable to virtually all slope geometries and soil profiles. A convenient complete equilibrium procedure for computing the seismic coefficient required to produce a given factor of safety. Side force assumptions are difficult to implement for any but simple slopes.

2.3.4 Numerical Modeling

Conventional limit equilibrium methods of analysis are most commonly applied for surface rock engineering due to being simple to use. However, the assessment of displacement or the development of failure surface are not possible by these methods. Many rock slope stability problems involve complexities relating to geometry, material anisotropy, non-linear behavior, in-situ stresses and the presence of several coupled processes (e.g. pore pressures, seismic loading, etc.) (Sjöberg, 1999). Therefore, in order to deal with complex rock slope failure processes, numerical modeling methods are used for stability analyses. Numerical modeling is considered as a very practical tool for the evaluation of complex failure mechanisms with respect to several proposed reasons by Lorig and Varona (2004):

- Numerical analysis can be utilized to assess several possibilities of geological models, failure modes and design options.
- Numerical models can be extrapolated outside their databases when compared with empirical methods.
- Comprehensive and accurate information about key geological features and better understanding of behavior of slopes can be gained by numerical models compared to analytical approaches.

The rock mass is divided into elements in numerical modeling. Stress-strain relation and material properties are assigned for each element. The elements are then connected in a model depends on specific factors of the problem. Jing and Hudson (2002) suggested several approaches for numerical methods:

- Continuum modeling – finite difference method (FDM), the finite element method (FEM) and the boundary element method (BEM)
- Discontinuum modeling – the discrete element method (DEM)
- Hybrid continuum/discrete modeling

Continuum modeling

In continuum modeling, material of the body is assumed as continuous. Although all large rock slopes involve discontinuities, the intact rock elastic properties and strength of discontinuities are reduced to the rock mass to be represented as a continuum. The rock mass is divided into zones or elements in numerical models and material properties which are stress-strain relations describing the material behavior are assigned to each element (Stead *et al.*, 2001). Linear elastic-perfectly plastic stress-strain relations which are commonly used rock mass material models are incorporated in numerical models. In order to restrict the shear strength parameters of an element, Mohr-Coulomb strength parameters are used in these models (Read and Stacey, 2009). The equivalent Mohr-Coulomb shear parameters are found by applying a failure surface tangent to the Hoek-Brown failure criterion, most widely used failure criterion for rock masses, with respect to specific confining stresses or ranges of confining stresses (Hoek, 1990a).

The continuum methods can be divided into groups depending on the way the problem is solved. There are mainly two various approaches:

- The integral (or boundary) methods; often called as the Boundary Element Method in which elements are only defined at the boundaries and can be divided into sub-methods based on types of formulations:
 - i. Fictitious stress method
 - ii. Displacement discontinuity method
 - iii. Direct integral method
- The differential methods; are normally known under the names Finite Difference Method and Finite Element Method based on different formulations in which the rock mass is divided into zones or elements.

The graphically illustrations of the continuum methods are presented in Figure 2.18.

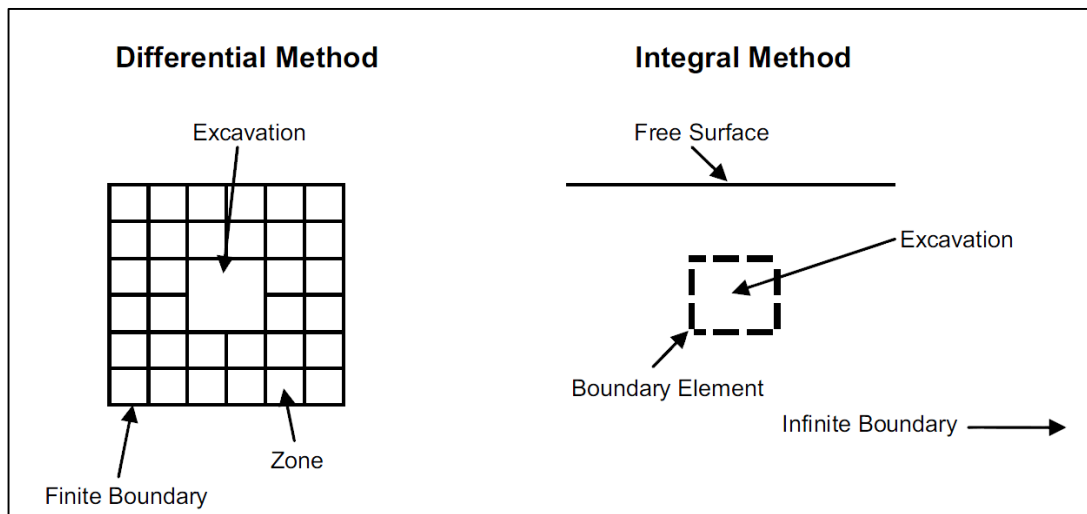


Figure 2.18 Graphical illustrations of differential and integral continuum methods
(Hoek *et al.*, 1990)

A common property of all of the continuum methods is that the model has to be discretized. The finer discretization or smaller the elements, the better the representation of the solutions of the original problem.

Boundary Element Method – Integral Methods

The method is based on the discretization of the boundaries of openings and ground surfaces. No artificial boundaries of the model have to be introduced and no boundary conditions have to be specified. This method is generally not suitable for analyzing non-elastic problems. In the method, the boundaries are divided into elements in which the stresses and displacements are relied on the order of the elements. Moreover, the stresses in the rock around the boundary is calculated using interpolation of the results from the boundary to interior points (Anon, 2011). There are three main types of formulations:

i. Fictitious stress method

The method is based on the exact solutions of stress vectors applied to an elastic body. The solution of a real problem is a procedure of finding the fictitious stresses that give the same stress field in the model as the excavation. The fictitious stresses are not used to anything else and they have no physical meaning. The method is suited for openings.

ii. Displacement discontinuity method

The displacement discontinuity method depends upon an exact solution of a relative displacement between two surfaces which means a discontinuity in displacement. The solution of a real problem is a procedure of finding the displacement discontinuity that gives the same stress field in the model as the analyzed discontinuity or excavation (Anon, 2011). The method is applicable to discontinuities such as fractures and joints.

iii. Direct integral method

The method is more generally used and it enables the direct solution for the unknown boundary displacements or stresses in terms of the specified boundary conditions (Anon, 2011). It can be used for the analysis of openings, joints and crack propagation. The key to the method is the reciprocal theorem which links the solution to two different boundary value problems for the same region. The theorem is a direct consequence of the linearity of the equilibrium equations and the generalized Hooke's law (Hibbeler, 2011).

Differential Methods

Finite Difference Method

The finite difference method is the oldest numerical modeling technique to solve the differential equations which apply the equations of motion. The rock mass is divided into interacting nodes to apply the equations including the strain-displacement relations and the stress-strain equations (Itasca, FLAC V7.00, 2011). Most commonly used explicit finite difference numerical code for geotechnical applications is FLAC

(The Fast Lagrangian Analysis of Continua). The two-dimensional program does not require any formation of matrices, unlike finite element programs and is formulated to analyze continuum problems. In the program, complicated geometries and several geological structures can be evaluated and even discontinuities are included in the form of interfaces. However, it is not appropriate to analyze the highly jointed structure by this program. Incremental velocities and displacements are derived by using the equations of motion and this constitutive relation produces new set of stresses or forces (Cundall, 1976). The equations are to be solved by using a time-marching schemes, presented in Figure 2.19.

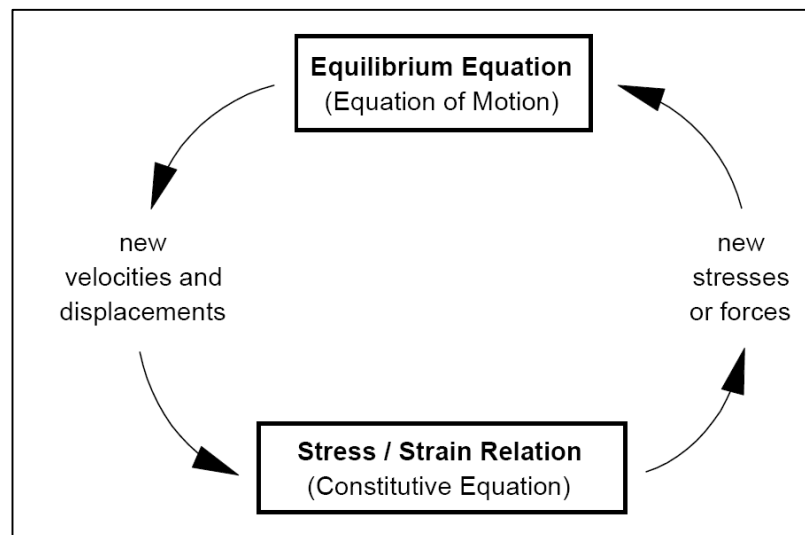


Figure 2.19 Explicit calculation cycle used in finite difference method (Itasca, 2011)

In addition to the two dimensional finite difference programs, three-dimensional code of FLAC3D (Itasca, 1997) has been developed to investigate the three-dimensional effects on slope stability. An example of a FLAC3D stability analysis including the computational mesh is presented in Figure 2.20.

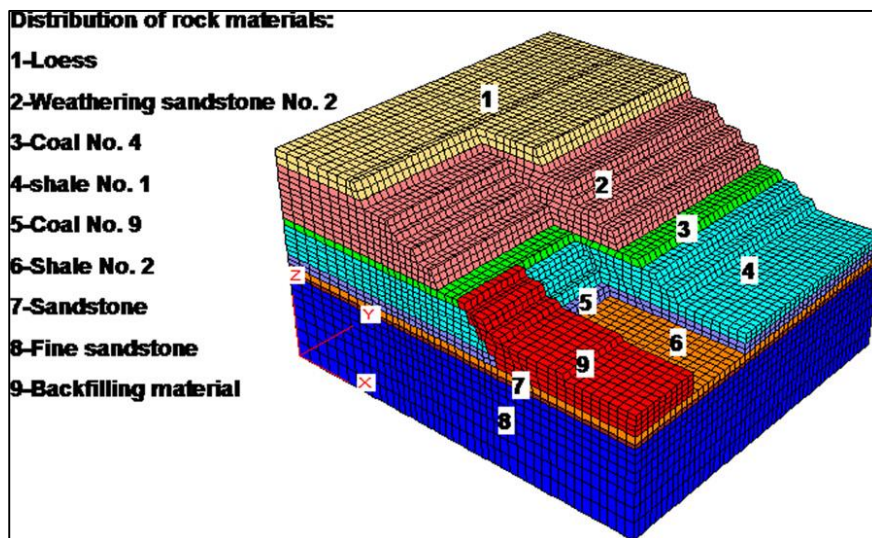


Figure 2.20 Three-dimensional finite difference model of FLAC3D showing the typical computational mesh and rock materials (He *et al.*, 2008)

Finite Element Method

Limit equilibrium methods of analysis are not generally concerned with the stress distribution in a slope above the assumed failure surface or the progressive failure due to the associated deformations. Since deformations and movements within a slope are controlled by the overall stress distribution, stress concentrations have an important influence on the initiation and growth of the failure surface. Therefore, information about stress and displacement distribution within the slopes can be analyzed by using the finite element method. Clough and Woodward (1967) firstly introduced the method for geotechnical engineering applications. Widely use of finite element method for slope stability analysis has developed further accuracy and reliability in the method.

The method can be considered as an alternative to limit equilibrium method for the evaluation of stability of slopes since the same input parameters are sufficient to be incorporated in finite element method to assess the slope stability. However, Griffiths and Lane (1999) presented the advantages of finite element method over conventional limit equilibrium methods for stability analysis:

- There is no need to assume about the shape and location of the failure surface because the failure occurs inherently along the zones in which the shear strength of the rock mass does not sustain the applied shear stresses.
- Division of the rock mass into slices is not needed and assumption of the slice side forces are not required.
- The method provides results about the deformations at working stress levels.

In the method, continua is divided into finite number of elements and the elements are connected to the nodes. The material properties are assigned to each element by concerning the stress strain relationship that describing the material behavior (Duncan, 1996). Such term definition used for finite element method and mesh generation for a rock slope are presented in Figure 2.21.

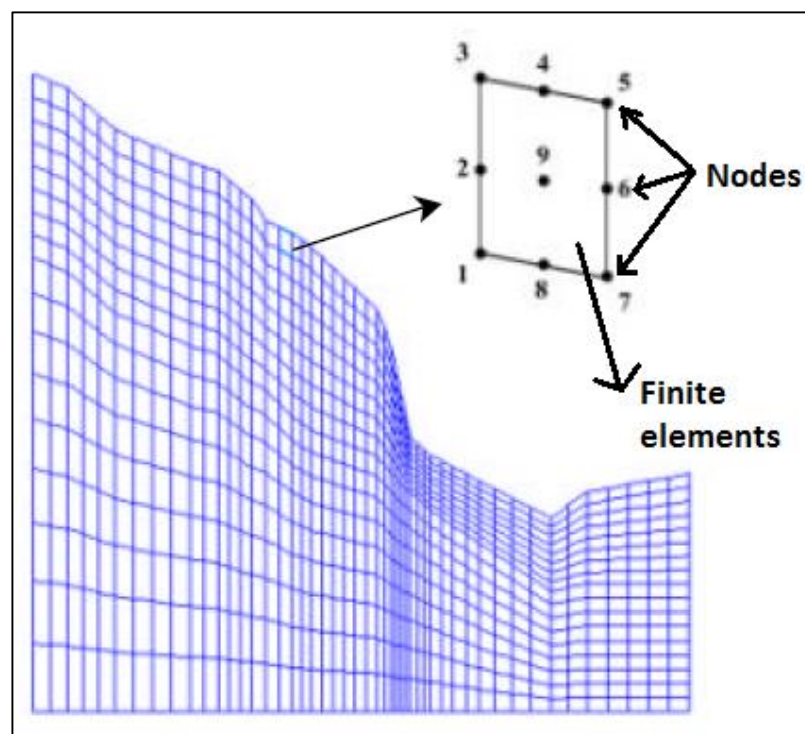


Figure 2.21 Terms used in finite element method and mesh generation using 9-noded elements (Eberhardt, 2003)

Various two and three dimensional finite element programs are available based on the implicit methods that use equations of equilibrium. The systems of equations are solved in matrix form (Wyllie and Mah, 2004). An example of two dimensional finite element coded program used for slope stability analysis is Phase² (Rocscience Inc., 2014). Besides, three-dimensional finite element code of RS³ (Rocscience, 2014) has been developed to investigate the three-dimensional influence on slope stability.

Shear Strength Reduction Method

In limit equilibrium method, factor of safety (FOS) is calculated in a straightforward manner by comparing resisting forces with driving forces. The shear strength reduction (SSR) method, however, can be used an alternative to limit equilibrium technique to determine FOS for stability of slopes by using finite element or finite difference program. The term strength reduction factor (SRF) is used instead of FOS that have the same meaning in principal. The FOS for both two and three dimensional slopes that is the ratio of rock/soil actual shear strength to the reduced shear strength at collapse is calculated by reducing the shear strength until failure occurs (Dawson *et al.*, 1999). In fact, Mohr-Coulomb shear strength parameters that are cohesion (c) and internal friction angle (ϕ) are reduced until the stability condition cannot be sustained. There are numerous advantages of shear strength reduction method over the limit equilibrium methods for slope stability analyses. First, the method does not require any assumption on the shape and location of failure surface. The critical failure surface is found automatically that the failure naturally takes place along the zones of the rock mass where shear strength of the rock mass yields against the shear stresses (Griffiths and Lane, 1999). Moreover, there is no any assumption on the inter-slice force distribution, location or inclinations. Translational and rotational equilibrium are both satisfied in the method. Secondly, the method is appropriate to be utilized for the complex progressive failure modes and can calculate the deformations or movements. Additionally, displacement controlled ground-structure interaction can be included by shear strength reduction method (Diederichs *et al.*, 2007).

The main disadvantage of the method is the long running time to perform the stability analysis and well trained users are required to conduct the analyses. However, with the advanced developments in the computer applications, computation time has become within the allowable time span for the both two and three dimensional design analyses. A continuum modeling approach of the method depends upon the conducted geotechnical program whether finite element or finite difference method based. Model convergence or predefined displacement limits at points of interest are considered as an indicator of stability equilibrium by analyzing the discretized zone in finite element or finite difference continuum models (Diederichs *et al.*, 2007). For finite difference continuum model, FLAC (Itasca, 2011) solves the sets of equations by utilizing the dynamic relaxation and the stability equilibrium is obtained in case a minimum tolerance has been achieved by the unbalanced forces (Dawson *et al.*, 1999). An example of the shear strength reduction method in finite difference program by considering the unbalanced forces as a stability indicator is presented in Figure 2.22.

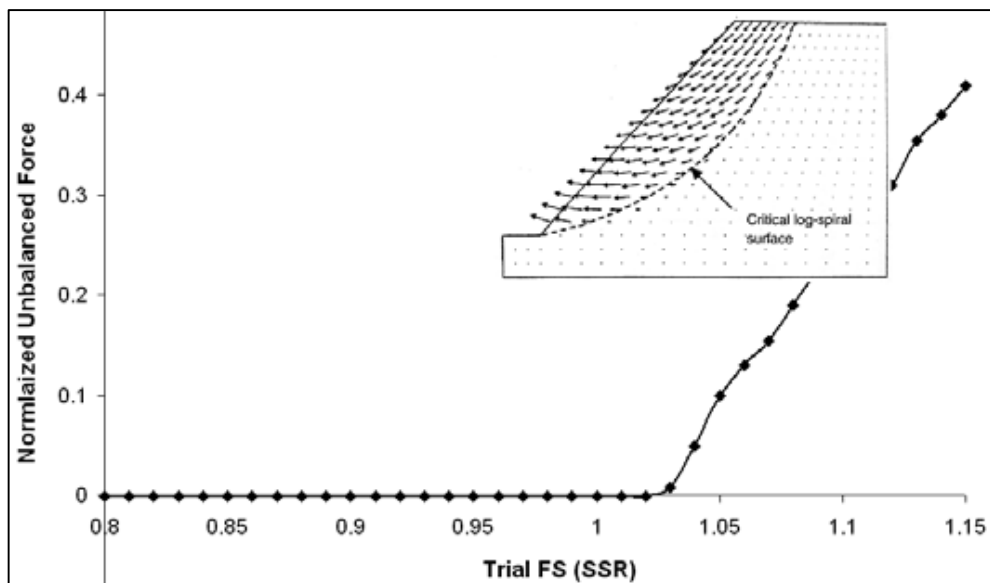


Figure 2.22 SSR conducted in finite difference analysis considering the unbalanced forces as stability indicator (Dawson *et al.*, 1999)

For SSR conducted in finite element continuum analysis, for instance Phase² (Rocscience Inc., 2014), model convergence is used as a stability indicator. Rapid increase in the displacements at any point in the model indicates the non-convergence and the slope is considered as unstable state. The convergence approach example is illustrated in Figure 2.23.

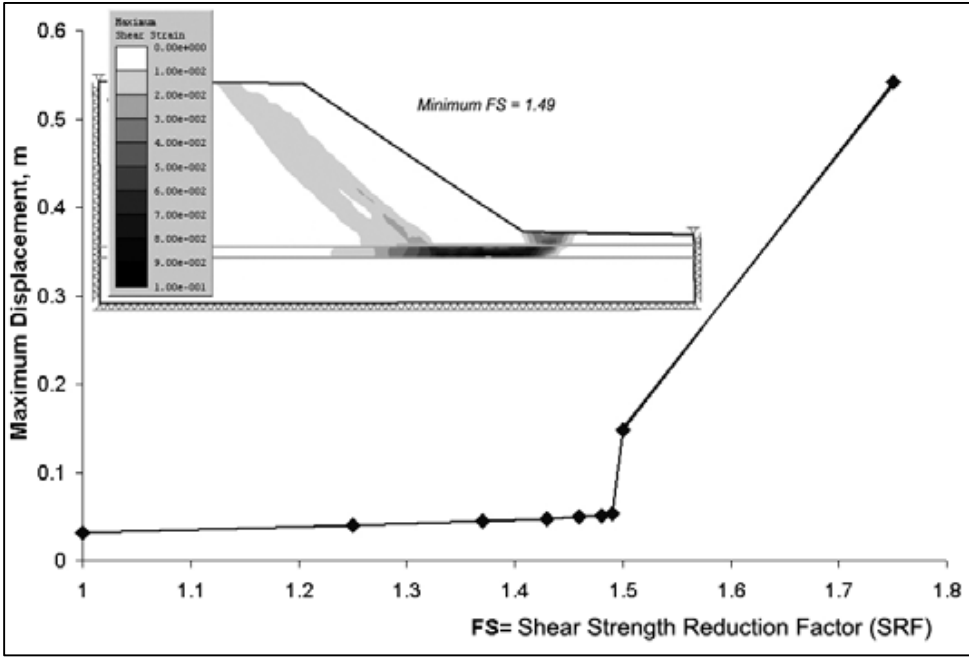


Figure 2.23 Convergence approach of SSR analysis for finite element method (Dawson *et al.*, 1999)

The strength reduction method was firstly used by (Zienkiewicz *et al.*, 1975) to investigate that the effects of associated and non-associated plasticity on the two dimensional composite embankment stability analysis. Accuracy of conventional limit analyses results and the development of failure was studied by Naylor (1981). Furthermore, Donald and Giam (1988) applied strength reduction method by using the nodal displacement to evaluate the failure state. The researchers pointed out that it is required to plot the displacement curves for the nodes in the failure region and investigated the factors that affect the FOS such as tolerance for nonlinear analysis, element type and size of the discretized mesh. Matsui and San (1992) assessed the

slope failure using the shear strength reduction technique in terms of shear strain failure criterion. A comparison of limit equilibrium methods and strength reduction method was conducted by Griffiths and Lane (1999) and stated that Mohr-Coulomb criterion is a reliable and efficient approach to determine FOS in those techniques and also indicated that strength reduction method may be used as an alternative to limit equilibrium methods. Accuracy of the SSR was evaluated by means of various slope angles, friction angles and pore pressure coefficients by Dawson *et al.*, (1999). FOS values were determined using the finite difference coded FLAC software considering the convergence criterion. The researchers pointed out that in case the finer mesh is used for the numerical solution, the obtained FOS difference decreases between SSR and limit analysis method. Ugai (1989) studied a two dimensional SSR method to compare the FOS results with limit equilibrium methods considering the corresponding critical failure surface for homogeneous slopes. The researcher stated that the method can be applied to nonhomogeneous slopes and the slopes reinforced using geosynthetics. The two dimensional approach of Ugai (1989) was extended to a three dimensional case comparing the SSR results with rigorous limit equilibrium methods for vertical cuts by Ugai and Leshchinsky (1995). The researchers indicated that 3-D analysis is well agreed with the conventional methods with respect to pseudo-static cases.

Discontinuum Modeling

When the rock slope including several sets of discontinuities which governs the failure mechanism with the combination of intact rock deformation, discontinuum modeling can be considered as an appropriate approach (Stead *et al.*, 2006). In the modeling method, discontinua (such as jointed rock mass) is composed of an assemblage of rigid or deformable discrete blocks and the media is subjected to either static or dynamic loading. In fact, the discontinuum modeling treats the jointed rock mass media as an assemblage of distinct, interacting bodies or blocks subjected to external loads to sustain significant motion with time (Eberhardt, 2003). In the method, large or finite

displacements or rotation of blocks are allowed and block kinematics is considered by recognizing the new contacts automatically during the system continues.

The two most commonly used principal elements are:

- The distinct element method and
- Discontinuous deformation analysis.

The distinct element method was developed by Cundall (1971) and enhanced the applications by Hart (1993) to point out the capabilities of the method and the importance in the design calculations for jointed rock. The method depends on force-displacement law which is used to determine the interaction between the deformable rock blocks regarding the Newton's second law of motion. The discontinuities are considered as interfaces between blocks and continuum behavior is assumed in the deformable blocks. Explicit time marching scheme is used to conduct the stability analysis for a problem in which dynamic equations of motion are considered for the calculations. In the cycle, contact forces are derived from known displacement by the application of a force-displacement law at all contacts and new velocities and displacements are derived from known forces acting on by the application of equations of motion (Itasca, 2004). The most widely used two dimensional distinct element code is UDEC (Itasca, 2004) that considers a plane-stain state for rock slope analysis including progressive failure in civil and mining engineering applications. Equivalent three dimensional distinct element code is 3DEC (Itasca, 2007) that is also applicable to model block medium by assuming deformable or rigid blocks.

The discontinuous deformation analysis (DDA) that was firstly suggested by Goodman and Shi (1985) to model the discontinuous rock mass in terms of rockslides and rock falls. In the analysis, jointed rock mass is considered as the assembly of discrete block similar with distinct element method. On the other hand, the main difference between those methods is that DDA uses implicit algorithm to solve displacements as unknowns, though explicit algorithm scheme is used for distinct element method. Moreover, DDA method is like finite element method in the manner

that the formulation solves a finite element mesh type in which each element represents an isolated block bounded by discontinuities. However, in distinct element method the deformation of blocks is incorporated by discretizing each block with finite difference mesh (Eberhardt, 2003).

Comparison of Continuum versus Discontinuum modeling

With the developments in geotechnical rock engineering, continuum and discontinuum modeling has become widely in use for stability analyses. It is significant to decide an appropriate method by considering the advantages and limitations of each approach. A comparison of continuum and discontinuum modeling are presented in Table 2.5.

Table 2.5 Comparison of continuum and discontinuum modeling techniques with advantages and limitations (Coggan *et al.*, 1998)

Analysis Method	Critical Input Parameters	Advantages	Limitations
Continuum Modeling (e.g., finite element, finite difference methods)	Representative slope geometry; constitutive criteria (e.g., elastic, elasto-plastic, creep, etc.); groundwater characteristics; shear strength of surfaces; in situ stress state	Allows for material deformation and failure. Can model complex behavior and mechanisms. Capability of 3-D modeling. Can model effects of groundwater and pore pressure. Able to assess effects of parameter variations on instability. Recent advances in computing hardware allow complex models to be solved on PC's with reasonable run times. Can incorporate creep deformation and dynamic analysis.	Users must be well trained, experienced and observe good modeling practice. Need to be aware of model/software limitations (e.g., boundary effects, mesh aspect ratios, symmetry, hardware memory restrictions). Availability of input data generally poor. Required input parameters not routinely measured. Inability to model effects of highly jointed rock. Can be difficult to perform sensitivity analysis due to run time constraints.
Discontinuum Modeling (e.g., distinct element, discrete element methods)	Representative slope and discontinuity geometry; intact constitutive criteria; discontinuity stiffness and shear strength; groundwater characteristics; in situ stress state.	Allows for block deformation and movement of blocks relative to each other. Can model complex behavior and mechanisms (combined material and discontinuity behavior coupled with hydro-mechanical and dynamic analysis). Able to assess effects of parameter variations on instability.	As above, experienced user required to observe good modeling practice. General limitations similar to those listed above. Need to be aware of scale effects. Need to simulate representative discontinuity geometry (spacing, persistence, etc.). Limited data on joint properties available.

For the slopes composed of massive, intact rock, weak rocks and soil-like or heavily fractured rock masses, the use of continuum modeling is more efficient technique (Stead *et al.*, 2001). However, for blocky medium, it is not proper to utilize continuum modeling. Most widely used continuum approaches for rock slope stability applications are finite element methods (Phase², RS³ software) and finite difference methods (FLAC, FLAC3D software).

Discontinuum modeling is more appropriate for the moderately jointed rock medium when it is difficult to model discontinuities and fractures in a continuum model. Failure through opening/closure of discontinuities that are controlled by the joint normal and shear stiffness are included in discontinuum modeling (Stead *et al.*, 2001). It is significant to gather the data about rigorous characterization of rock mass such as discontinuity orientation, block size, joint persistence and spacing which are required to conduct discontinuum modeling.

Two-dimensional versus three-dimensional analysis

It is significant to choose a model whether two dimensional or three dimensional to conduct numerical stability analysis. Most of the slope design analyses are utilized with two dimensional modeling by considering the plane strain conditions. However, with the advances in computer technology, three dimensional stability analysis have become more commonly used since 2003. Many factors such as time requirement for simulation, critical parameters, field conditions or computer configuration have a crucial aspect to decide the dimension of a model. In practice, safe slope angle depends on the radius of curvature for open pit mining (Diering and Stacey, 1987). Therefore, three dimensional complex structures or stress conditions of mining problems can be investigated with three dimensional analysis in an efficient manner by increasing the accuracy. Lorig and Varona (2004) suggested such conditions to apply three dimensional analysis:

- The direction of principal geological structures does not strike within 20-30° of the strike of the slope.
- The material anisotropy axis should not strike within 20-30° of the slope.
- The directions of principal stresses are neither parallel nor perpendicular to the slope.
- The geomechanical unit distribution differs through the strike of the slope.
- The slope geometry in plan cannot be represented by two dimensional analysis, which assumes axisymmetric or plane strain.

The curvature characteristic of open pit slopes are neglected in two dimensional methods, though it has a significant influence on safe slope angle, presented in Figure 2.24.

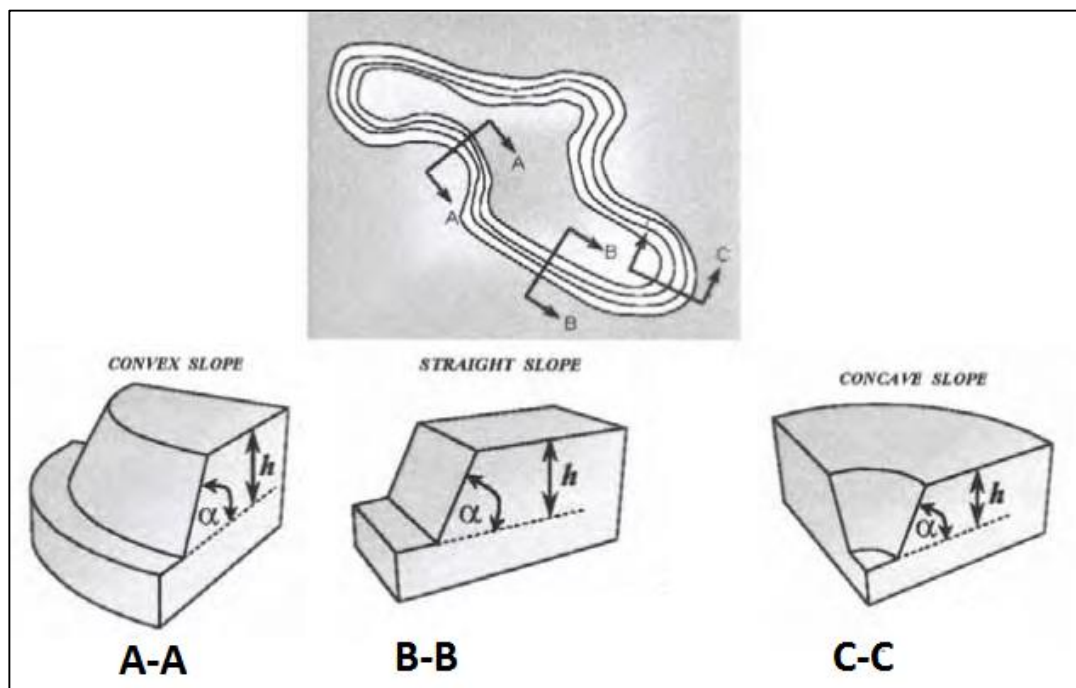


Figure 2.24 Influence of plan geometry for stability of a slope

A numerous stability analyses were carried out using FLAC3D software on concave and convex slopes with assuming 500 m height and 45° face angle in a dry condition

to evaluate the curvature effect for instability by Lorig and Varona (2004). As a result, the researchers pointed out that FOS is inversely proportional with the radius of curvature. In fact, when the radius of curvature is decreased, FOS is always getting higher. Moreover, they stated that two dimensional slopes are more tend to be unstable than concave and convex slopes. All statements can be considered as valid providing that slopes are massive, continuous or with relatively short joint trace lengths.

2.3.5 Comparison of Limit Equilibrium Methods and Numerical Modeling

In geotechnical and rock engineering, limit equilibrium methods are most commonly used for stability analyses. However, for complex mechanisms or model geometries, numerical modeling may be more appropriate to analyze the stability of a slope due to considering the instability mechanism or in situ stress state. A general comparison of numerical modeling and limit equilibrium methods was conducted by Lorig & Varona (2004), presented in Table 2.6.

Table 2.6 Summary of differences of numerical modeling and limit equilibrium methods (Wyllie and Mah, 2004)

Analysis result	Numerical solution	Limit Equilibrium
Equilibrium	Satisfied everywhere	Satisfied only for specific objects, such as slices
Stresses	Computed everywhere using field equations	Computed approximately on certain surfaces
Deformation failure	Part of the solution; yield condition satisfied everywhere; slide surfaces develop “automatically” as conditions dictate	Not considered; failure allowed only on certain pre-defined surfaces; no check on yield condition elsewhere
Kinematics	The “mechanisms” that develop satisfy kinematic constraints	A single kinematic condition is specified according to the particular geologic conditions

Numerical modeling has various advantages over limit equilibrium methods:

- No assumption is needed for location of the failure surface, critical failure surface is formed automatically in any shape in which the shear strength of the rock mass yields.
- Complex mechanisms can be analyzed.
- Stresses, deformations or movements can be calculated.
- Kinematical conditions that are translational and rotational equilibrium are satisfied.

The main drawback of the numerical modeling is to take longer time to compute the analysis and set up the model, although numerous of FOS values are calculated about instantly in limit equilibrium methods. Moreover, qualified analyst is required to assess the continuum mechanics of the problem and the instability progress since the related software are not easy to conduct analysis.

A comparison of numerical modeling and limit equilibrium methods was performed to verify the results of slope stability programs by Hammah *et al.*, (2005). The researchers, conducted analyses on several slope cases and pointed out that such conditions are necessary to determine similar FOS values with those methods:

- Same Young's/rock mass modulus must be used for the materials in a multiple-material model.
- A single valid Poisson's ratio must be assumed for the materials.
- Assume a dilation angle as zero.
- For post-peak behavior, elastic-perfectly plastic constitutive models must be used.

2.4 Summary of Literature Review

In the literature review, rock slope design terms in open pit mining are introduced and discussed. Several modes of slope failure mechanisms that are controlled by the geological structure and the stress conditions of the rock mass are described in detail. Moreover, currently used rock slope design methods are introduced and discussed. In order to determine and predict the time span of failure, those design techniques are being conducted. Therefore, conventional methods and numerical modeling used in rock slope engineering are mentioned and compared. Kinematic analysis is considered as a practical tool for investigating the possible structurally controlled modes of failure such as planar, wedge and toppling failures by means of stereographic projection. However, it is proper to use kinematical approach as a preliminary design method in order to eliminate the stable slopes for the analyses being conducted further. Within the scope of this study, kinematic analysis is not included since any dominating discontinuity set cannot be observed during the fieldwork investigations due to the complex matrix of the rock mass in the mine sites. Empirical design charts that are also significant preliminary guide for slope design applications can be efficient way to extend the database with numerous stability cases. The most widely used conventional slope stability analysis and design approach is considered as limit equilibrium methods depending on the force and moment equilibrium conditions. Conducting the method, factor of safety which is an indicator of instability can be calculated and assessed. To determine the FOS value, method of slices techniques are utilized that relies on different assumptions and equilibrium conditions. Due to being simple to use and quick estimation, conventional rock slope analysis and design methods are commonly applied for surface rock engineering. However, continuum and discontinuum numerical modeling can be used for more detailed analyses. Complex failure mechanism and large scale progressive failures are performed and evaluated with the numerical analysis methods by considering the stress-strain relations, displacements, deformations and movements. Although numerical modeling has several advantages over limit equilibrium methods, combined use of both methods is a more powerful and practical way to optimize the overall slope stability by increasing the reliability and

accuracy (Stead *et al.*, 2006). Additionally, it is significant to decide the model of stability analysis to be whether in two dimensional or three dimensional. Due to the recent advances in computer applications, three dimensional stability analysis has occupied an important place on rock slope and geotechnical engineering. Though the complex structures and stress conditions are in three dimensional in mining problems, most of the design analyses are simplified the assumptions to model in two dimensional plane strain condition. Therefore, it is essential for a rock slope engineer or an analyst to apply a proper and accurate analysis type for stability and design purposes. However, in the research, two dimensional stability analyses were considered as proper way to determine the optimized safe overall slope angle for open pit slopes. For the further detailed slope stability assessment, three dimensional stability analysis can be conducted to verify and supplement the analysis results in 2D by increasing the accuracy and reliability.

CHAPTER 3

GENERAL INFORMATION ABOUT THE STUDY AREA AND GEOTECHNICAL STUDIES

3.1 Research Area

The mine site in Bizmişen region is located around Kemaliye district of Erzincan province in eastern Turkey. The mine site is owned by BİLFER Mining Corp. and currently in the area there is not any mining activities. The location map of the region is shown in Figure 3.1.

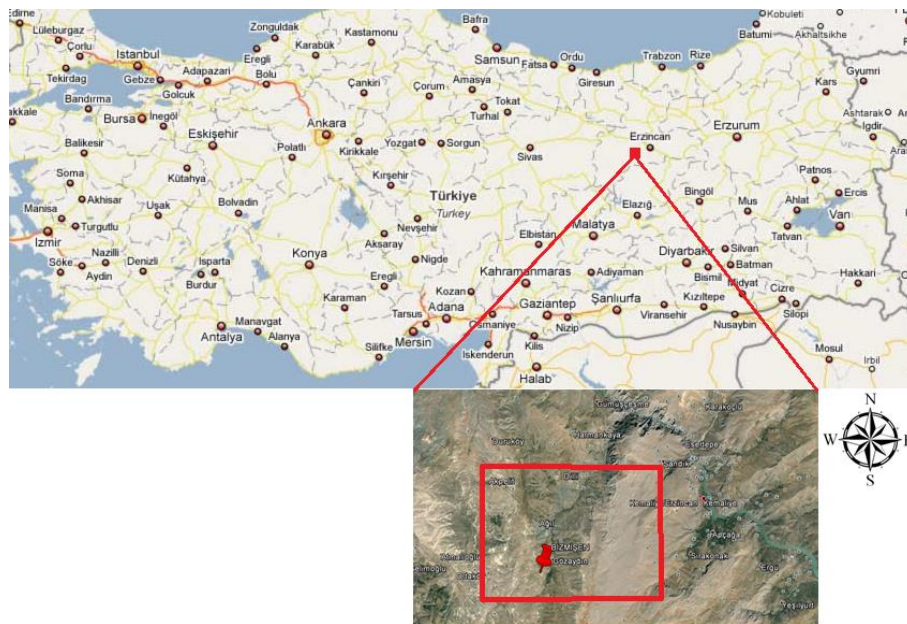


Figure 3.1 Location map of Bizmişen (Erzincan) region (Google Earth, 2015)

In Bizmişen area, 95 drilling operations total length of which is almost 12 km have been conducted by Mineral Research and Exploration Institute (MTA) since 1963. Besides, BİLFER Corp. has carried those working a step further with 83 more exploration drillings, total length of the drillings approximately is 14 km. Iron (Fe), Sulphur (S) and silica (SiO₂) grades were determined by MTA. On the other hand, only iron (Fe) and copper (Cu) grades were reported on the workings of BİLFER Corp. The mine administration is planning to operate open pit mines in four sectors which are Dönentaş, Taştepe, Ayşe Ocağı and Orta Ocak, that settle in the northwest, northeast and south of the region respectively (Figure 3.2).

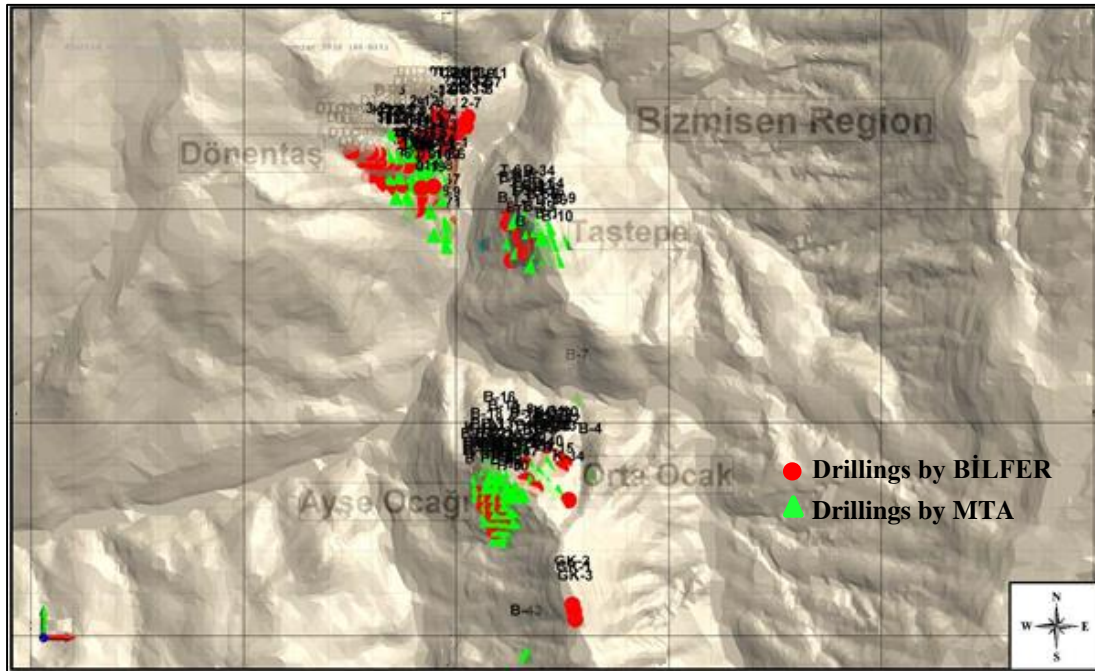


Figure 3.2 Plan view of the location of drilling operations in Bizmişen region

3.2 General Geology of the Area

The mine site settles in the south of Ankara-Erzincan suture zone and north of the Toros block according to the studies about tectonic units of Turkey by Durand *et al.*, (1999), shown in Figure 3.3.

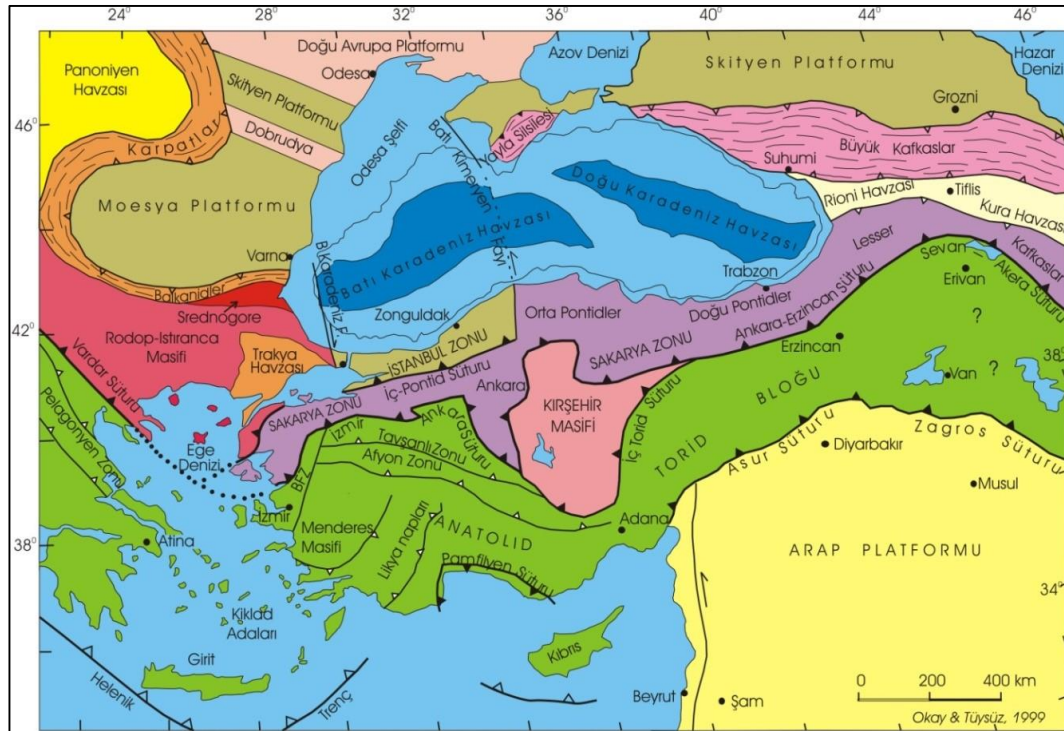


Figure 3.3 Tectonic units of Turkey (Durand *et al.*, 1999)

The oldest formation around the region is carboniferous-campanian aged Munzur limestone embedded as blocks in serpentines. Granite rock formations are covered incompatibly by sedimentary rocks with nummulites. In the region, this formation is abducted by Oligocene-Upper Miocene including various local inconsistencies. Plio-anthropogene, aged terrestrial sediments are the youngest rock formation (Özgül, *et al.*, 1981).

The tectonic subgrade of the region is composed of lower carboniferous-campanian aged Munzur limestone and aged ophiolite rocks consisting of intense serpentized perioditic rocks. In the upper layer, aged maastrichtian is incompatibly involved. Paleocene aged granitic rocks possibly interrupt these formations. Mineralization and granitic rocks are nonconformably covered by Neogene aged formation consisting of partly limestone. The youngest formations around the region are anthropogene aged

slope debris and alluviums. The tectonic stratigraphic sequencing in Bizmişen iron mineralization field is shown in Figure 3.4 (Yıldırım and Hamarat, 1985).

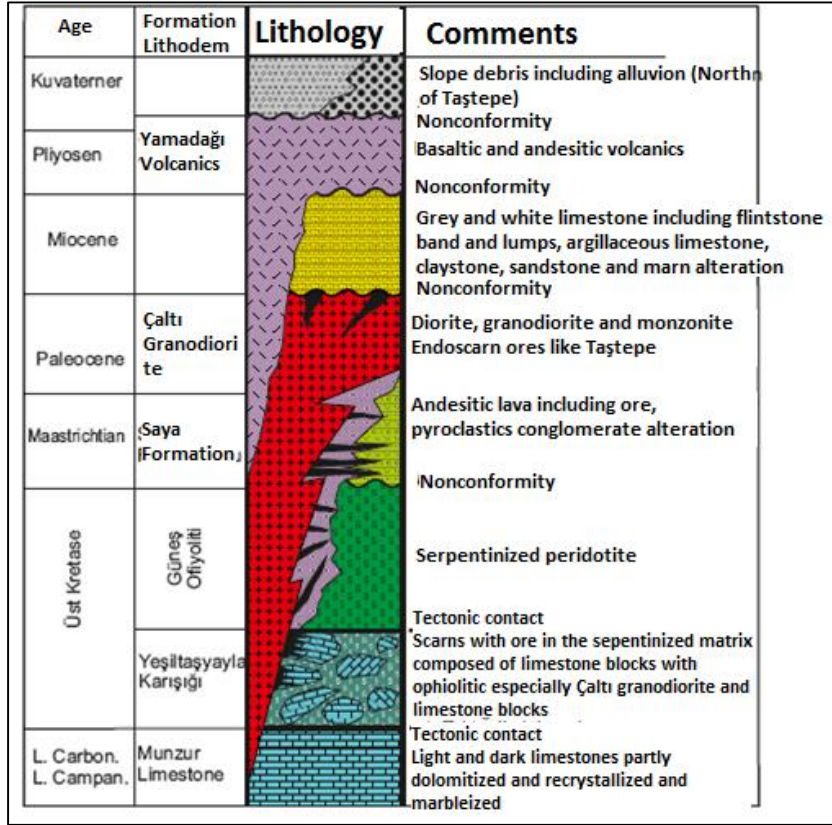


Figure 3.4 Generalized tectonostratigraphic column cross-section of the Bizmişen region (Yıldırım and Hamarat, 1985)

3.3 Geotechnical Site Characterization

On the purpose of geological and geotechnical survey, technical field trips to the mine site in Kemaliye-Bizmişen region were arranged. To determine the quality of the rock mass, fieldwork and geotechnical core logging were also conducted. Additionally, in order to determine the physico-mechanical properties of the rock materials, core samples from the logged drillholes and rock blocks were taken directly from the mine site.

3.3.1 Geotechnical Survey

In the region, according to the reserve evaluation studies, four open pit mines will be operated for different ore bodies. Thus, fieldwork for Dönentaş, Taştepe, Ayşe Ocağı and Orta Ocak sectors was carried out to gain sufficient relevant data for geotechnical assessment prior to stability analyses. Slopes in which mining activities had been operated were investigated to determine the rock mass characteristics around the mine site. Dönentaş, Taştepe, Ayşe Ocağı and Orta Ocak sectors and the locations of the drillholes are shown in Figure 3.5 and Figure 3.6.

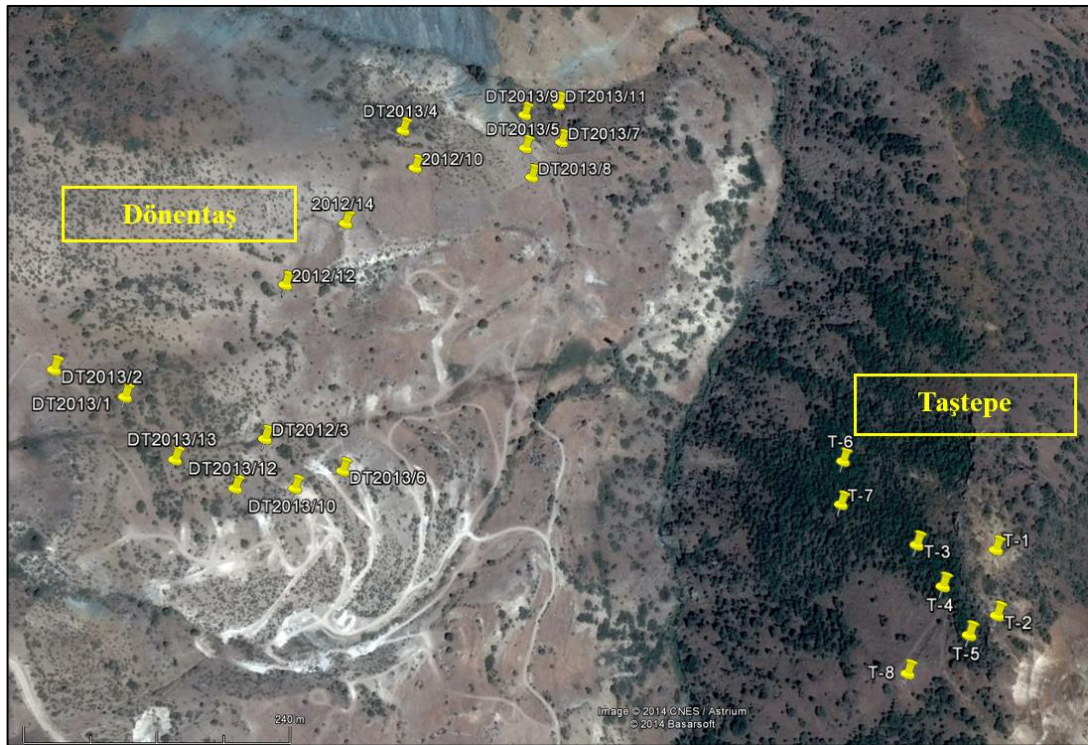


Figure 3.5 Satellite view of Dönentaş and Taştepe sectors and the drillhole locations (Karpuz, *et al.*, 2014)

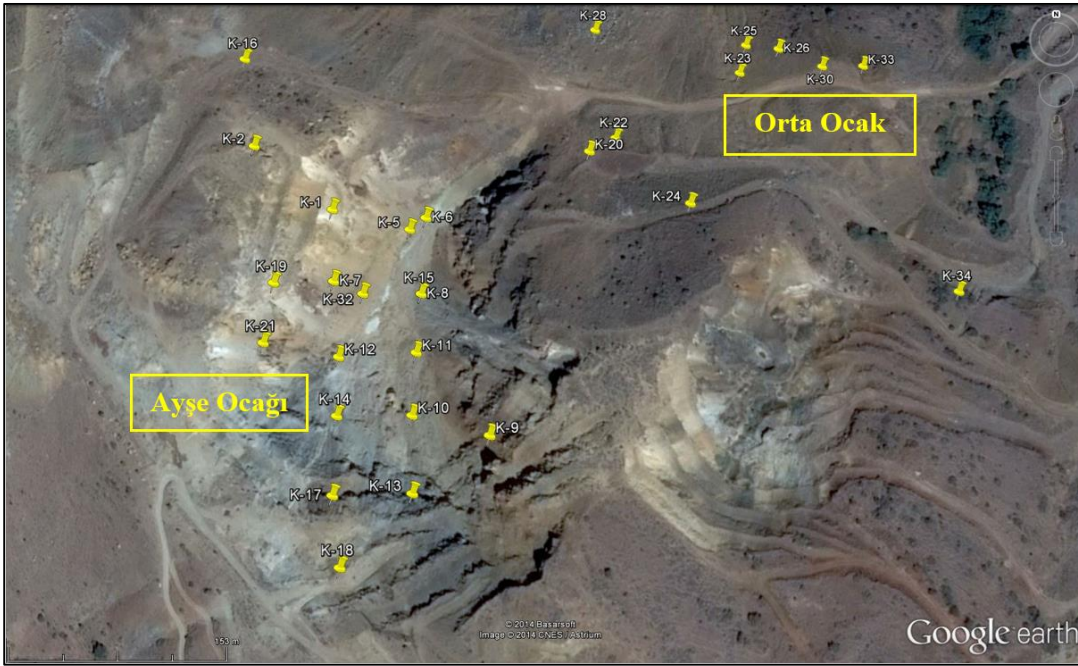


Figure 3.6 Satellite view of Ayşe Ocağı and Orta Ocak sectors and the drillhole locations (Karpuz, *et al.*, 2014)

To designate and obtain sufficient data about the rock mass properties of the region, geotechnical studies were conducted in all sectors except Dönentaş due to the lack of old available face or open pits. Geological strength index (GSI) values were assigned for the dominating lithological units from the field observations in those sectors as proposed by Hoek *et al.*, (2005). In rock engineering, it is important to gain reliable data about rock mass properties to be used as inputs into numerical analysis for designing rock constructions. The GSI system is a rock mass characterization that enables engineers to determine the rock mass properties with visual evaluation of the rock mass. Its use provides a better understanding of rock mass behavior and it enhances geologic logic and reduces rock engineering uncertainty by assisting rock mass to be explained more clearly. The GSI assessment depends upon the lithology, structure and conditions of the discontinuities of the rock mass. GSI rating is applicable mostly on the rock mass as an outcrop, tunnel surface, road cut and drill hole cores by visual observations. Its rating is determined with the combination of two parameters

which are considered as the fundamentals throughout the geological process. The parameters are the conditions of the discontinuities that governs the degree of blocky characteristics and the formation of the rock mass relying on the geological restrictions (see Appendix Figure A.1). Geotechnical investigation areas within these mining sectors are shown in Figure 3.7-Figure 3.9. The ranges of GSI values for lithological units observed in these sectors are presented in Table 3.1 and marked in Figure 3.10.

Table 3.1 Estimated GSI ratings for the lithological units in Bizmişen sectors
(Karpuz, *et al.*, 2014)

Lithological Unit	GSI
Hematite with limonite	30-40
Magnetite	60-70
Limestone	25-35
Magnetite + Hematite	55-70
Serpentinite	25-35



Figure 3.7 Investigation area in Taştepe sector (Karpuz, *et al.*, 2014)



Figure 3.8 Investigation area in Ayşe Ocağı sector (Karpuz, *et al.*, 2014)



Figure 3.9 Investigation area in Orta Ocak sector (Karpuz, *et al.*, 2014)

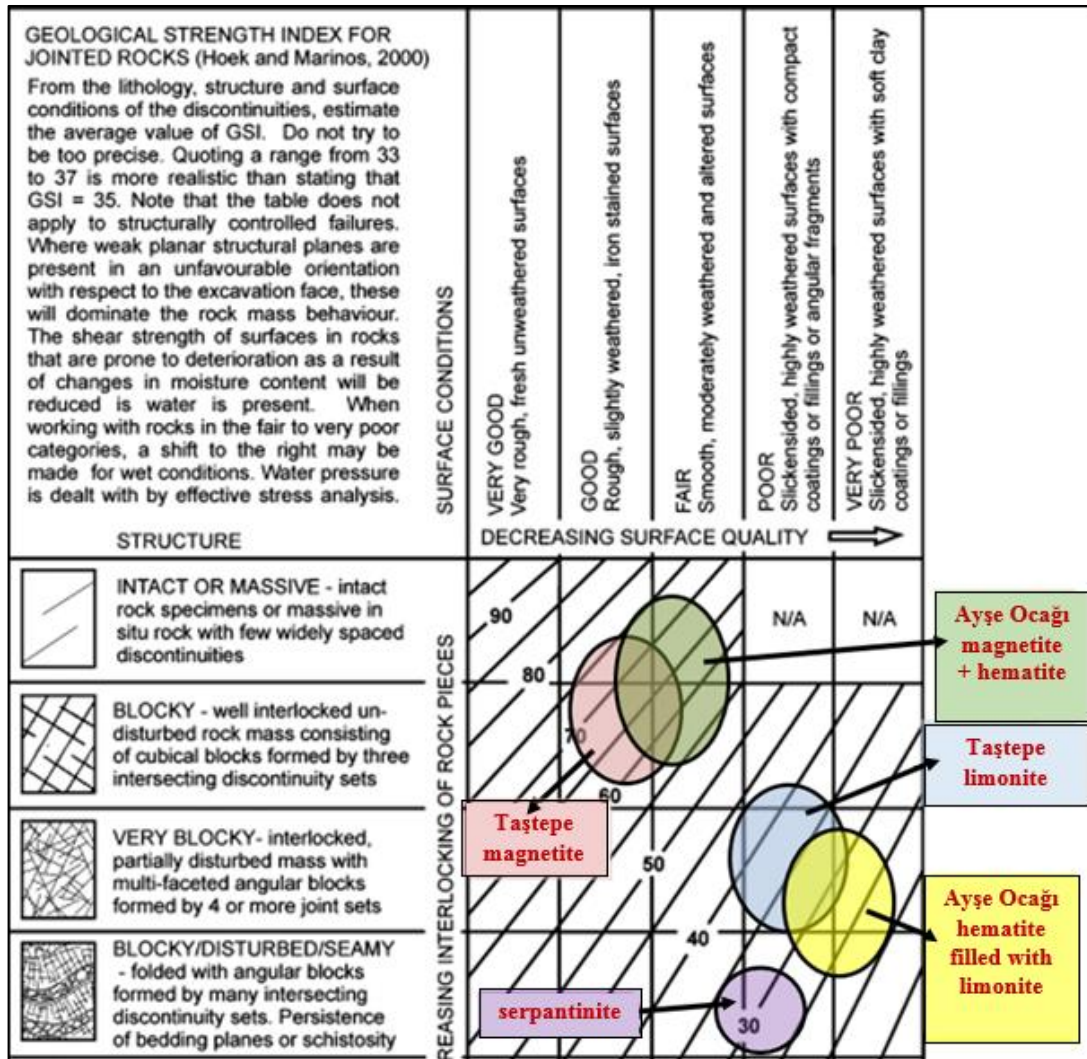


Figure 3.10 GSI ranges for the lithological units in Bizmişen sectors (Karpuz, *et al.*, 2014)

Besides field investigations, geotechnical core logging was also performed on representative exploration drillings. To increase the accuracy and reliability, as much as possible core logging was carried out and plenty of samples were taken for laboratory tests. For the core logging assessment, the geotechnical borehole data sheet was used, presented in Appendix A (Figure A.2). Geotechnical core logging were carried out on 11 exploration drillings with a total length of almost 4 km. In Dönentaş sector, 7 representative drillings were selected regarding the orebody orientation. The

codes and the depths of drillholes are DT-2011-1, DT-2011-4, DT-2011-7, DT-2012-2, DT-2012-5, DT-2013-1, DT-2013-3 and 295 m, 284 m, 306 m, 367 m, 397 m, 551 m and 363 m, respectively. Likewise, in Ayşe Ocağı sector, 4 representative exploration drillings were selected for core logging. The drillholes are named as K-6, K-12, K-15 and K-20 with a depth of 192 m, 172 m, 191 m and 170 m respectively. An example of drillhole core used in the core logging studies is shown in Figure 3.11.

To designate the rock mass quality, Rock Mass Rating (RMR_{89}) method proposed by Bieniawski (1989) and Q-system proposed by Barton *et al.*, (1974) were used to evaluate the geotechnical rock mass properties of the dominating lithological units by means of core logging. The RMR system and the required parameters are presented in Appendix A (Figure A.3). Furthermore, descriptions and ratings for the rock mass quality by using the Q-system are presented in Appendix A (Figure A.4).



Figure 3.11 An example of drillhole core in Bizmişen region (Karpuz, *et al.*, 2014)

Regarding both the data obtained from field observations and core logging, average RMR_{89} , Q and GSI ratings for the dominating lithological units were estimated, presented in Table 3.2. Therefore, rock mass properties and rock quality characterization were constituted for Bizmişen region prior to stability analyses that provides a better understanding about characteristics of rock mass behavior.

Table 3.2 Estimated rock mass properties for the lithological units in Bizmişen region

Lithology	Rock Mass Properties		
	RMR_{89}	Q	GSI
	Avg.	Avg.	Avg.
Skarnfels	48	2.57	44
Limestone	40	1.2	35
Granodiorite	60	4.28	57
Ore	55	3.22	55
Mudstone	47	1.51	48
Serpentinite	40	1.18	44

Considering both Q system and RMR method of rock mass classification, serpentinite and limestone can be classified as poor rocks, whereas granodiorite can be qualified as fair rock. Moreover, skarnfels, limestone, ore, mudstone and serpentinite can be considered as poor rocks, but granodiorite as fair rock with respect to Q-system. According to RMR method, serpentinite and limestone can be considered as poor rocks, whereas ore, skarnfels, mudstone and granodiorite can be characterized as fair rock units. An example of compiled results of core logging with evaluated parameters and lithological units is shown in Figure 3.12.

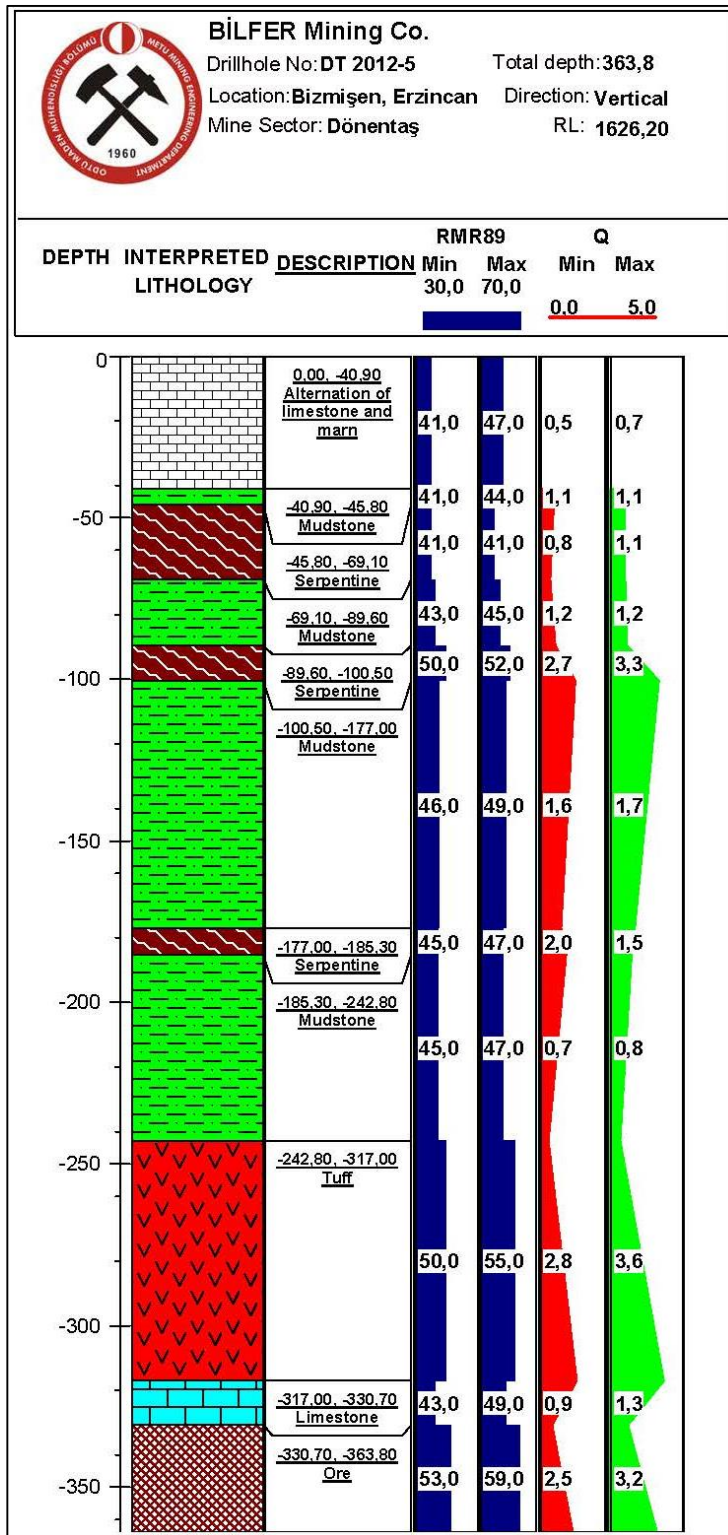


Figure 3.12 An example of compiled results of core logging with evaluated parameters and lithological units in Dönentaş sector

3.3.2 Laboratory Studies

Gaining relevant information about the properties of intact rock for prediction of rock mass, laboratory testing is significant aspect. In fact, physical and mechanical characteristics of the rock mass can be estimated using the intact rock parameters determined by means of laboratory experiments. Within this scope, representative specimens collected during the core logging and block samples were taken. The tests were conducted in Rock Mechanics Laboratory at Mining Engineering Department of METU. Prior to stability analyses, comprehensive laboratory tests with 408 rock specimens were carried out. Based on the laboratory experiment results, rock material properties were determined. Unit weight (γ), Poisson's ratio (ν), Young's modulus (E), indirect tensile strength (σ_t), uniaxial compressive strength (σ_c) and m_i constant were obtained by proper laboratory work. The number and percentage of experiments conducted are shown in Table 3.3 and Figure 3.13. Furthermore, the percentage distribution of the laboratory tests with respect to each lithology are presented in Table 3.4.

Table 3.3 Number and type of laboratory tests

Experiment Type	Number of Test
Uniaxial Compressive Strength Test	152
Static Deformability Test	90
Indirect Tensile Strength Test (Brazilian)	112
Triaxial Compression Test	54 (18 sets)
Unit Weight Determination Test	408

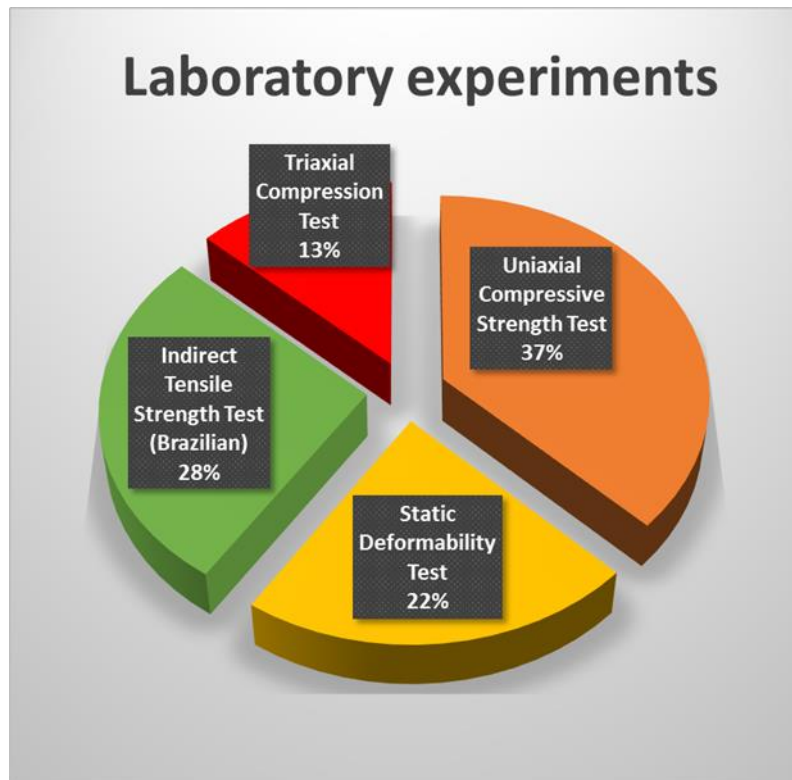


Figure 3.13 Percentage distribution of laboratory tests

Table 3.4 Percentage distribution of laboratory tests for each lithological unit

Percentage of Laboratory Tests (%)				
Lithological Unit	Triaxial Compression Test	Uniaxial Compressive Strength Test	Indirect Tensile Strength Test (Brazilian)	Static Deformability Test
Granodiorite	29	19	33	19
Skarnfels	18	31	28	23
Mudstone	16	49	16	19
Ore	19	33	27	21
Limestone	21	28	27	24
Serpentine	8	35	32	25

The rock material properties of dominating lithological units observed in the field are presented in Table 3.5.

Table 3.5 Rock material properties of dominating lithological units

Rock Material Properties					
Lithology	Unit Weight, γ (kN/m³)	Poisson's Ratio, ν	Elastic Modulus, E (GPa)	Indirect Tensile Strength, σ_t (MPa)	Uniaxial Compressive Strength, σ_c (MPa)
	Avg \pm Std	Avg \pm Std	Avg \pm Std	Avg \pm Std	Avg \pm Std
Skarnfels	26.51 \pm 2.62	0.10 \pm 0.04	12.19 \pm 7.04	7.77 \pm 5.05	35.2 \pm 23.0
Limestone	26.15 \pm 0.94	0.16 \pm 0.05	24.54 \pm 7.05	7.10 \pm 4.55	48.8 \pm 18.8
Granodiorite	26.90 \pm 0.44	0.08 \pm 0.02	36.05 \pm 4.37	13.19 \pm 2.50	123.9 \pm 56.9
Ore	39.48 \pm 2.31	0.05 \pm 0.03	26.68 \pm 4.56	14.30 \pm 4.98	58.3 \pm 23.5
Mudstone	25.65 \pm 0.85	0.13 \pm 0.07	7.54 \pm 5.70	2.25 \pm 0.91	16.9 \pm 12.7
Serpentinite	24.01 \pm 1.99	0.15 \pm 0.11	8.08 \pm 6.73	4.67 \pm 4.29	17.1 \pm 14.5

According to the results of the laboratory test results, strength of both ore and limestone can be classified as hard rock and skarnfels as medium rock, on the other hand, serpentine and mudstone units can be considered as weak rock.

Uniaxial Compression Testing

In mining and civil engineering purposes, Uniaxial Compression Testing (UCS) is most frequently used laboratory experiment. The test is intended to measure the uniaxial compressive strength of a rock sample. A cylindrical or prismatic with regular geometry rock specimen is loaded axially without any confining pressure until failure. The length (L) to diameter (D) ratio (L/D) of 2:1 is required for compressive strength tests. ASTM D2938-79 testing standards was used for Uniaxial Compression Tests. An example of UCS test illustration is presented in Figure 3.14.



Figure 3.14 Illustration of UCS test

Static Deformability Test

The aim of this test is to determine the stress-strain curves, Young's modulus (E) and Poisson's ratio (ν). ASTM D3148-02 testing standards was used for Static Deformability Tests. The test set up and used equipment are shown in Figure 3.15.



Figure 3.15 Illustration of Static Deformability Test

Indirect Tensile Strength Test (Brazilian)

Tensile strength of the intact rock is supposed to be determined in order to gain information about the strength of rock specimen. The aim of the test is to measure the uniaxial tensile strength of rock specimen indirectly. The test sample should be circular having a thickness to diameter ratio (t/D) between 0.2-0.75. ASTM D3967-81 testing standards was used for indirect tensile strength test. An example of the test is shown in Figure 3.16.



Figure 3.16 Illustration of indirect tensile strength test

Triaxial Compression Test

The test is intended to determine the strength of a cylindrical rock sample under triaxial compression and to determine the internal friction angle (ϕ) and cohesion (c). The confining pressure is applied by means of oil inside the testing rig. As a brief procedure, the specimen is loaded both axially and laterally until a specific point. When the point is reached this point, the sample is loaded only axially until failure

occurs. ASTM D2664-80 testing standards were used for triaxial compression tests. The test set up is presented in Figure 3.17.



Figure 3.17 Illustration of triaxial compression test

3.4 Rock Mass Design Parameters for Stability Analyses

Rock mass and material properties were determined by means of both geotechnical field survey and laboratory tests prior to stability analyses. Generalized Hoek-Brown failure criterion and GSI data were used to determine the design input parameters which represent the rock mass behavior for stability analyses. For the intact rock specimen that constitutes the rock mass, the criterion is expressed by the equation as below:

$$\sigma_1' = \sigma_3' + \sigma_{ci} \left(m_b \frac{\sigma_3'}{\sigma_{ci}} + s \right)^a \tag{3.1}$$

where,

σ_1 and σ_3 are the major and minor effective principal stresses at failure,
 σ_{ci} is the uniaxial compressive strength (UCS) of the intact rock material,
 m_b is the value of Hoek-Brown constant for the rock mass,
 s and a are the rock mass constants, where $s = 1$ for intact rock.

The value of m_b , s and a are calculated by,

$$m_b = m_i \exp\left(\frac{GSI - 100}{28 - 14D}\right) \quad (3.2)$$

$$s = \exp\left(\frac{GSI - 100}{9 - 3D}\right) \quad (3.3)$$

$$a = \frac{1}{2} + \frac{1}{6}(e^{-GSI/15} - e^{-20/3}) \quad (3.4)$$

where, D is the disturbance factor depends upon the degree of disturbance of the rock mass has been subjected to by blasting and stress relaxation.

Moreover, the deformation of the rock mass E_m is calculated by using the equation as follows,

$$E_m = \left(1 - \frac{D}{2}\right) \sqrt{\frac{\sigma_{ci}}{100}} \times 10^{\left(\frac{GSI-10}{40}\right)} \quad (3.5)$$

The Generalized Hoek-Brown criterion assumes isotropic rock and rock mass behavior and it is applicable to intact rock or heavily jointed rock masses which can be considered as homogeneous and isotropic (Hoek *et al.*, 1995). The transition from an isotropic intact rock specimen through a highly anisotropic rock mass in which failure is controlled by one or two discontinuities, and to an isotropic heavily jointed rock mass is summarized schematically as shown in Figure 3.18 (Hustrulid *et al.*, 2001).

In the criterion the rock material properties are reduced to estimate the equivalent rock mass values by using σ_{ci} , m_i , E_i (modulus of deformation of intact rock), GSI system and disturbance factor. By using the equations mentioned, Rocdata software of Rocscience (RocData v5.0, 2014) can determine the rock mass parameters in terms of convenience of computation.

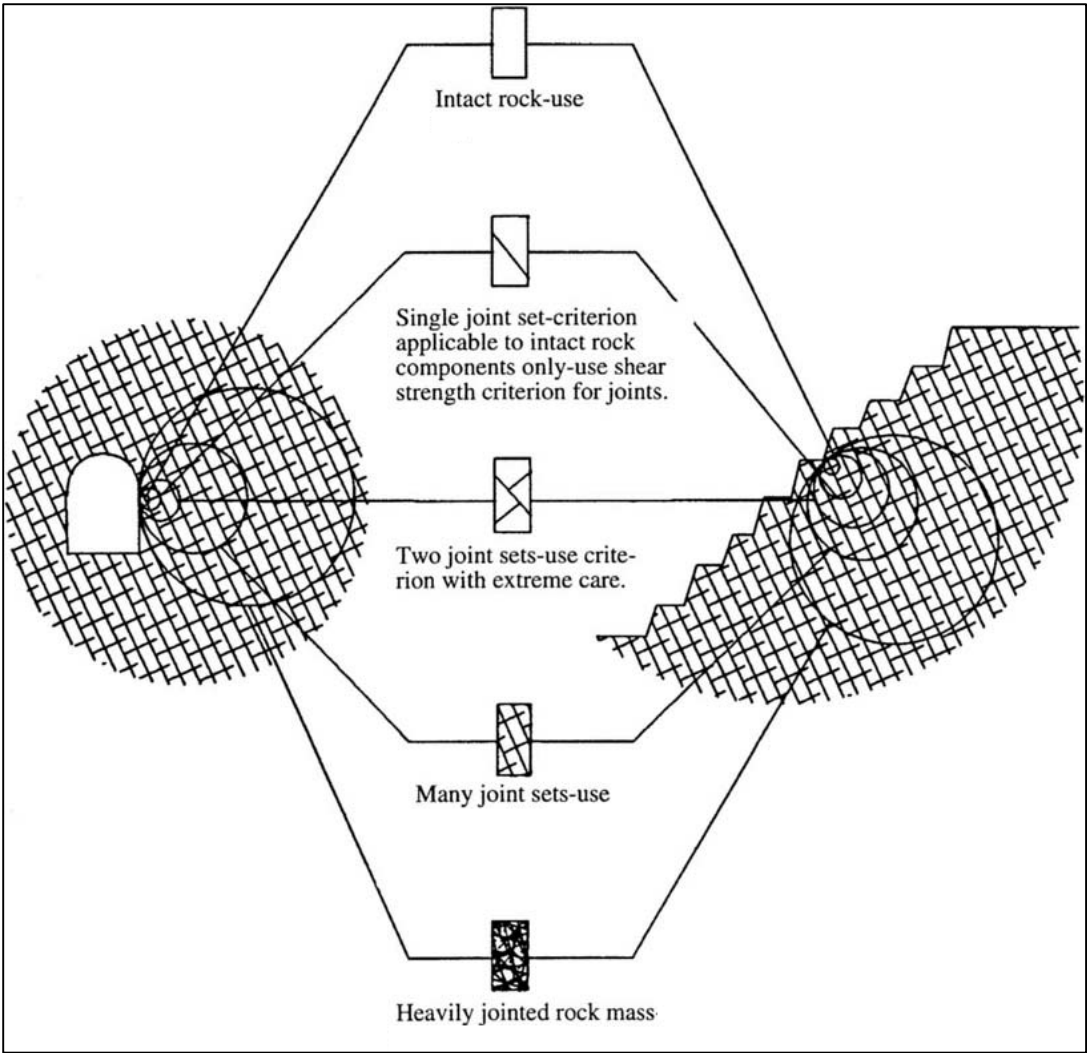


Figure 3.18 Schematic representation of rock mass and material condition (Hoek *et al.*, 1995)

For stability analyses, most of the geotechnical calculations are conducted in terms of the Mohr-Coulomb failure criterion, Therefore, it is required to determine the equivalent Mohr-Coulomb parameters, cohesion (c), and internal friction angle (ϕ). In the process, Hoek-Brown failure envelope is translated to a linear Mohr-Coulomb failure envelope to estimate the inputs used into stability analysis. Considering the studies of Hoek and Brown (1997) and Hoek *et al.*, (2002), equivalent Mohr-Coulomb parameters were determined by using the equations as followed.

$$\phi' = \sin^{-1} \left[\frac{6am_b(s + m_b\sigma'_{3n})^{a-1}}{2(1+a)(2+a) + 6am_b(s + m_b\sigma'_{3n})^{a-1}} \right] \quad (3.6)$$

$$c' = \frac{\sigma_{ci}[(1+2a)s + (1-a)m_b\sigma'_{3n}](s + m_b\sigma'_{3n})^{a-1}}{(1+a)(2+a)\sqrt{1 + (6am_b(s + m_b\sigma'_{3n})^{a-1})/((1+a)(2+a))}} \quad (3.7)$$

where ϕ' is the internal friction angle, c' is the cohesion and $\sigma'_{3n} = \frac{\sigma'_{3\max}}{\sigma_{ci}}$ is the upper limit of confining stress.

The equivalent rock mass parameters can also be estimated by using both RocLab v1.0 (2014) and RocData v5.0 (2014) softwares in which all these methods are implemented.

Since the groundwater has a significant influence on the deeper parts of the open pits in Bizmişen region, effective stress analyses were used and for slope stability analyses, effective values of cohesion (c') and internal friction angle (ϕ') were used as design inputs.

Due to the orebody orientation and the topographic conditions of the mines to be operated in Bizmişen region, mining depths are various for each open pit mine. Rock mass characteristics may differ with respect to the height from the actual ground surface. Therefore, to represent the rock mass characterization of planned open pit

mines accurately, effective Mohr-Coulomb strength parameters, cohesion (c') and internal friction angle (ϕ'), were determined by considering the operated ultimate mining depth.

Serpentinite and mudstone are the mostly observed units in the hanging wall. The properties of these rock units are close to each other. Therefore, it was decided to merge their properties and assign them to the host rock. GSI system rating was utilized as 48 to represent the rock mass of intended open pits, having higher than 160 m mining depth, whereas GSI values were reduced to 43 for open pits with lower than 160 m mining depth in order to reflect the effect of weakening due to alteration.

Results of the laboratory work states that σ_{ci} for mudstone and serpentinite are the lowest among all the dominating rock units. Design inputs of host rock that is composed of serpentine and mudstone, were assigned as $\sigma_{ci} = 17 \text{ MPa}$ and $m_i = 10$. An intact modulus E_i was assigned as 7.81 GPa in order to estimate the rock mass modulus E_m (Hoek and Diederichs, 2006). Disturbance factor (D) was also involved for prediction of rock mass parameters to consider blast damage, stress relief and Hoek-Brown classification (Hoek *et al.*, 2002). The disturbance factor ranges from 0 to 1 according to disturbance condition of the rock mass. D=0 indicates an undisturbed rock slope, whereas D=0.7 and D=1 considers the rock slope as damaged caused by blasting and stress relief due to overburden removal. D=0 generally overestimates the slope stability (Pierce *et al.*, 2001). Therefore D=0.7 and D=1.0 are suggested to represent the rock mass condition as disturbed by poor or good blasting related with mechanical excavation and heavy production blasting respectively (Hoek *et al.*, 2001). Appropriate disturbance factor for slopes can be assigned by using the guideline proposed by Hoek *et al.*, (2002), see in Appendix A (Figure A.5). The rock mass strength and deformation properties for the stability model based on cross section, Section #A-A' are presented as input and output in Table 3.6.

Table 3.6 Rock mass strength and deformation properties for the host rock of model based on Section #A-A'

	$\sigma_{ci} = 17.1$ MPa			$m_i = 10$		GSI = 48			
Input	Slope Height, H = 380 m					Unit Weight = 0.025 MN/m ³			
	Disturbance Factor, D = 0.7					$E_i = 7.81$ GPa			
	Hoek-Brown			Mohr-Coulomb		Rock Mass Parameters			
	Criterion			Fit					
Output	m_b	s	a	c (MPa)	φ (°)	σ_t (MPa)	σ_c (MPa)	σ_{cm} (MPa)	E_m (GPa)
	0.574	0.0005	0.507	0.715	19.56	0.016	0.376	1.694	0.738

The estimation of rock mass properties from intact rock specimen based on Hoek-Brown classification that is translated to Mohr-Coulomb failure envelope was done using RocLab software failure envelopes of which are presented in Figure 3.19.

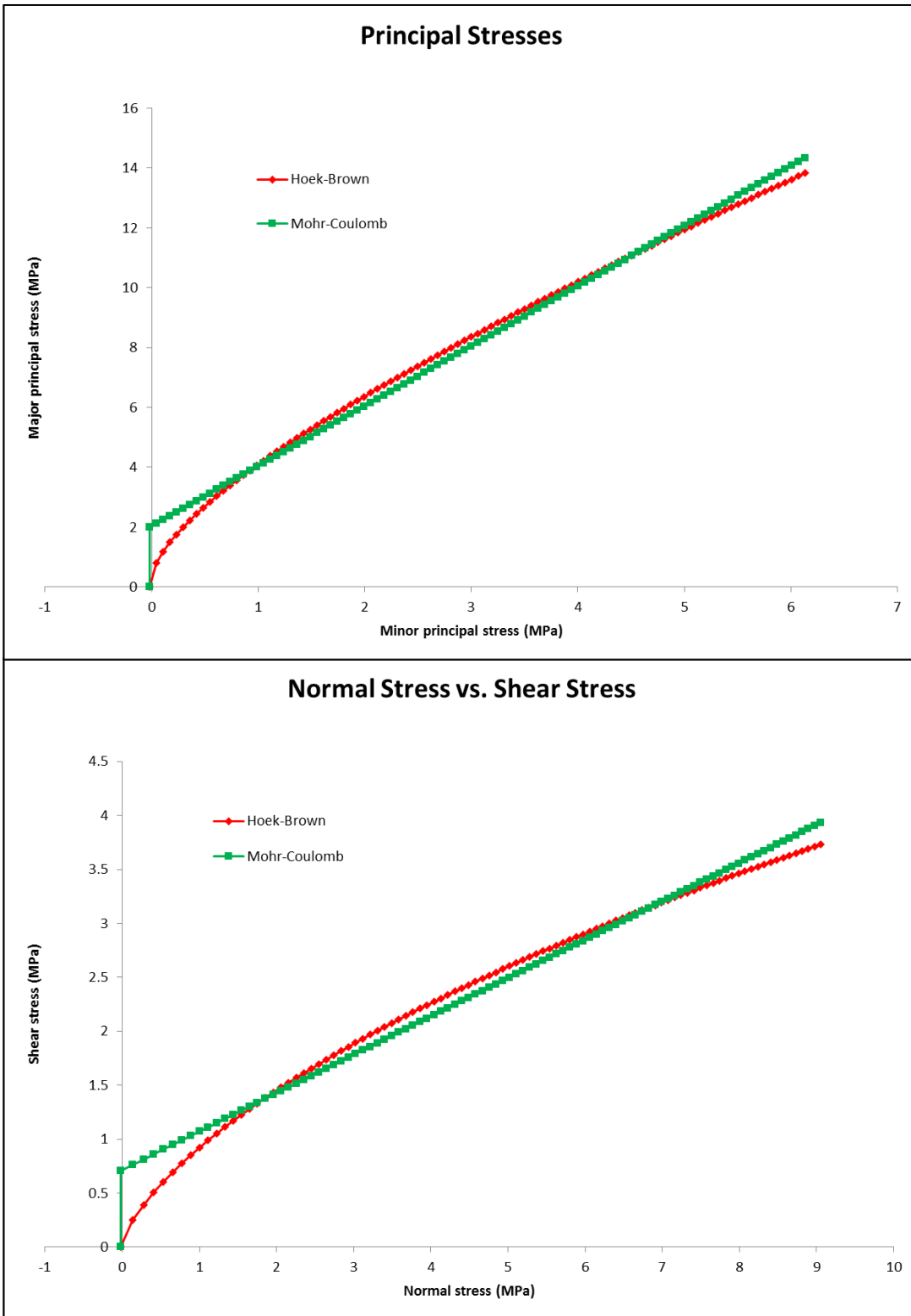


Figure 3.19 Hoek-Brown and Mohr-Coulomb failure envelopes

CHAPTER 4

SLOPE STABILITY ANALYSES

4.1 Introduction

Stability analysis of slopes in an open pit has become significant with an increase in the mining depth. On the other hand, since steeper slope angle can reduce the amount of stripping waste rock, it is necessary to optimize the overall slope angle by increasing it as much as possible without jeopardizing the mining safety.

There are several alternatives available in order to investigate the slope stability analysis. Limit equilibrium methods and numerical modeling are the most widely used techniques in slope stability. However, optimum design can be achieved with the combined use of both methods based on determination of FOS and SRF.

4.2 Selection of Critical Cross-section for Stability Analyses

For convenient and reliable stability analyses, critical cross sections were determined by regarding the areas with high potential of instability. According to the mining plans, west slope of Dönentaş open pit reaches approximately 400 m mining depth considering the topography and ore body orientation. Therefore, a 2D cross section, Section #A-A', including the deepest part of the open pit was prepared for overall slope angle optimization studies (Figure 4.1). Since mining depth would differ by regarding the advance in mining operations, several cross sections were also prepared to conduct stability analyses for different mining depths. The plan view of these cross sections can be seen in Figure 4.1.

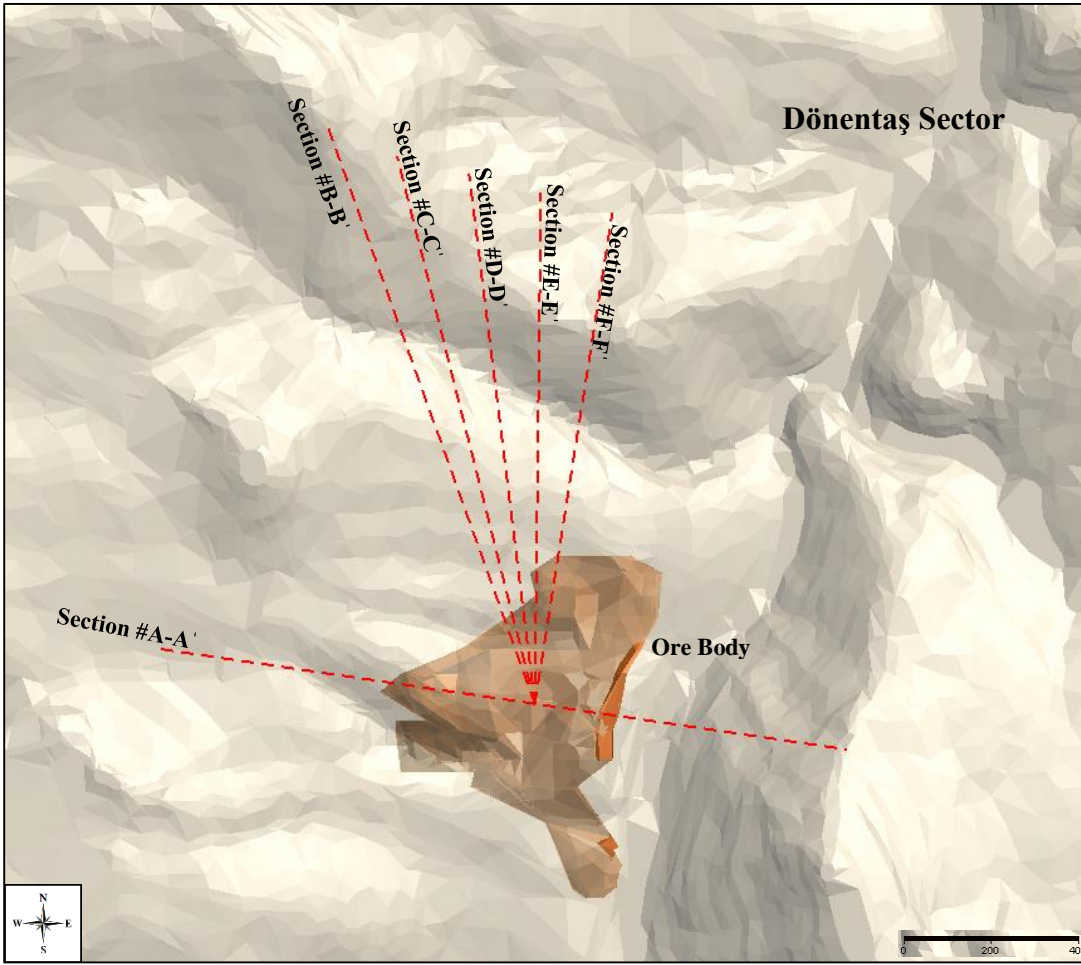


Figure 4.1 Cross sections for different mining depths

Initially, in order to achieve optimum design of the west wall of Dönentaş open pit, 11 various scenarios were studied. In the scenarios, different overall slope angle values ranging from 32° to 42° were considered. Since mining depth reaches almost 400 m on the west slope of the pit, it is crucial to optimize the overall slope angle to reduce the amount of stripping in terms of economic viability. Therefore, by conducting both limit equilibrium methods and numerical modeling, optimum overall slope angle was determined with respect to the results of FOS and SRF. On the other hand, since east wall of the open pit was designed as pursuing the dip of the ore body with 30° , slope angle optimization studies were not carried out for that part of the open pit.

After achieving the optimum overall slope angle for the deepest slope, for different mining depths, corresponding overall slope angles were predicted by satisfying FOS and SRF value of 1.2 (Table 4.1). With the combined use of limit equilibrium methods and numerical modeling, FOS and SRF results were assessed and optimum geotechnical mine design was performed.

Table 4.1 Overall slope angles for various mining depths

Mining Depth (m)	Overall Slope Angle (°)
380	36
300	40
280	41
270	42
260	43
240	44
230	45
220	46
210	47
195	48
180	49
170	50
160	51
150	52
140	53
130	54
120	55
85	60

4.3 Model Generation

Stability models were prepared with respect to the various overall slope angle schemes for the west slope of Dönentaş open pit by regarding the most critical cross section, Section #A-A'. In representative model geometry of the cross section, the bench angle was designed as 80° in order to take precautions against local spalling on the benches

for further working operations. Regarding the equipment qualifications, bench height was designed as 10 m. On the west wall of Dönentaş open pit, inter-ramps with approximately 30 m width were designed to ensure both safe workings conditions at deeper levels of the open pit and to reduce the instability risk. Ideal bench width was adjusted as regarding the conditions of the working benches and haul roads.

Slope stability is influenced by the occurrence of groundwater in mine sites. Effective stress and pore pressure are influenced by groundwater. An increase in pore pressure within discontinuities and rock mass reduces the shear strength which causes a potential slope failure. Stability of a slope is affected by the position and potentiometric level of groundwater (Ulusay *et al.*, 2014). Therefore, hydrogeological investigation was also conducted during fieldwork to gain a general comprehension about regional groundwater trends. Based on the field observations, the groundwater within the rock mass was assumed around 1500-1530 m level. In the models generated for stability analyses, groundwater level was included to represent the interaction between pore pressure and stresses and deformation.

Same slope design parameters were used for all the models prepared based on the cross sections for different mining depths and overall slope angle. Example illustrations for the models based on GSI:48 and GSI:43 prepared for stability analyses to optimize the corresponding overall slope angles can be seen in Figure 4.2 and Figure 4.3.

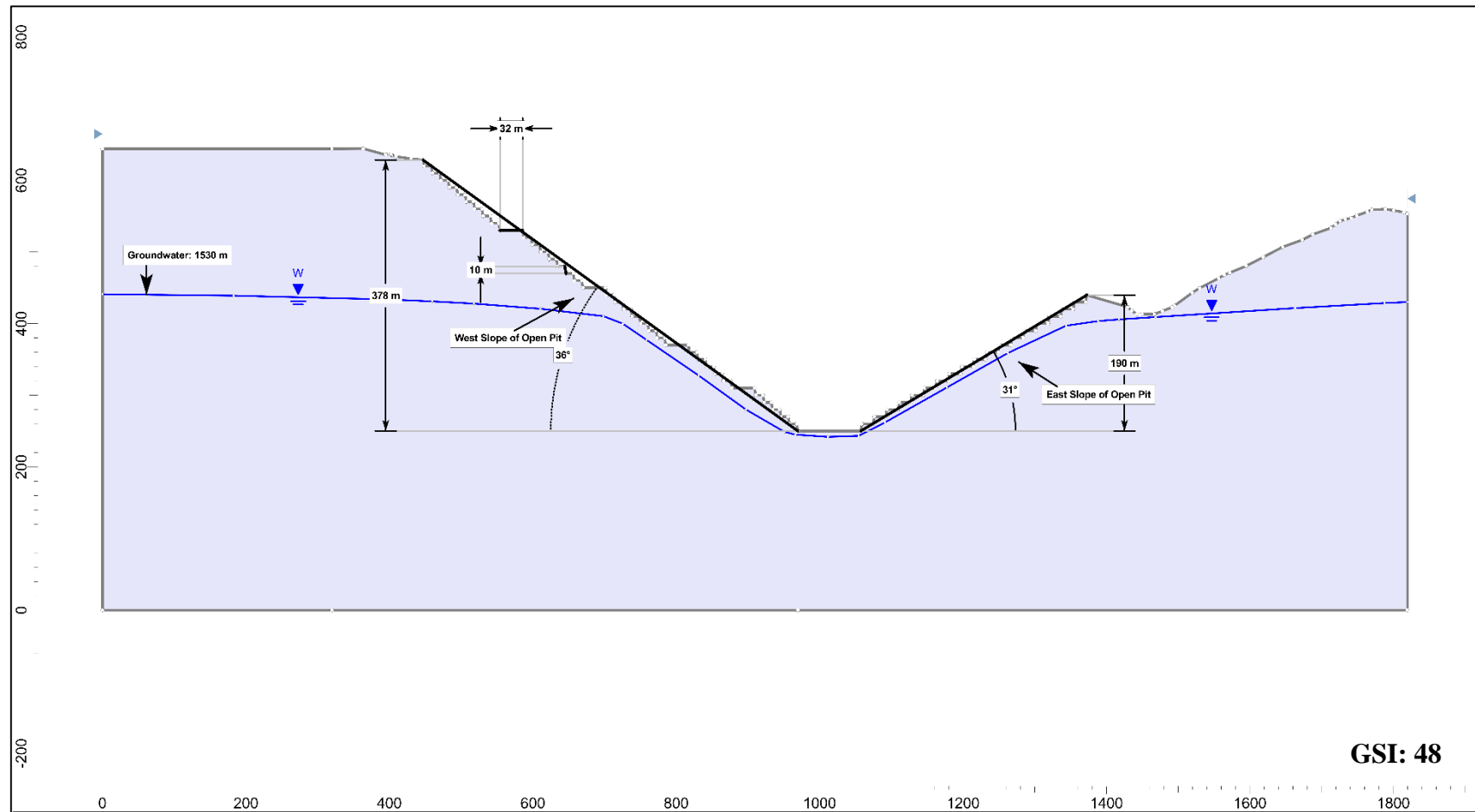


Figure 4.2 Illustration of model geometry based on cross section, Section # A-A'

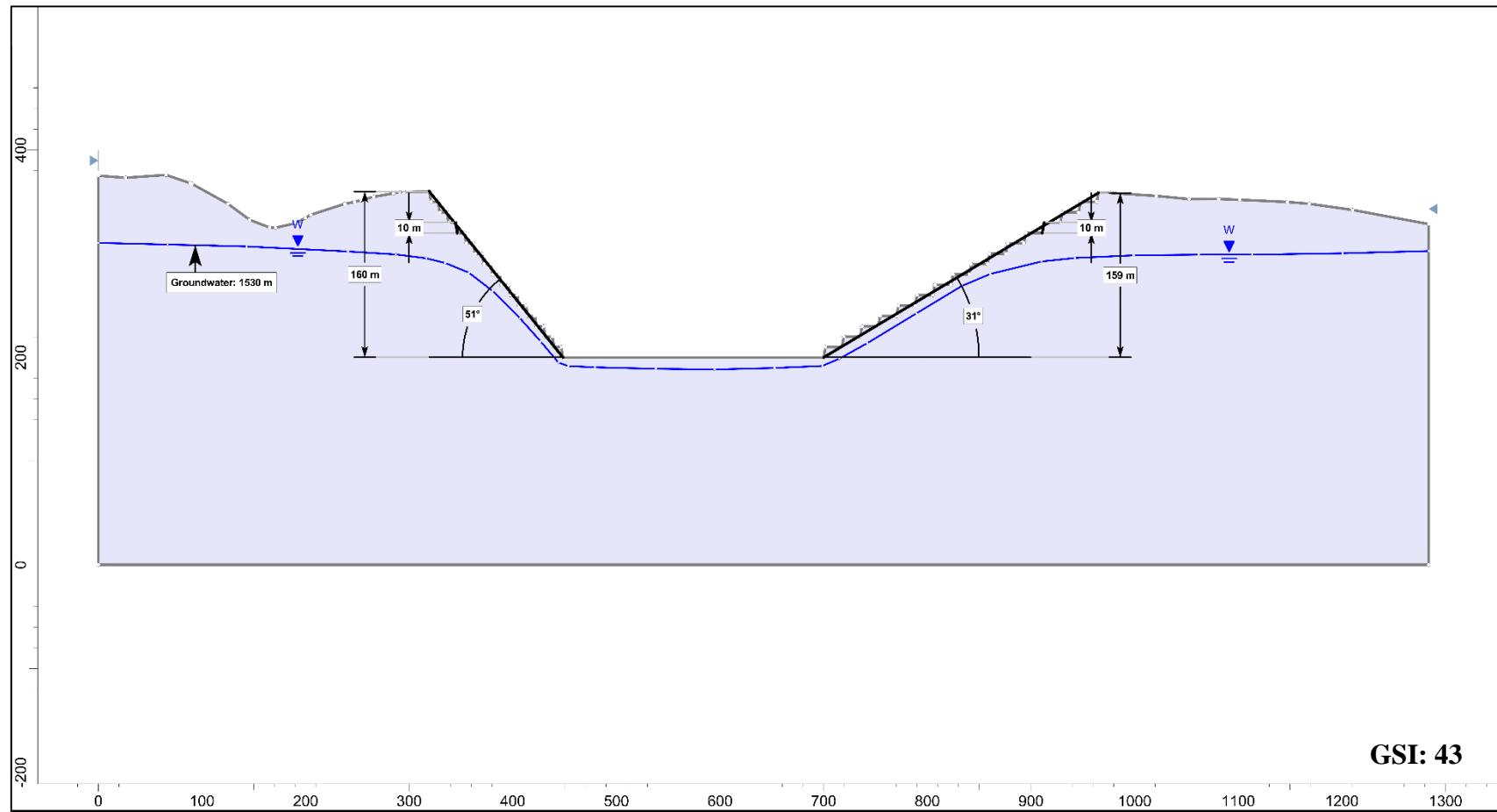


Figure 4.3 Illustration of model geometry based on cross section, Section #E-E'

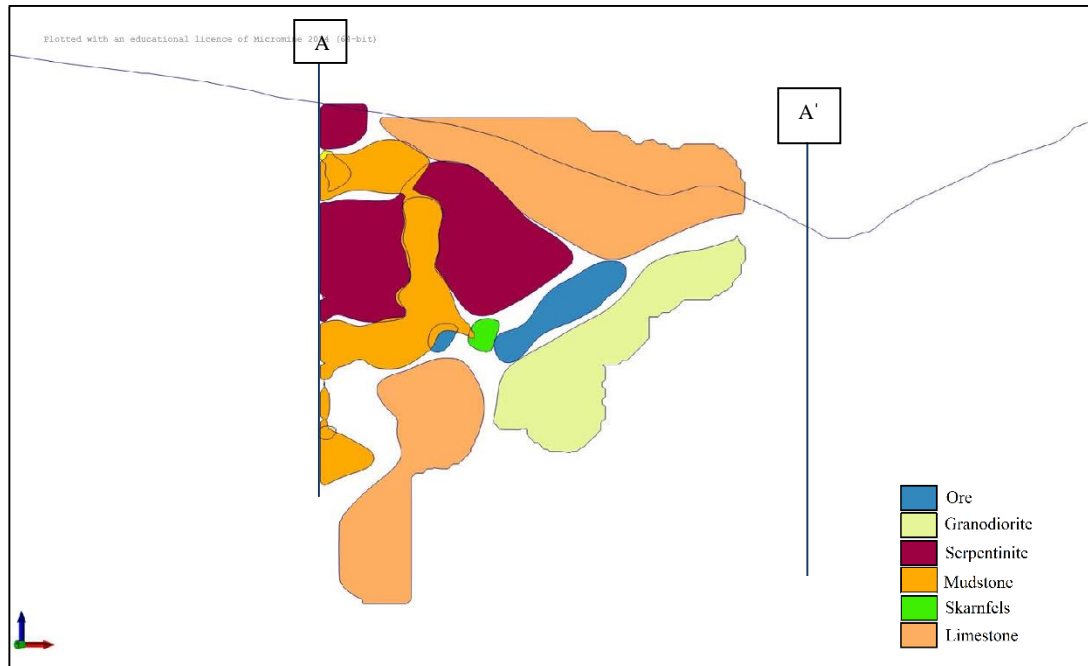


Figure 4.4 Lithological illustration of Dönentaş region based on Section #A-A' (Micromine Pty, 2014)

As mentioned previously in Chapter 3, serpentinite and mudstone are the most dominantly observed rock units around the region. In Figure 4.4, it can be seen that most of the rock mass is composed of serpentinite and mudstone within the rock mass based on the prepared cross section, Section #A-A'. Thus, rock mass properties of these rock units were considered to be merged and assigned as inputs to the host rock for all the models prepared for stability analyses.

4.4 Limit Equilibrium Analysis

Limit equilibrium methods depend upon the force and moment equilibrium conditions. It predicts critical FOS value by ensuring that the rock mass can maintain the stability on the assumed possible failure surface (Read and Stacey, 2009).

Several approaches based on method of slices were proposed by some researchers for limit equilibrium methods. Simplified Bishop (1955), Morgenstern-Price (1965) and Spencer (1967) are the most widely used slicing techniques for stability analysis.

For all limit equilibrium analyses, most commonly used two dimensional software Slide v6.0 (Rocscience Inc., 2014) was selected to assess the FOS values by considering the circular and non-circular failure surfaces. To represent proper and realistic rock mass characteristics around Bizmişen region, possible failure surfaces were considered as circular failures.

4.4.1 Model Input Parameters

Prepared model geometry is governed by such project settings such as units of stress, time and permeability. Metric system with meter and second was used to perform the analyses. The methods of slices were conducted by using 25 slices regarding the 0.5% tolerance which may be sufficient to obtain accurate results. Mohr-Coulomb failure criterion was used for the analyses, thus equivalent effective cohesion and internal friction angle represent the material properties of the host rock in the models. By means of laboratory experiments, a unit weight of $\gamma=25 \text{ kN/m}^3$ was assigned to the host rock mass. To represent the groundwater condition of the models, H_u values, used for the calculation of the pore pressure, were assigned with respect to the mining depth. Slide v6.0 software offers various search methods for both circular and non-circular surface types to calculate the minimum FOS value. However, circular failure mechanism was estimated as search method for the analyses regarding the rock mass characteristics of Bizmişen region. The used slope search method for circular failure surfaces that available in Slide v6.0 software to generate slip surfaces is presented in Figure 4.5.

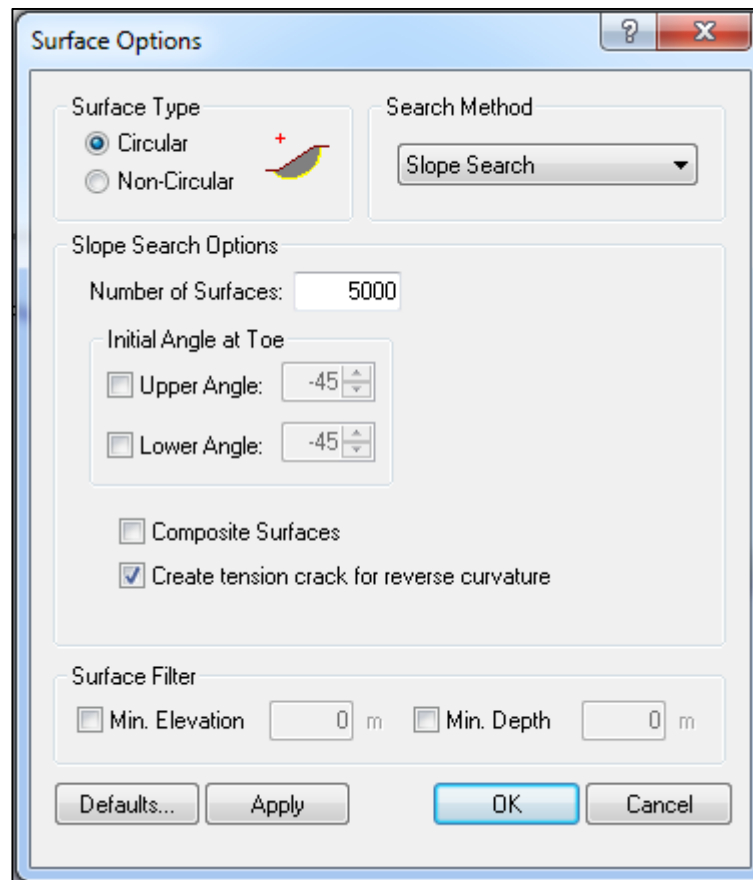


Figure 4.5 Slope search option for circular failure surface in Slide v6.0 (Rocscience Inc., 2014)

The slope search analysis is conducted with 5000 surfaces by considering the steps to generate slip circles (Rocscience Inc., 2014):

- Two points on the slope as starting point and ending points of the slip surface on the slope are generated considering the slope limits.
- The program defines the slip circle by using a third point using the initial angle at toe.
- All steps mentioned above are repeated until the number of valid slip surfaces and the number of surfaces specified in the slope search get equal to each other.

The location of the critical surface with the minimum FOS is found by means of an iterative procedure based on Monte Carlo technique suggested by Greco (1996).

Model input parameters for the analysis of most critical cross section, Section #A-A' that includes the west wall of the Dönentaş open pit are shown in Table 4.2.

Table 4.2 Model inputs of most critical section, Section #A-A', in Bizmişen region

Parameter	Unit	Design Domain with 36° overall slope angle
Unit Weight (γ)	kN/m ³	25
Cohesion (c)	kN/m ² (kPa)	715
Internal friction angle (ϕ)	[°]	19.6
H _u	[-]	0.5

4.5 Numerical Modeling

Although limit equilibrium methods are easy to be used, the evaluation of deformation and development of failure surface automatically are not possible. Deformation or displacement is a significant parameter in slope design due to being an indicator to suggest precautions for maintaining stability. Moreover, they are most frequently recorded parameters to assess the stability condition of the slopes. Limit equilibrium methods may be inadequate for the analysis of the slopes composed of complex material properties. However, numerical modeling provides an insight for model with complex geology by considering the theoretical system of stress-strain relations in realistic manner. As stated by Hoek (2009), shear strength reduction method is the most commonly used for open pit slope stability studies. The method is a powerful valid alternative to limit equilibrium methods to determine FOS based on using finite element or finite difference analysis. In this study, however, shear strength reduction method based on finite element analysis was conducted for the evaluation of open pit stability. The main advantage of the method is the lack of priori assumptions on the shape and location of failure surface. The failure occurs inherently within the slope in

which shear strength or the rock mass cannot sustain the applied shear stresses (Griffiths and Lane, 1999). The model convergence is considered as the failure indicator by analyzing the discretized zones. Mohr-Coulomb strength parameters that are cohesion (c) and internal friction angle (ϕ) best explain the slope material in the method (Hammah *et al.*, 2007). These parameters are reduced gradually for each trial and the strength reduction factor (SRF) and the corresponding displacement at each node are recorded. In the method, SRF has the same meaning with FOS that used in conventional limit equilibrium methods and it is equal or slightly less than FOS (Dawson *et al.*, 1999). When there is a rapid increase in the nodal displacements within the model, non-convergence occurs in which the slope failure take place and at that point SRF is recorded as critical strength reduction factor (CSRf). In fact, stress and displacement distributions which are included in the equations of equilibrium cannot be created for the slope material in case the convergence is not ensured within a user specified number of iterations and tolerance. Hence, a dramatic increase in slope displacements characterizes the failure.

Considering the results from limit equilibrium methods, all estimated overall slope angles were verified by conducting numerical modeling. Shear strength reduction method was utilized for all analyses to increase the reliability and accuracy of the results by using a 2D finite element program, Phase2 v9.0 (Rocscience Inc., 2014) based on plane strain condition. FOS values were compared and verified with SRF results that is described as the ratio of actual rock shear strength to the reduced shear strength at failure.

4.5.1 Model Input Parameters

As previously mentioned in Chapter 3, equivalent Mohr-Coulomb parameters of the rock mass, c' and ϕ' , were obtained by using Hoek-Brown classification including GSI values from the field investigations, σ_{ci} and m_i values from laboratory tests. Due to the influence of groundwater on slopes, effective values of cohesion and internal friction angle were used for the analyses.

Peak values of those parameters are considered as a break-even point from elastic to plastic behavior. Residual values are used after the failure and the post-failure progress proceeds according to the plastic analysis with increasing deformations. In plastic analyses, for instance, the material fails and volumetrically swells which would cause more deformation. This swelling progress is represented with the dilation angle. In the models, for the post-failure, the peak parameters were reduced to residual values with controlled by dilatation angle and proceeded the computation with residual parameters.

In the models, Mohr-Coulomb failure criterion was assigned for both peak and residual parameters. GSI_{res} of the rock mass was calculated according to Cai *et al.*, (2007):

$$GSI_{res} = GSI e^{-0.0134GSI} \quad (4.1)$$

The equation below was used to determine the dilation angle of the rock mass (Alejano *et al.*, 2009):

$$\Psi = (5GSI - 125)\phi'/1000 \quad (4.2)$$

In Phase² software, four different finite element types are available, presented in Figure 4.6. The analyses were carried out by using uniform 6 noded triangular elements with the number of over 3000 elements to increase the accuracy of the results.

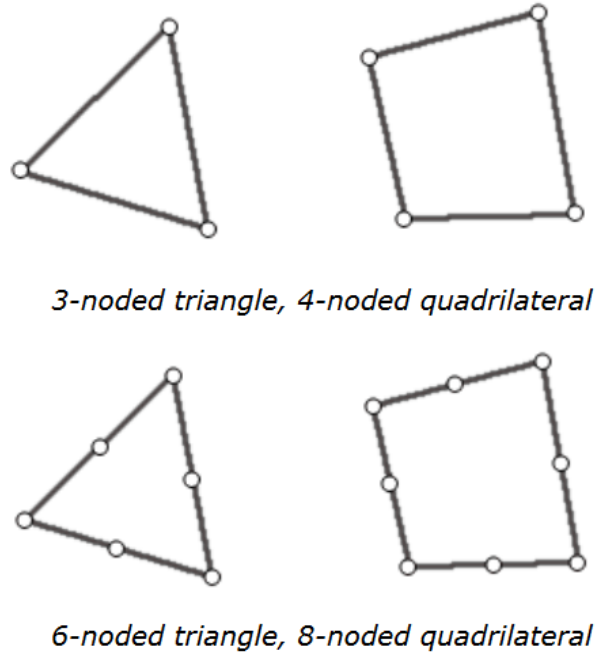


Figure 4.6 Finite element mesh type used in Phase² software (Rocscience Inc., 2014)

To solve the matrices in the analyses, Gaussian Elimination solver type was selected. Convergence was controlled by Absolute Energy criterion. All analyses were conducted by 500 iterations with 0.1% tolerance. Gravitational field stress was assigned by using the actual ground surface utility. k ratio (horizontal/vertical stress) as 1 in all analyses. Field stress & Body force option was assigned for the initial element loading conditions of the analyses.

Model input parameters for the strength reduction analysis of most critical cross section, Section #A-A' that includes the west wall of the Dönentaş open pit in Bizmişen region are shown in Table 4.3.

Table 4.3 Model inputs of most critical section, Section #A-A'

Parameter	Unit	Design Domain with 36° overall slope angle
Unit weight	kN/m ³	25
Poisson's ratio	[-]	0.14
Young's modulus	GPa	7.81
Peak cohesion	kN/m ² (kPa)	715
Residual cohesion	kN/m ² (kPa)	715
Internal friction angle	°	19.6
Residual friction angle	°	19.6
Dilatation angle	°	2.3
H _u	[-]	0.5

As a result, slope stability analyses were carried out to optimize the overall slope angle of open pits in Bizmişen region by using the determined design input parameters and the prepared models mentioned in this chapter.

CHAPTER 5

STABILITY ANALYSES RESULTS AND DISCUSSION

5.1 Assessment of Factor of Safety (FOS) as Design Criterion

Slope stability efficiency of open pit mines has been evaluated based on the allowable factor of safety (FOS) which can be defined as the ratio of resisting forces and driving forces over rock mass. It is a practical concept for engineering design purposes by predicting slope instability and estimating the potential failure. FOS is determined both using limit equilibrium method and numerical modeling by considering force-moment equilibrium and stress-strain analyses that are used in geotechnical purposes of large-scale rock slopes for mining and civil engineering applications.

Based on the safety requirement of engineering, allowable level of FOS differs with respect to various design projects. Several researchers have made recommendations for acceptable FOS values for design. Priest and Brown (1983) suggested a guideline based on the consequence of failure and recommends FOS values for design which is presented in Table 5.1. Another applicable judgement of allowable FOS was proposed by Hoek and Bray (1981). Acceptable FOS values are considered with respect to geotechnical conditions and engineering design purposes to ensure the long term or short term stability, shown in Table 5.2. In mining industry, typical acceptance design criteria for both FOS and POF (Possibility of Failure) is presented in Table 5.3. The performance of pit slope can also be evaluated by using this recommended design criteria based on the consequence of failure.

Table 5.1 Allowable FOS guideline (Priest and Brown, 1983)

Consequence of failure	Examples	Acceptable values
Not serious	Individual benches; small (<50 m), temporary slopes, not adjacent to haulage roads	1.3
Moderately serious	Any slope of a permanent or semi-permanent nature	1.6
Very serious	Medium-sized (50-100 m) and high slopes (<150 m) carrying major haulage roads or underlying permanent mine installations	2.0

Table 5.2 Design factors of safety for pit slope design (Sullivan, 2006)

DESIGN SITUATION		FACTORS OF SAFETY COMMONLY USED OR ACCEPTED IN PRACTICE	
Applicability	Geotechnical Conditions	Range	Preferred Value
General slope design	simple geological and geotechnical conditions	1.2 - 1.3	1.2
	complex geology, soil and or soft rock; groundwater		1.3
	to stabilize a large moving slope	1.0 - 1.3	1.1
	rigorous back analysis of large failure available		1.1
Slope below haul road or important infrastructure		1.2 - 1.5	1.3

Table 5.3 Allowable FOS and POF criteria values (Read and Stacey, 2009)

Slope scale	Consequences of failure	Acceptance criteria		
		FOS (min)(static)	FOS (min) (dynamic)	POF (max) P[FOS≤1]
Bench	Low-high	1.1	NA	25-50%
	Low	1.15-1.2	1.0	25%
Inter-ramp	Medium	1.2	1.0	20%
	High	1.2-1.3	1.1	10%
	Low	1.2-1.3	1.0	15-20%
Overall	Medium	1.3	1.05	5-10%
	High	1.3-1.5	1.1	≤5%

Recommended design criteria above provide a guideline to assess the performance of pit slopes and quantify the slope failure risk with respect to safety and economics. In this research, the minimum FOS was considered as 1.2 based on the safety requirement of the engineering.

5.2 Results of Analyses with Limit Equilibrium Methods

After determining the most critical cross section, Section #A-A', based on high risk of instability, to conduct stability analysis, models were prepared with respect to several overall slope angle design geometries for the west slope of Dönentaş open pit. The scenarios are based on the overall slope angles varying between 32° and 42° to achieve the optimum.

GLE/Morgenstern-Price, Bishop and Spencer method of slices techniques were decided to assess the stability analyses. The analyses were utilized based on Mohr-Coulomb failure criterion and critical failure mechanism was considered as circular (rotational) type of failure. According to the computation results of all methods for the

west slope of Dönentaş open pit, predicted FOS values for overall slope angles varying between 32° and 42° are summarized in Table 5.4.

Table 5.4 FOS computation results by limit equilibrium analysis for the most critical section, Section #A-A' with various overall slope angle scenarios

Overall Slope Angle of West Wall of Dönentaş Open Pit	Factor of Safety, FOS		
	GLE/Morgenstern- Price	Bishop	Spencer
32	1.284	1.290	1.288
33	1.271	1.273	1.268
34	1.232	1.235	1.235
35	1.217	1.220	1.220
36	1.206	1.208	1.208
37	1.197	1.199	1.198
38	1.174	1.181	1.179
39	1.165	1.170	1.169
40	1.153	1.156	1.152
41	1.137	1.140	1.136
42	1.118	1.120	1.116

As seen in Table 5.4, FOS decreases when the overall slope angle increases. The FOS results calculated by using different method of slices are close to each other and range from 1.116 to 1.290. Based on the safety requirement of rock engineering, the minimum allowable value of FOS as 1.2 is satisfied for overall slope angle of 36°. Since amount of waste rock increases as the overall slope angle gets lower, an optimum overall slope angle for the west wall of Dönentaş open pit with around 400 m mining depth was proposed to be adjusted as 36°. Computation results based on method of slices for optimum overall slope angle scenarios are presented in Figure 5.1.

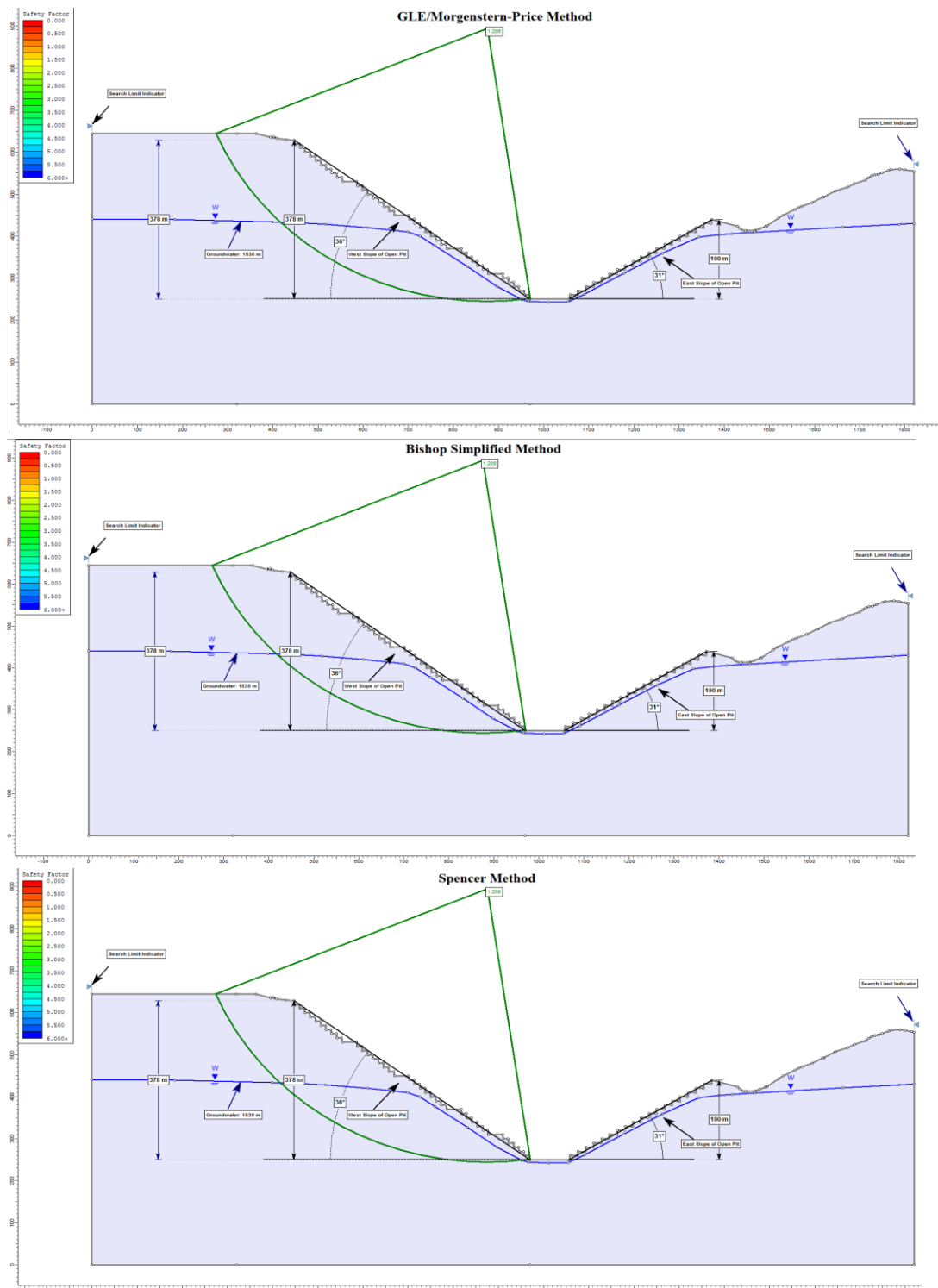


Figure 5.1 Results of analyses with limit equilibrium methods for Section #A-A' with overall slope angle of 36°

After determining optimum overall slope angle for the deepest slope of Dönentaş open pit, stability analyses were conducted on the models based on the other cross sections. Each cross sections was prepared for different mining depth and overall slope angle. Likewise, same bench geometry parameters, method of slices, failure criteria and failure mechanism characteristics were used for the models of other cross sections (Section #B-B', Section #C-C', Section #D-D', Section #E-E', Section #F-F'). Computation results and predicted FOS values based on method of slices for different mining depths with corresponding overall slope angle are summarized in Table 5.5.

Table 5.5 Estimated FOS values for various mining depths with corresponding overall slope angle

Overall Slope Height (m)	Overall Slope Angle (°)	FOS		
		GLE/Morgenstern-Price	Bishop	Spencer
380	36	1.206	1.208	1.208
300	40	1.207	1.209	1.207
280	41	1.200	1.203	1.200
270	42	1.208	1.211	1.209
260	43	1.202	1.205	1.202
240	44	1.229	1.233	1.231
230	45	1.222	1.226	1.225
220	46	1.242	1.244	1.243
210	47	1.231	1.234	1.230
195	48	1.254	1.259	1.254
180	49	1.274	1.271	1.274
170	50	1.272	1.276	1.279
160	51	1.200	1.202	1.202
150	52	1.200	1.205	1.200
140	53	1.201	1.204	1.203
130	54	1.204	1.209	1.205
120	55	1.209	1.206	1.203

As it is seen in Table 5.5, all predicted FOS values by means of Slide v6.0 (Rocscience Inc., 2014) software are higher than 1.2 that was considered as the allowable design criteria based on the safety requirements of engineering. Thus optimum overall slope

angles for various mining depths were satisfied with a stable condition by limit equilibrium analyses based on method of slices.

To increase the reliability and accuracy of the stability analyses, numerical modeling was also conducted to evaluate and compare the predictions of limit equilibrium analyses.

5.3 Results of Analyses with Numerical Modeling

All stability analyses carried out by limit equilibrium methods were also performed by using finite element method with the software of Phase² v9.0 (Rocscience Inc., 2014). FOS assessment was done by the shear strength reduction technique in which SRF is predicted by reducing the shear strength parameters of rock mass until failure occurs. To verify the accuracy of the results obtained for the overall slope angle designs, same model geometries were used in the numerical modeling analyses. An example of model showing the typical mesh dimensions and boundary conditions from Section #A-A' with overall slope angle of 36° can be seen in Figure 5.2.

Initially, several schemes for the optimization of the west slope of Dönentaş open pit were analyzed with SSR technique and SRF results were compared with predicted FOS values. Computation results of the analyses from Section #A-A' with predicted SRF values for overall slope angles varying between 32° and 42° are summarized in Table 5.6.

As seen in Table 5.6, SRF results change between 1.09 to 1.27 for analyses of west slope of Dönentaş open pit with different overall slope angles between 32° and 42°. Accepted design criteria of minimum FOS of 1.2 was satisfied for the overall slope angles lower than 37°. However, an optimum design can be achieved with the overall slope angle of 36° in terms of economic efficiency. Therefore, optimization of the west slope angle of Dönentaş open pit was satisfied with 36° overall slope angle by regarding and verifying the results of method of slices and shear strength reduction technique.

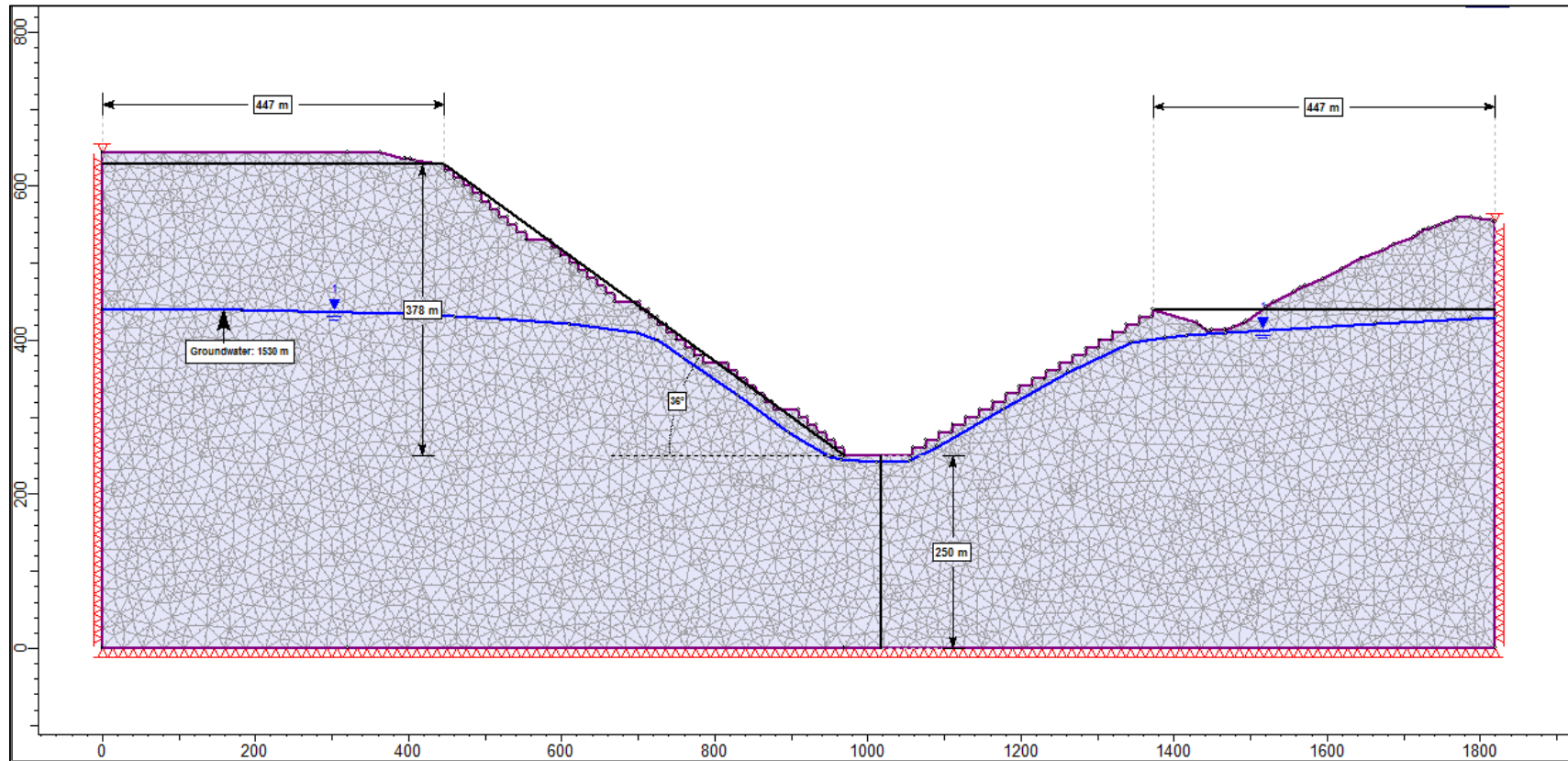


Figure 5.2 Typical mesh dimensions and boundary conditions of the model based on Section #A-A' with overall slope angle of 36°

The progress of automatically generated failure surface and the deformation vectors within the rock mass for Section #A-A' with optimum overall slope angle of 36 are presented in Figure 5.3.

Table 5.6 SRF results by SSR method for Section #A-A' with several schemes of overall slope angle

Overall Slope Angle of West Wall of Dönentaş Open Pit	Strength Reduction Factor (SRF)
32	1.27
33	1.25
34	1.22
35	1.21
36	1.20
37	1.18
38	1.16
39	1.14
40	1.13
41	1.11
42	1.09

SSR analyses with SRF results and corresponding displacement for the optimization analyses of west overall slope angle of Dönentaş open pit are shown in Figure 5.4. Moreover, the plot of maximum displacement with corresponding SRF for the analysis of model based on Section #A-A' with the determined optimum overall slope angle of 36 are presented in Figure 5.5.

After verifying the analyses results of optimization scenarios on the west slope of Dönentaş open pit by using SSR method, models prepared for different mining depth and overall slope angle were also performed by numerical modeling. Computation results and predicted SRF values based on SSR method for different mining depths with corresponding overall slope angle are summarized in Table 5.7. All SRF results evaluated by SSR technique can be seen to satisfy the acceptable design criteria of minimum FOS of 1.2, based on the safety requirements.

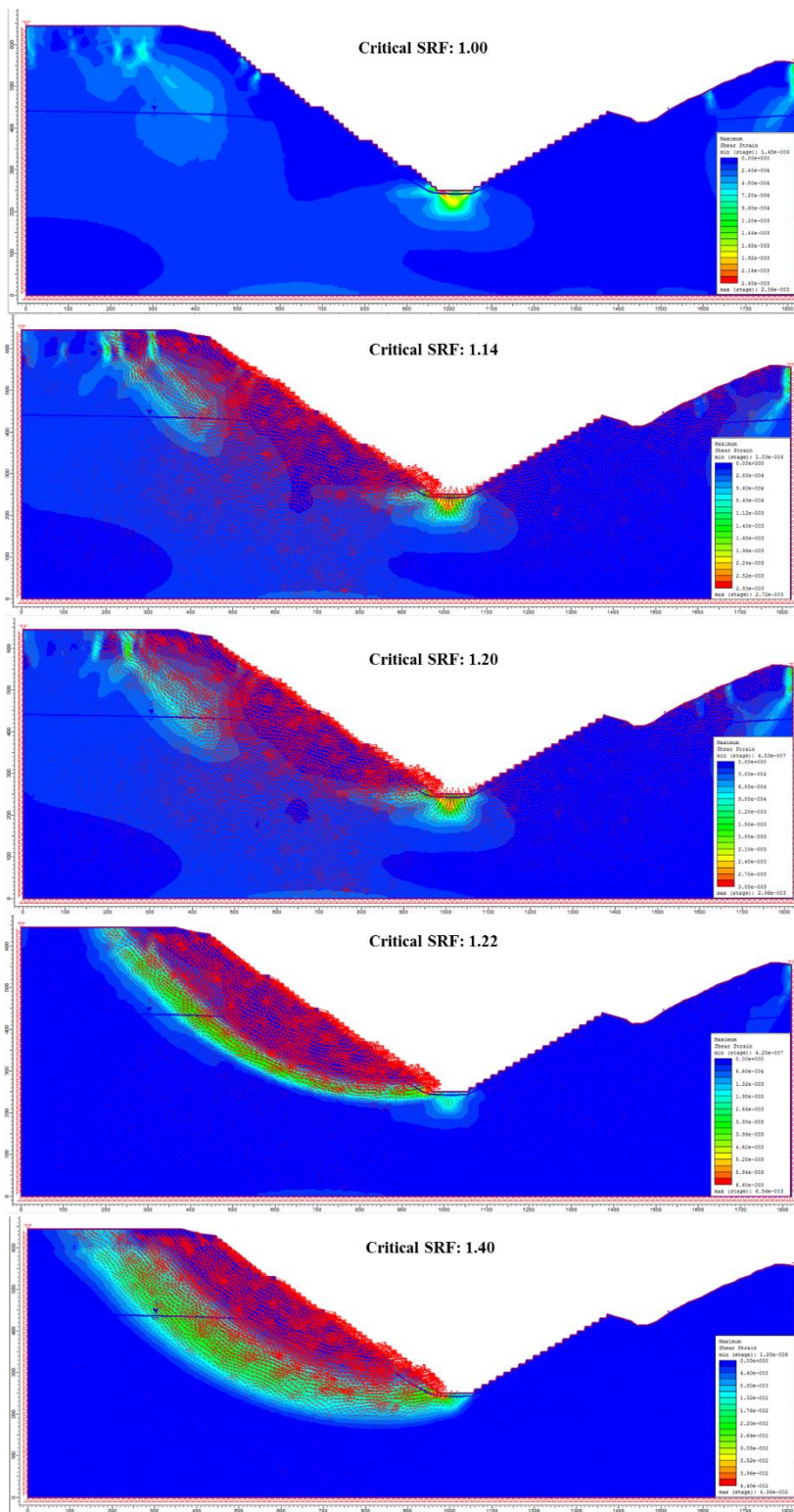


Figure 5.3 SSR analysis of Section #A-A' with overall slope angle of 36° showing the progress of failure surface by maximum shear strain and deformation vectors

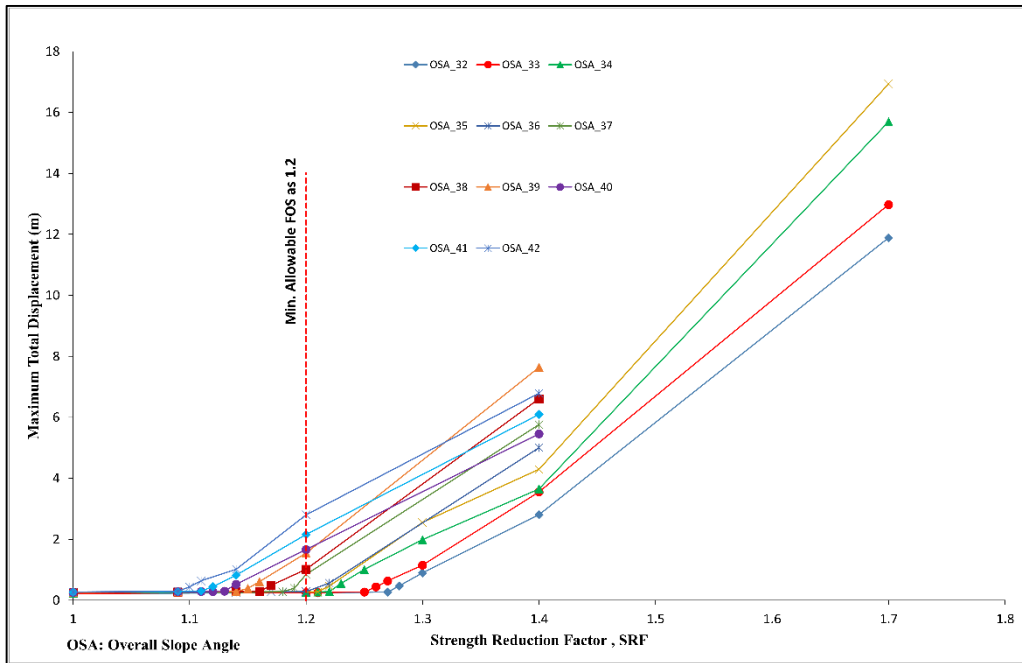


Figure 5.4 SSR analyses with SRF results and corresponding displacement for the west slope of Dönentaş open pit

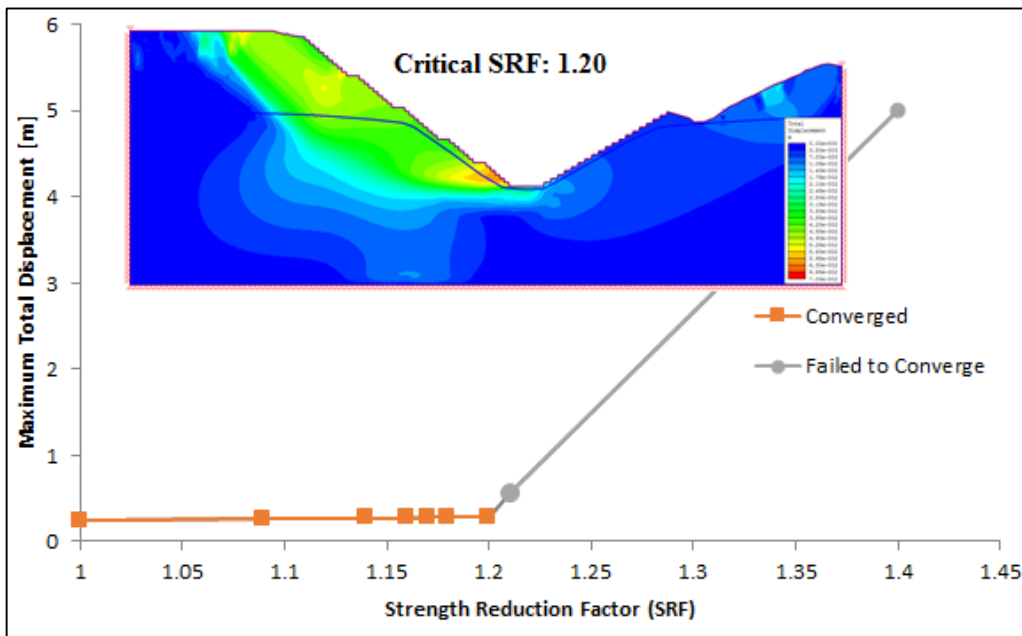


Figure 5.5 SSR solution for the west slope of Dönentaş open pit for model Section #A-A' with overall slope angle of 36° at SRF: 1.20 indicating the total displacement

Table 5.7 Computed SRF results by SSR technique for different mining depths and corresponding overall slope angle

Overall Slope Height (m)	Overall Slope Angle (°)	Strength Reduction Factor (SRF)
380	36	1.20
300	40	1.20
280	41	1.20
270	42	1.20
260	43	1.20
240	44	1.21
230	45	1.21
220	46	1.22
210	47	1.21
195	48	1.23
180	49	1.25
170	50	1.26
160	51	1.20
150	52	1.20
140	53	1.21
130	54	1.20
120	55	1.22

The plot of maximum displacement with corresponding SRF for SSR solutions of different mining depths and overall slope angle analyses are presented in Figure 5.6.

As a result, with the combined use of method of slices and SSR method, overall slope angles for the west wall of Dönentaş open pit and for different mining depths were optimized by regarding the evaluation of both FOS and SRF results. Since they were predicted higher than the required criteria of 1.2, mining design can be achieved with optimized overall slope angles.

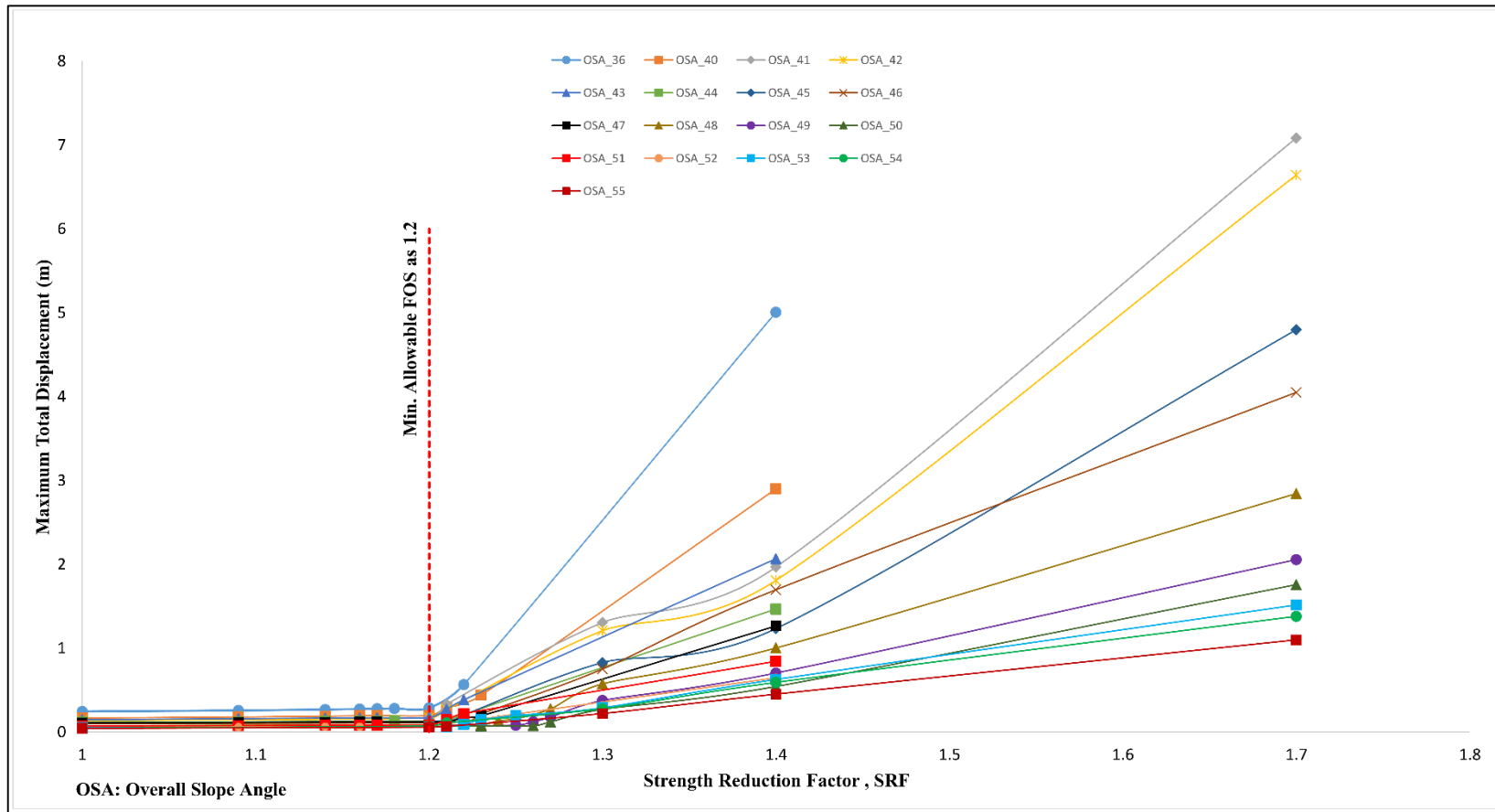


Figure 5.6 SSR analyses with SRF results and corresponding displacement for the analyses of different mining depths and corresponding overall slope angle

5.4 Discussion on the Analysis Results

Initially, in Dönentaş open pit, an optimization study of overall slope angle for the west slope was carried out by investigating the prepared 11 schemes. For the most critical section, Section #A-A' with H= 380 m, overall slope angle was changed between 32° and 42° and stability analyses were performed to estimate FOS and SRF values. Based on the engineering safety requirements, allowable FOS was considered as 1.2 and obtained results from limit equilibrium methods and numerical modeling were compared. In Figure 5.7, estimated FOS and SRF values from method of slices and SSR technique are presented.

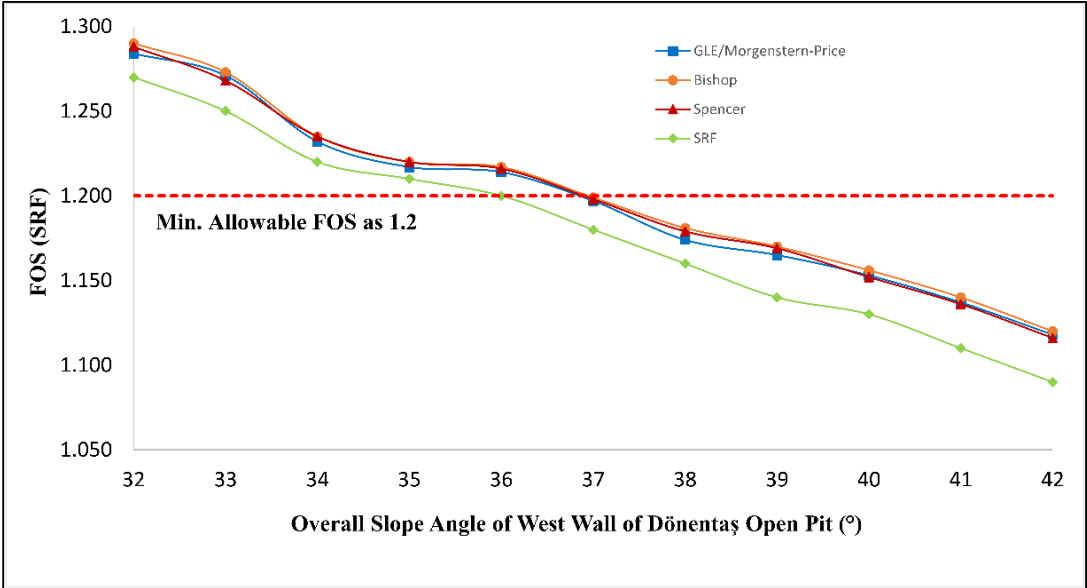


Figure 5.7 FOS and SRF results of overall slope angle optimization analyses for the west slope of Dönentaş open pit with varying angle between 32° and 42°

As shown in Figure 5.7, limit equilibrium methods and numerical modeling estimate relatively close computation results and they are consistent with each other. SSR method underestimates the slope stability by approximately 3% when compared to the limit equilibrium methods. An optimum overall slope angle design for the west slope of Dönentaş open pit can be achieved by 36° based on the accepted design criteria. Moreover, it can be stated that steepening the overall slope angle can reduce the amount of stripping. Micromine software (Micromine Pty Ltd., 2014) was used to calculate the change in the amount of stripping waste rock with respect to the overall slope angle for the west slope of Dönentaş open pit. The relationship between FOS-OSA and FOS-AS are presented in Figure 5.8.

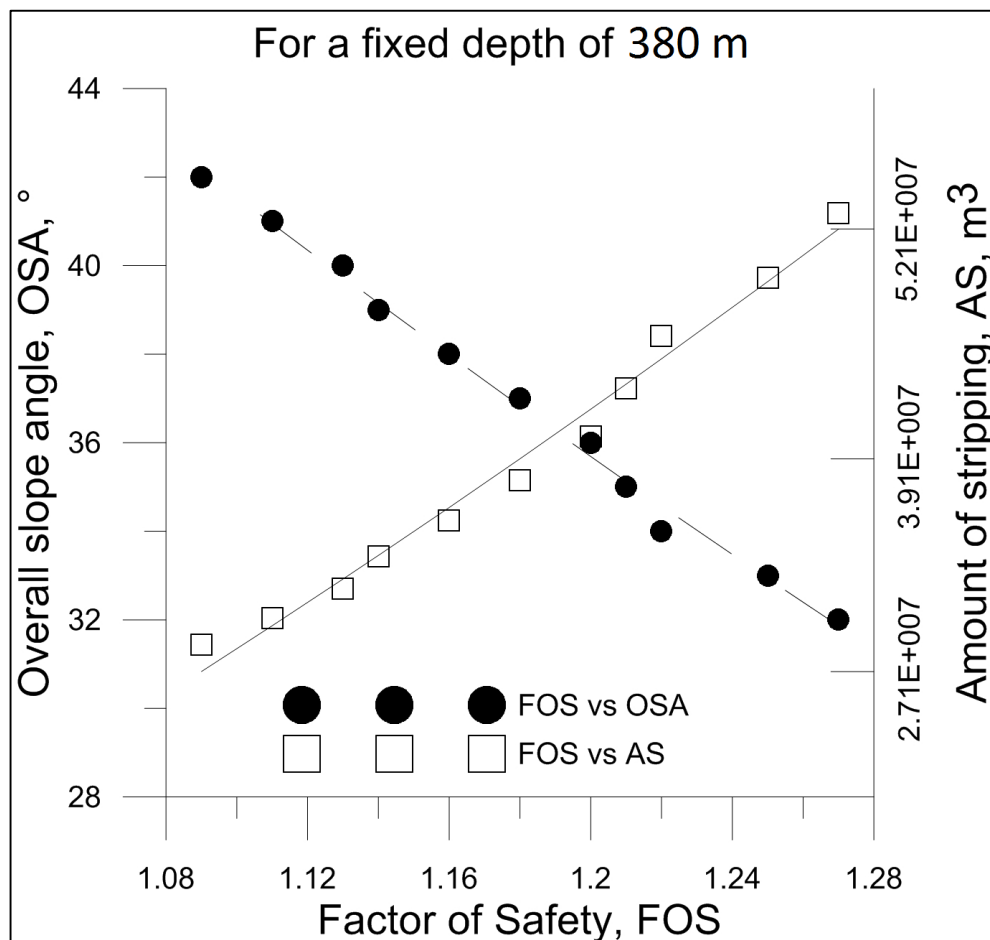


Figure 5.8 Overall Slope Angle, FOS and Amount of Overburden Stripping relation

Furthermore, stability analyses of predicted overall slope angles for different mining depths determined by satisfying minimum FOS and SRF values of 1.2, were performed with the combined use of method of slices and finite element method based on shear strength reduction technique. Computation results of FOS and SRF for the models of varying mining depth with corresponding overall slope angle are presented in Table 5.8.

Table 5.8 FOS and SRF results of analyses for different mining depth and corresponding overall slope angle

Overall Slope Height (m)	Overall Slope Angle (°)	FOS			SRF
		GLE/Morgenstern-Price	Bishop	Spencer	
380	36	1.206	1.208	1.208	1.20
300	40	1.207	1.209	1.207	1.20
280	41	1.200	1.203	1.200	1.20
270	42	1.208	1.211	1.209	1.20
260	43	1.202	1.205	1.202	1.20
240	44	1.229	1.233	1.231	1.21
230	45	1.222	1.226	1.225	1.21
220	46	1.242	1.244	1.243	1.22
210	47	1.231	1.234	1.230	1.21
195	48	1.254	1.259	1.254	1.23
180	49	1.274	1.271	1.274	1.25
170	50	1.272	1.276	1.279	1.26
160	51	1.200	1.202	1.202	1.20
150	52	1.200	1.205	1.200	1.20
140	53	1.201	1.204	1.203	1.21
130	54	1.204	1.209	1.205	1.20
120	55	1.209	1.206	1.203	1.22

According to the computation results, predicted optimum overall slope angles for different mining depths are higher than FOS of 1.2 which was considered as the accepted design criteria. It can be indicated that SSR method relatively underestimates the instability, approximately 5% difference, which enables a safe design by regarding the worst case.

5.5 Development of Slope Performance Chart

Several slope performance charts are used as practical tools for the preliminary design of slopes. They were composed of the geotechnical data of various rock types from stable and unstable mine sites. Therefore, slope performance charts include general stability cases that makes the applicability of the charts restricted for specific local cases. However, they can be enhanced and improved by increasing the local conditions in the database. In this study, a slope design chart was created for iron ore mines located in Bizmişen region. According to the results of stability analyses conducted for different mining depths with various overall slope angles, the slope performance chart was constituted by adopting FOS and SRF values as a minimum of 1.2, presented in Figure 5.9. Proposed slope performance chart that was created by using the relation between mining depth and overall slope angle based on the geotechnical data of Bizmişen region, can assist for the further designs of open pits with the same geotechnical characteristics.

Using the Minitab software (2010), a mathematical expression for the proposed slope performance chart was also determined by using non-linear regression and represented by the equation with $R^2 = 0.9986$,

$$\alpha = 88.234 + 0.0372H - 3.41726 \times H^{0.5} \quad (5.1)$$

where

$$85 \text{ m} \leq H \leq 380 \text{ m}$$

α = Overall Slope Angle (°)

H = Mining Depth (m)

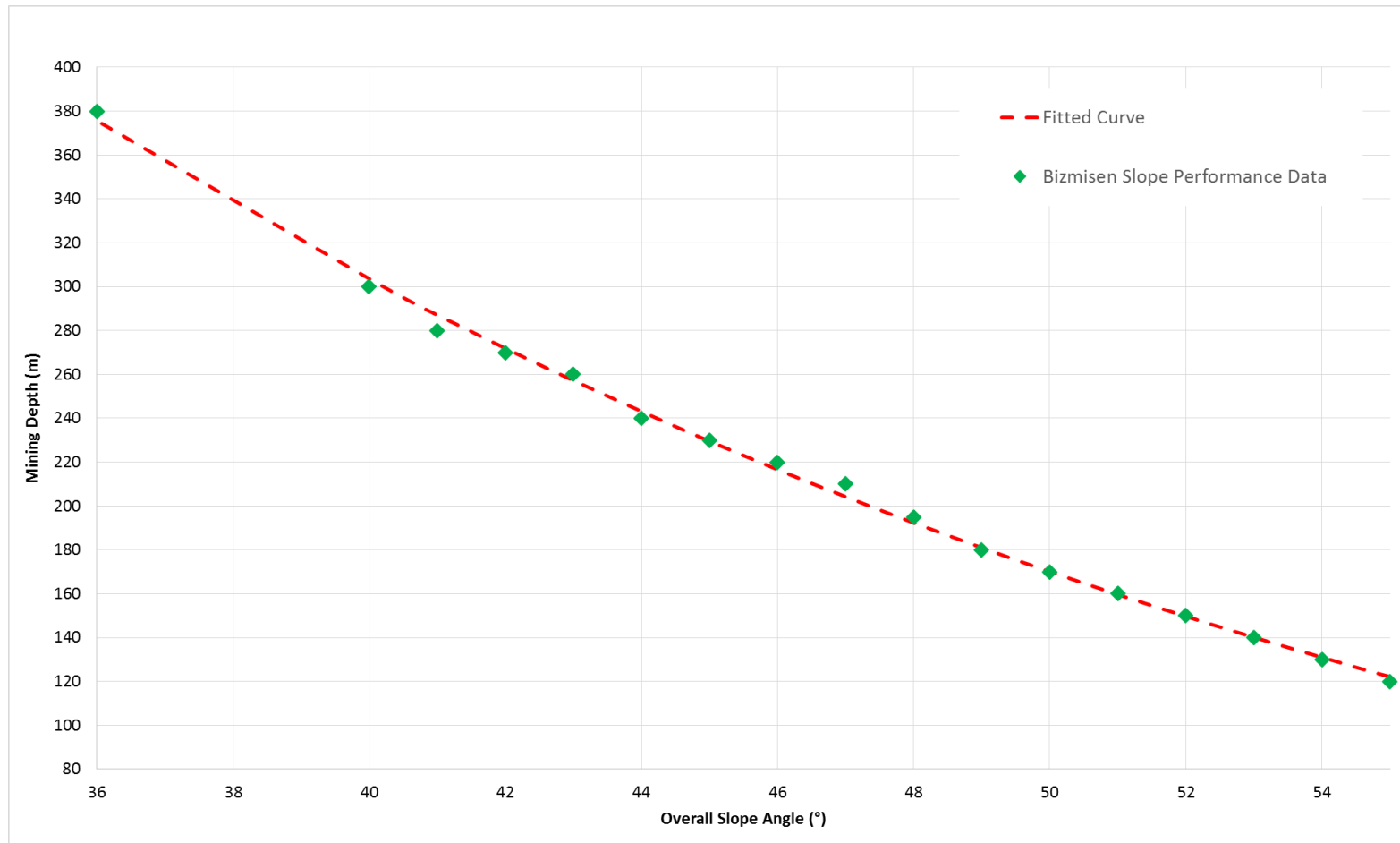


Figure 5.9 Slope performance chart created based on Bizmişen geotechnical characteristics

CHAPTER 6

CONCLUSIONS AND RECOMMENDATIONS

This research covers the optimum safe overall slope angle design of open pit mines in Bizmişen region. It is essential to make the slope design optimized for open pit mines by ensuring mining safety. For deep open pit mines, making the overall slope angle as high as possible can reduce the amount of stripped waste rock and decreases the production cost under safety requirements. In Bizmişen region, for an approximately 400 m deep open pit mine, 1° rise in overall slope angle can reduce almost 3 million m³ of overburden amount. Therefore, the optimization attempts were carried out for the open pits in Bizmişen region, Erzincan.

The following main conclusions can be drawn from this research:

- i. Combined use of limit equilibrium methods and numerical modeling has increased the reliability and accuracy of the stability analyses results.
- ii. Considering the acceptable design criteria FOS with 1.2, optimum overall slope angle was determined as 36° for the west slope of Dönentaş open pit which is planned to reach approximately 400 m maximum mining depth.
- iii. Considering minimum FOS and SRF values of 1.2, for different mining depths corresponding overall slope angles were estimated in Bizmişen region.
- iv. According to the stability analyses results, a relation is obtained between overall slope angles and different mining depths (Equation 5.1).
- v. Using the obtained relation between various mining depths and optimized overall slope angles, a slope performance chart is proposed to be used as a practical guide for preliminary design of open pit mines in Bizmişen region.
- vi. The proposed slope performance chart can also be applied to other open pit iron mines with similar geotechnical characteristics in Turkey. For instance, safe overall slope angle was predicted as 55° for 130 m mining depth in

Ayazmant open pit iron mine (Karpuz, *et al.*, 2013). Using the proposed performance chart, a consistent overall slope angle of 54° was found.

According to the reached conclusions, the following items can be recommended for further studies:

- i. 3D stability analyses should be conducted to achieve more effective and representative results.
- ii. Comparative stability analyses can be developed considering discontinuum models following detailed discontinuity mapping studies.
- iii. Seismic loads should be considered for the stability analyses in order to analyze the effects of seismic and dynamic events on the slope stability.
- iv. The analyses conducted in this study should also be performed considering different ground water levels to prevent possible problems that may occur due to climatic conditions.
- v. Considering local geotechnical characteristics, individual slope performance charts can be constituted for preliminary slope design purposes for different regions.
- vi. Sensitivity analyses can be performed to discuss the effects of rock material properties on optimization studies of overall slope angle.

REFERENCES

- Abramson, L. W., Lee, T. S., Sharma, S., & Boyce, G. M. (2002). *Slope Stability and Stabilization Methods* (Second ed.). New York: JOHN WILEY & SONS, INC.
- Alejano, L. R., Rodriguez-Dono, A., Alonso, E., & Fdez-Manin, G. (2009). Ground reaction curves for tunnels excavated in different quality rock masses showing several types of post-failure behaviour. *Tunnelling and Underground Space Technology*, 24, 689-705.
- Anon. (2003). *Slope stability engineering manual*. Washington, DC: US Army Corps of Engineers.
- Anon. (2011). *Compendium for Design of Rock Constructions - T7002B*. Lulea: Lulea University of Technology.
- Barton, N. R., Lien, R., & Lunde, J. (1974). Engineering classification of rock masses for the design of tunnel support. *Rock Mechanics*, 6(4), 189-239.
- Bieniawski, Z. T. (1976). Rock mass classifications in rock engineering. *Proceedings of the Symposium on Exploration for Rock Engineering*, (s. 97-107). Johannesburg.
- Bieniawski, Z. T. (1989). *Engineering rock mass classifications*. Wiley.
- Bishop, A. W. (1955). The use of the slip circle in the stability analysis of earth slopes. *Geotechnique*, 7-17.
- Cai, M., Kaiser, P. K., Tasaka, Y., & Minami, M. (2007). Determination of residual strength parameters of jointed rock masses using the GSI system. *International Journal of Rock Mechanics and Mining Sciences*, 44, 247-265.
- Cheng, Y. M., & Lau, C. K. (2008). *Slope stability analysis and stabilization*. Milton Park, Abingdon, Oxon, OX14-4RN: Routledge.
- Chowdhury, R., Flentje, P., & Bhattacharya, G. (2010). *Geotechnical Slope Analysis*. London, UK: CRS Press.
- Clough, R. W., & Woodward, R. J. (1967). Analysis of Embankment Stresses and Deformations. *Journal of Geotechnical Division*, 529-549.

- Coggan, J. S., Stead, D., & Eyre, J. M. (1998). Evaluation of techniques for quarry slope stability assessment. *Transactions of the Institutions of Mining and Metallurgy*, 107, 139-147.
- Cundall, P. A. (1971). A computer model for simulating progressive large-scale movements in blocky rock systems. *Proceedings of the Symposium of the International Society of Rock Mechanics*, 1.
- Cundall, P. A. (1976). Explicit Finite Difference Methods in Geomechanics. *2nd International Conference on Numerical Methods in Geomechanics*, 1, pp. 132-150. Virginia.
- Dawson, E. M., Roth, W. H., & Drescher, A. (1999). Slope stability analysis by strength reduction. *Geotechnique*, 49(6), 835-840.
- Diederichs, M. S., Lato, M., Hammah, R., & Quinn, P. (2007). Shear strength reduction approach for slope stability analyses. *Proceedings of the 1st Canada-US Rock Mechanics Symposium*. Vancouver.
- Diering, J. C., & Stacey, T. R. (1987). Three-dimensional stress analysis: a practical planning tool for mining problems. *Proceedings of the 20th International Symposium on the Application of Computers and Mathematics in the Mineral Industries*. 1, pp. 33-42. Johannesburg: SAIMM.
- Donald, I. B., & Giam, S. K. (1988). Application of the nodal displacement method to slope stability analysis. *Proceedings of the 5th Australia-New Zealand conference on geomechanics*, (pp. 456-460). Sydney.
- Douglas, K. J. (2002). *The Shear Strength of Rock Masses*. PhD Thesis, The University of New South Wales, School of Civil and Environmental Engineering, Sydney.
- Duncan, J. M. (1996). State of the Art: Limit Equilibrium and Finite Element Analysis of Slopes. *Journal of Geotechnical Engineering Division*, 122, 577-596.
- Duncan, J. M., Wright, S. G., & Brandon, T. L. (2014). *Soil Strength and Slope Stability* (Second ed.). USA: WILEY.
- Durand, B., Jolivet, L., Horvath, F., & Seranne, M. (1999). *The mediterranean basins: Tertiary extension within the Alpine Orogen*. Brassmill Lane, UK: The Geological Society.

Eberhardt, E. (2003). *Rock Slope Stability Analysis - Utilization of Advanced Numerical Techniques*. The University of British Columbia, Geological Engineering/Earth and Ocean Sciences, Vancouver.

Fellenius, W. (1936). Calculation of the stability of earth dams. *Transactions of 2nd Congress on Large Dams*, (pp. 445-462). Washington DC.

Goodman, R. E. (1989). *Introduction to Rock Mechanics* (Second ed.). New York: WILEY.

Goodman, R. E., & Bray, J. (1976). Toppling of rock slopes. In C. ASCE: Boulder (Ed.), *Proceedings of the Specialty Conference on Rock Engineering for Foundations and Slopes, 2*, pp. 201-234. Colorado.

Goodman, R. E., & Shi, G. (1985). *Block theory and its application to rock engineering*. New Jersey: PRENTICE-HALL.

(2015). *Google Earth*.

Greco, V. R. (1996). Efficient Monte Carlo technique for locating critical slip surface. *Journal of Geotechnical Engineering*, 122(7).

Griffiths, D. V., & Lane, P. A. (1999). Slope stability analysis by finite elements. *Geotechnique*, 49(3), 387-403.

Haines, A., & Terbrugge, P. J. (1991). Preliminary estimation of rock slope stability using rock mass classification systems. *Proceedings 7th International Society Rock Mechanics*, 2, pp. 887-892. Aachen.

Hammah, R. E., Yacoub, T., Corkum, B., & Curran, J. (2005). A comparison of finite element slope stability analysis with conventional limit equilibrium investigation. *Proceedings of the 58th Canadian Geotechnical and 6th Joint IAH-CNC and CGS Groundwater Specialty Conferences*. Saskatoon, Canada.

Hammah, R. E., Yacoub, T., Corkum, B., Wibowo, F., & Curran, J. H. (2007). Analysis of blocky slopes with finite element shear strength reduction analysis. *Proceedings of the 1st Canada-US Rock Mechanics Symposium*, (pp. 329-334). Vancouver, Canada.

Hart, R. D. (1993). An introduction to distinct element modelling for rock engineering. In *Comprehensive Rock Engineering: Principles, Practice & Projects* (Vol. 2, pp. 245-261). Pergamon Press, Oxford.

Hartman, H. L. (1992). *SME MINING ENGINEERING HANDBOOK* (3rd ed.). (P. Darling, Ed.) United States of America: SOCIETY FOR MINING, METALLURGY, AND EXPLORATION, INC.

He, M. C., Feng, J. L., & Sun, X. M. (2008). Stability evaluation and optimal excavated design of rock slope at Antaibao open pit coal mine, China. *International Journal of Rock Mechanics and Mining Sciences*, 45, 289-302.

Hibbeler, R. C. (2011). *Mechanics of Materials* (8th ed.). PEARSON.

Hocking, G. (1976). A method for distinguishing between single and double plane sliding of tetrahedral wedges. *International Journal of Rock Mechanics and Mining Sciences and Geomechanics Abstracts*, 13(7), 225-226.

Hoek, E. (1990a). Estimating Mohr-Coulomb friction and cohesion values from the Hoek-Brown failure criterion. *International Journal of Rock Mechanics and Mining Sciences and Geomechanics Abstracts*, 27, 227-229.

Hoek, E. (2009). *Fundamentals of slope design*. Slope Stability 2009, Santiago, Chile.

Hoek, E., & Bray, J. W. (1981). *Rock Slope Engineering*. London: The Institute of Mining and Metallurgy.

Hoek, E., & Brown, E. T. (1997). Practical estimates of rock mass strength. *International Journal of Rock Mechanics and Mining Sciences*, 34(8), 1165-1186.

Hoek, E., & Diederichs, M. S. (2006). Empirical estimation of rock mass modulus. *International Journal of Rock Mechanics and Mining Sciences*, 43, 203-215.

Hoek, E., Carranza-Torres, C., & Corkum, B. (2002). Hoek-Brown failure criterion-2002 edition. *Proc. NARMS-TAC Conference*, 1, pp. 267-273. Toronto.

Hoek, E., Grabinsky, M., & Diederichs, M. (1990b). Numerical modelling for underground excavation design. *100(A21-A30)*.

Hoek, E., Kaiser, P. K., & Bawden, W. F. (1995). *Support of underground excavations in hard rock*. Rotterdam, Netherlands: A.A. BALKEMA.

Hoek, E., Marinos, P., & Marinos, V. (2005). The geological strength index: applications and limitations. *Bulletin of Engineering Geology and the Environment*, 65, 55-65.

- Hoek, E., Rippere, K. H., & Stacey, P. F. (2001). Large-scale slope designs - A review of the state of the art. In W. A. Hustrulid, M. K. McCarter, & D. A. Zyl (Eds.), *Slope Stability in Surface Mining* (pp. 3-11). Littleton, Colorado, USA: Society for Mining, Metallurgy and Exploration, Inc. (SME).
- Hustrulid, W. A., McCarter, M. K., & Van Zyl, D. J. (2001). *Slope stability in surface mining*. USA: Society for Mining, Metallurgy, and Exploration, INC. (SME).
- Itasca. (1997). *FLAC3D. Fast Lagrangian Analysis of Continua in 3 Dimensions*. Minneapolis: Itasca Consulting Group Inc.
- Itasca. (2004). *UDEC V4.0: Universal Distinct Element Code, User's Guide* (2nd ed.). Minnesota: Itasca Consulting Group.
- Itasca. (2007). *3 Dimensional Distinct Element Code, User's Guide* (3rd ed.). Minnesota: Itasca Consulting Group.
- Itasca. (2011). *FLAC V7.00. Fast Lagrangian Analysis of Continua User's Guide*. (Fifth, Ed.) Minneapolis, Minnesota, USA: Itasca Consulting Group Inc.
- Janbu, N. (1954). Application of composite slip surface for stability analysis. *Proc. European Conference on Stability of Earth Slopes*, (pp. 43-49). Stockholm.
- Jing, L., & Hudson, J. A. (2002). Numerical methods in rock mechanics. *International Journal of Rock Mechanics and Mining Sciences*, 39, 409-427.
- Karpuz, C., Tutluoğlu, L., Başarır, H., Demirel, N., Yardımcı, A. G., & Akdağ, S. (2014). *Erzincan Bizmişen Demir Cevheri Maden İşletme Projesi Sonuç Raporu*.
- Karpuz, C., Tutluoğlu, L., Bilgin, H. A., Öztürk, H., Öge, İ. F., Güner, D., & Yardımcı, A. G. (2013). *Ayazmant Demir Bakır Cevheri Maden İşletme Projesi*.
- Laubscher, D. H. (1977). Geomechanics classification of jointed rock masses. *Transactions of the Institution of Mining and Metallurgy, Section A, Mining Industry*, A1-A8.
- Laubscher, D. H. (1990). A geomechanics classification system for the rating of rock mass in mine design. *Journal of the South African Institute of Mining and Metallurgy*, 257-273.

- Lorig, L., & Varona, P. (2004). Numerical analysis. In D. C. Wyllie, & C. W. Mah (Eds.), *Rock Slope Engineering* (4th ed.). New York: Spon Press.
- Lowe, J., & Karafiath, L. (1960). Stability of earth dams upon drawdown. *Proceedings of the 1st Pan-American Conference on Soil Mechanics and Foundation Engineering*, 2, pp. 537-552. Mexico City.
- Lutton, R. J. (1970). Rock Slope Chart from Empirical Slope Data. In *Transactions of the Society of Mining Engineers, A.I.M.E*, 247 (pp. 160-162).
- Markland, J. T. (1972). *Auseful technique for estimating the stability of rock slopes when the rigid wedge sliding type of failure is expected*. Imperial Collage Rock Mechanics Research Report No.19.
- Matsui, T., & San, K. C. (1992). Finite element slope stability analysis by shear strength reduction technique. *Soils and Foundations*, 32(1), 59-70.
- McMahon, B. K. (1976). *Estimation of Upper Bounds to Rock Slopes by Analysis of Existing*. Canada Centre for Mineral and Energy Technology.
- Micromine Pty Ltd. (2014). Micromine.
- Minitab 17 Statistical Software. (2010). *Minitab, Inc.*
- Morgenstern, N., & Price, V. E. (1965). The analysis of the stability of general slip surfaces. *Geotechnique*, 79-93.
- Naylor, D. J. (1981). Finite elements and slope stability. In J. B. Martins (Ed.), *Proceedings of the NATO Advanced Study Institute*, (pp. 229-244). Braga.
- Özgül, N., Turşucu, A., Özyardımcı, N., Şenol, M., Bingöl, İ., & Uysal, Ş. (1981). *Munzur dağlarının jeolojisi*. Ankara: MTA.
- Phase2 v9.0 . (2014). Toronto, Canada: Rocscience Inc.
- Pierce, M., Brandshaug, T., & Ward, M. (2001). Slope stability assessment at the Main Cresson Mine. In W. A. Hustrulid, M. K. McCarter, & D. A. Zyl (Eds.), *Slope Stability in Surface Mining* (pp. 239-250). Society for Mining Metallurgy and Exploration Inc.
- Priest, S. D., & Brown, E. T. (1983). Probabilistic stability analysis of variable rock slopes. *Transactions of Institution of Mining and Metallurgy, Section A*, pp. A1-12.

Read, J., & Stacey, P. (2009). *Guidelines for Open Pit Slope Design*. Collingwood: CSIRO.

Robertson, A. M. (1988). Estimating weak rock strength. *SME Annual Meeting* (pp. 1-5). Phoenix, Arizona: Society of Mining Engineers.

RocData v5.0. (2014). Toronto, Ontario, Canada: Rocscience Inc.

RocLab v1.0. (2014). Toronto, Ontario, Canada: Rocscience Inc.

RS3 1.0. (2014). Rock and soil 3D User's manual. Toronto, Canada: Rocscience Inc.

Simmons, J. V., & Simpson, P. J. (2006). Composite failure mechanisms in coal measures' rock masses. *The Journal of The South African Institute of Mining and Metallurgy*, 106, 459-469.

Sjöberg, J. (1999). *Analysis of Large Scale Rock Slopes: Ph. D Thesis*. Lulea University of Technology, Department of Civil and Mining Engineering Division of Rock Mechanics.

Slide v6.0. (2014). Toronto, Canada: Rocscience Inc.

Sönmez, H., & Ulusay, R. (2002). A discussion on the Hoek-Brown failure criterion and suggested modifications to the criterion verified by slope stability case studies. *Yerbilimleri*, 26, 77-99.

Spencer, E. (1967). A method of the analysis of the stability of embankments assuming parallel inter-slice forces. *Geotechnique*, 11-26.

Stead, D., Eberhardt, E., & Coggan, J. S. (2006). Developments in the characterization of complex rock slope deformation and failure using numerical modelling techniques. *Engineering Geology*, 83, 217-235.

Stead, D., Eberhardt, E., Coggan, J., & Benko, B. (2001). Advanced numerical techniques in rock slope stability analysis - Applications and limitations. *International Conference on Landslides - Causes, Impacts and Countermeasures*, (pp. 615-624). Davos, Switzerland.

Sullivan, T. D. (2006). Pit slope design and risk - a view of the current state of the art. *International Symposium on Stability of Rock Slopes in Open Pit Mining and Civil Engineering* (pp. 51-78). The South African Institute of Mining and Metallurgy.

- Tablacı, A. (2010). Bizmişen-Çaltı (Kemaliye-Erzincan) töresindeki Fe'lere bağlı Cu-Au-Ag ve Ni cevherleşmeleri. *MSc. thesis*.
- Ugai, K. (1989). A method of calculation of total facator of safety of slopes by elasto-plastic FEM. *Soils and Foundations*, 29(2), 190-195.
- Ugai, K., & Leshchinsky, D. (1995). Three dimensional limit equilibrium and finite element analyses: a comparison of results. *Soils and Foundations*, 35(4), 1-7.
- Ulusay, R., Ekmekci, M., Tuncay, E., & Hasancebi, N. (2014). Improvement of slope stability based on integrated geotechnical evaluations and hydrogeological conceptualisation at a lignite open pit. *Engineering Geology*, 261-280.
- Whitman, R. V., & Bailey, W. A. (1967). Use of computer for slope stability analysis. *Journal of the Soil Mechanics and Foundation Division*, 93 (SM4).
- Wright, S. G. (1970). *A study of slope stability and the undrained shear strength of clay shales: Ph. D Thesis*. University of California, Berkeley.
- Wyllie, D. C., & Mah, C. W. (2004). *Rock slope engineering civil and mining* (4th ed.). Milton Park, Abingdon, Oxon, OX14 4RN: The Institute of Mining and Metallurgy.
- Yıldırım, A., & Hamarat, O. (1985). *Erzincan-Kemaliye-Bizmişen demir madeni jeoloji ve rezerv raporu - Cilt-I*. MTA.
- Zienkiewicz, O. C., Humpheson, C., & Lewis, R. W. (1975). Associated and non-associated visco-plasticity and plasticity in soil mechanics. *Geotechnique*, 25(4), 671-689.

APPENDIX A

ROCK MASS CLASSIFICATION AND CHARACTERIZATION SYSTEMS

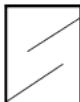





<p>GEOLOGICAL STRENGTH INDEX FOR JOINTED ROCKS (Hoek and Marinos, 2000)</p> <p>From the lithology, structure and surface conditions of the discontinuities, estimate the average value of GSI. Do not try to be too precise. Quoting a range from 33 to 37 is more realistic than stating that GSI = 35. Note that the table does not apply to structurally controlled failures. Where weak planar structural planes are present in an unfavourable orientation with respect to the excavation face, these will dominate the rock mass behaviour. The shear strength of surfaces in rocks that are prone to deterioration as a result of changes in moisture content will be reduced if water is present. When working with rocks in the fair to very poor categories, a shift to the right may be made for wet conditions. Water pressure is dealt with by effective stress analysis.</p>		SURFACE CONDITIONS				
STRUCTURE		DECREASING SURFACE QUALITY →				
 <p>INTACT OR MASSIVE - intact rock specimens or massive in situ rock with few widely spaced discontinuities</p>	VERY GOOD Very rough, fresh unweathered surfaces	GOOD Rough, slightly weathered, iron stained surfaces	FAIR Smooth, moderately weathered and altered surfaces	POOR Slickensided, highly weathered surfaces with compact coatings or fillings or angular fragments	VERY POOR Slickensided, highly weathered surfaces with soft clay coatings or fillings	
	 <p>BLOCKY - well interlocked undisturbed rock mass consisting of cubical blocks formed by three intersecting discontinuity sets</p>	90			N/A	N/A
		80				
		70				
		60				
		50				
 <p>VERY BLOCKY- interlocked, partially disturbed mass with multi-faceted angular blocks formed by 4 or more joint sets</p>	40					
	 <p>BLOCKY/DISTURBED/SEAMY - folded with angular blocks formed by many intersecting discontinuity sets. Persistence of bedding planes or schistosity</p>	30				
		20				
 <p>DISINTEGRATED - poorly interlocked, heavily broken rock mass with mixture of angular and rounded rock pieces</p>	10					
	 <p>LAMINATED/SHEARED - Lack of blockiness due to close spacing of weak schistosity or shear planes</p>	N/A	N/A			

Figure A.1 General Chart for GSI Estimates with respect to Geological Observations

(Hoek *et al.*, 2005)

A. CLASSIFICATION PARAMETERS AND THEIR RATINGS									
Parameter			Range of values						
1	Strength of intact rock material	Point-load strength index	>10 MPa	4 - 10 MPa	2 - 4 MPa	1 - 2 MPa	For this low range - uniaxial compressive test is preferred		
		Uniaxial comp. strength	>250 MPa	100 - 250 MPa	50 - 100 MPa	25 - 50 MPa	5 - 25 MPa	1 - 5 MPa	< 1 MPa
	Rating	15	12	7	4	2	1	0	
2	Drill core Quality /RQD	90% - 100%	75% - 90%	50% - 75%	25% - 50%	< 25%			
	Rating	20	17	13	8	3			
3	Spacing of discontinuities	> 2 m	0.6 - 2 . m	200 - 600 mm	60 - 200 mm	< 60 mm			
	Rating	20	15	10	8	5			
4	Condition of discontinuities (See E)	Very rough surfaces Not continuous No separation Unweathered wall rock	Slightly rough surfaces Separation < 1 mm Slightly weathered walls	Slightly rough surfaces Separation < 1 mm Highly weathered walls	Slickensided surfaces or Gouge < 5 mm thick or Separation 1-5 mm Continuous	Soft gouge >5 mm thick or Separation > 5 mm Continuous			
	Rating	30	25	20	10	0			
5	Groundwater	Inflow per 10 m tunnel length (l/m)	None	< 10	10 - 25	25 - 125	> 125		
		(Joint water press./ Major principal σ)	0	< 0.1	0.1, - 0.2	0.2 - 0.5	> 0.5		
	General conditions	Completely dry	Damp	Wet	Dripping	Flowing			
	Rating	15	10	7	4	0			
B. RATING ADJUSTMENT FOR DISCONTINUITY ORIENTATIONS (See F)									
Strike and dip orientations		Very favourable	Favourable	Fair	Unfavourable	Very Unfavourable			
Ratings	Tunnels & mines	0	-2	-5	-10	-12			
	Foundations	0	-2	-7	-15	-25			
	Slopes	0	-5	-25	-50				
C. ROCK MASS CLASSES DETERMINED FROM TOTAL RATINGS									
Rating	100 ← 81	80 ← 61	60 ← 41	40 ← 21	< 21				
Class number	I	II	III	IV	V				
Description	Very good rock	Good rock	Fair rock	Poor rock	Very poor rock				
D. MEANING OF ROCK CLASSES									
Class number	I	II	III	IV	V				
Average stand-up time	20 yrs for 15 m span	1 year for 10 m span	1 week for 5 m span	10 hrs for 2.5 m span	30 min for 1 m span				
Cohesion of rock mass (kPa)	> 400	300 - 400	200 - 300	100 - 200	< 100				
Friction angle of rock mass (deg)	> 45	35 - 45	25 - 35	15 - 25	< 15				
E. GUIDELINES FOR CLASSIFICATION OF DISCONTINUITY conditions									
Discontinuity length (persistence)	< 1 m	1 - 3 m	3 - 10 m	10 - 20 m	> 20 m				
Rating	6	4	2	1	0				
Separation (aperture)	None	< 0.1 mm	0.1 - 1.0 mm	1 - 5 mm	> 5 mm				
Rating	6	5	4	1	0				
Roughness	Very rough	Rough	Slightly rough	Smooth	Slickensided				
Rating	6	5	3	1	0				
Infilling (gouge)	None	Hard filling < 5 mm	Hard filling > 5 mm	Soft filling < 5 mm	Soft filling > 5 mm				
Rating	6	4	2	2	0				
Weathering	Unweathered	Slightly weathered	Moderately weathered	Highly weathered	Decomposed				
Rating	6	5	3	1	0				
F. EFFECT OF DISCONTINUITY STRIKE AND DIP ORIENTATION IN TUNNELLING**									
Strike perpendicular to tunnel axis					Strike parallel to tunnel axis				
Drive with dip - Dip 45 - 90°		Drive with dip - Dip 20 - 45°			Dip 45 - 90°		Dip 20 - 45°		
Very favourable		Favourable			Very unfavourable		Fair		
Drive against dip - Dip 45-90°		Drive against dip - Dip 20-45°			Dip 0-20 - Irrespective of strike°				
Fair		Unfavourable			Fair				

* Some conditions are mutually exclusive . For example, if infilling is present, the roughness of the surface will be overshadowed by the influence of the gouge. In such cases use A.4 directly.

** Modified after Wickham et al (1972).

Figure A.3 Rock Mass Rating System (Bieniawski, 1989)

Required parameters to classify a rock mass by using Q-system are presented as below:

1. Rock Quality Designation (RQD).
2. Joint set number (J_n).
3. Joint roughness number (J_r).
4. Joint alteration number (J_a).
5. Joint water reduction factor (J_w).
6. Stress reduction factor (SRF).

$$\text{Rock mass quality, } Q = \frac{RQD}{J_n} \times \frac{J_r}{J_a} \times \frac{J_w}{SRF}$$

DESCRIPTION	VALUE	NOTES
1. ROCK QUALITY DESIGNATION	RQD	
A. Very poor	0 - 25	1. Where RQD is reported or measured as ≤ 10 (including 0), a nominal value of 10 is used to evaluate Q.
B. Poor	25 - 50	
C. Fair	50 - 75	
D. Good	75 - 90	2. RQD intervals of 5, i.e. 100, 95, 90 etc. are sufficiently accurate.
E. Excellent	90 - 100	
2. JOINT SET NUMBER	J_n	
A. Massive, no or few joints	0.5 - 1.0	
B. One joint set	2	
C. One joint set plus random	3	
D. Two joint sets	4	
E. Two joint sets plus random	6	
F. Three joint sets	9	1. For intersections use ($3.0 \times J_n$)
G. Three joint sets plus random	12	
H. Four or more joint sets, random, heavily jointed, 'sugar cube', etc.	15	2. For portals use ($2.0 \times J_n$)
J. Crushed rock, earthlike	20	
3. JOINT ROUGHNESS NUMBER	J_r	
a. Rock wall contact		
b. Rock wall contact before 10 cm shear		
A. Discontinuous joints	4	
B. Rough and irregular, undulating	3	
C. Smooth undulating	2	
D. Slickensided undulating	1.5	1. Add 1.0 if the mean spacing of the relevant joint set is greater than 3 m.
E. Rough or irregular, planar	1.5	
F. Smooth, planar	1.0	
G. Slickensided, planar	0.5	2. $J_r = 0.5$ can be used for planar, slickensided joints having lineations, provided that the lineations are oriented for minimum strength.
c. No rock wall contact when sheared		
H. Zones containing clay minerals thick enough to prevent rock wall contact	1.0 (nominal)	
J. Sandy, gravely or crushed zone thick enough to prevent rock wall contact	1.0 (nominal)	
4. JOINT ALTERATION NUMBER	J_a	ϕ_r degrees (approx.)
a. Rock wall contact		
A. Tightly healed, hard, non-softening, impermeable filling	0.75	1. Values of ϕ_r , the residual friction angle, are intended as an approximate guide to the mineralogical properties of the alteration products, if present.
B. Unaltered joint walls, surface staining only	1.0	25 - 35
C. Slightly altered joint walls, non-softening mineral coatings, sandy particles, clay-free disintegrated rock, etc.	2.0	25 - 30
D. Silty-, or sandy-clay coatings, small clay-fraction (non-softening)	3.0	20 - 25
E. Softening or low-friction clay mineral coatings, i.e. kaolinite, mica. Also chlorite, talc, gypsum and graphite etc., and small quantities of swelling clays. (Discontinuous coatings, 1 - 2 mm or less in thickness)	4.0	8 - 16

Figure A.4 Classification of Individual Parameters used in Q-system (Barton *et al.*, 1974)

DESCRIPTION	VALUE	NOTES
4. JOINT ALTERATION NUMBER	J_a	ϕ r degrees (approx.)
b. Rock wall contact before 10 cm shear		
F. Sandy particles, clay-free, disintegrating rock etc.	4.0	25 - 30
G. Strongly over-consolidated, non-softening clay mineral fillings (continuous < 5 mm thick)	6.0	16 - 24
H. Medium or low over-consolidation, softening clay mineral fillings (continuous < 5 mm thick)	8.0	12 - 16
J. Swelling clay fillings, i.e. montmorillonite, (continuous < 5 mm thick). Values of J_a depend on percent of swelling clay-size particles, and access to water.	8.0 - 12.0	6 - 12
c. No rock wall contact when sheared		
K. Zones or bands of disintegrated or crushed rock and clay (see G, H and J for clay conditions)	6.0	
L. rock and clay (see G, H and J for clay conditions)	8.0	
M. conditions)	8.0 - 12.0	6 - 24
N. Zones or bands of silty- or sandy-clay, small clay fraction, non-softening	5.0	
O. Thick continuous zones or bands of clay	10.0 - 13.0	
P. & R. (see G.H and J for clay conditions)	6.0 - 24.0	
5. JOINT WATER REDUCTION	J_w	approx. water pressure (kgf/cm ²)
A. Dry excavation or minor inflow i.e. < 5 l/m locally	1.0	< 1.0
B. Medium inflow or pressure, occasional outwash of joint fillings	0.66	1.0 - 2.5
C. Large inflow or high pressure in competent rock with unfilled joints	0.5	2.5 - 10.0
D. Large inflow or high pressure	0.33	2.5 - 10.0
E. Exceptionally high inflow or pressure at blasting, decaying with time	0.2 - 0.1	> 10
F. Exceptionally high inflow or pressure	0.1 - 0.05	> 10
1. Factors C to F are crude estimates; increase J_w if drainage installed.		
2. Special problems caused by ice formation are not considered.		
6. STRESS REDUCTION FACTOR		SRF
a. Weakness zones intersecting excavation, which may cause loosening of rock mass when tunnel is excavated		
A. Multiple occurrences of weakness zones containing clay or chemically disintegrated rock, very loose surrounding rock (any depth)		10.0
1. Reduce these values on the relevant shear zones only influence but f SRF by 25 - 50% if do not intersect the excavation		
B. Single weakness zones containing clay, or chemically disintegrated rock (excavation depth < 50 m)		5.0
C. Single weakness zones containing clay, or chemically disintegrated rock (excavation depth > 50 m)		2.5
D. Multiple shear zones in competent rock (clay free), loose surrounding rock (any depth)		7.5
E. Single shear zone in competent rock (clay free). (depth of excavation < 50 m)		5.0
F. Single shear zone in competent rock (clay free). (depth of excavation > 50 m)		2.5
G. Loose open joints, heavily jointed or 'sugar cube', (any depth)		5.0

Figure A.4 (cont'd) Classification of Individual Parameters used in Q-system (Barton *et al.*, 1974)

DESCRIPTION		VALUE	NOTES
6. STRESS REDUCTION FACTOR		SRF	
b. Competent rock, rock stress problems			
	σ_c/σ_1	σ_t/σ_1	
H. Low stress, near surface	> 200	> 13	2.5
J. Medium stress	200 - 10	13 - 0.66	1.0
K. High stress, very tight structure (usually favourable to stability, may be unfavourable to wall stability)	10 - 5	0.66 - 0.33	0.5 - 2
L. Mild rockburst (massive rock)	5 - 2.5	0.33 - 0.16	5 - 10
M. Heavy rockburst (massive rock)	< 2.5	< 0.16	10 - 20
c. Squeezing rock, plastic flow of incompetent rock under influence of high rock pressure			
N. Mild squeezing rock pressure			5 - 10
O. Heavy squeezing rock pressure			10 - 20
d. Swelling rock, chemical swelling activity depending on presence of water			
P. Mild swelling rock pressure			5 - 10
R. Heavy swelling rock pressure			10 - 15
ADDITIONAL NOTES ON THE USE OF THESE TABLES			
When making estimates of the rock mass Quality (Q), the following guidelines should be followed in addition to the notes listed in the tables:			
1. When borehole core is unavailable, RQD can be estimated from the number of joints per unit volume, in which the number of joints per metre for each joint set are added. A simple relationship can be used to convert this number to RQD for the case of clay free rock masses: $RQD = 115 - 3.3 J_V$ (approx.), where J_V = total number of joints per m^3 ($0 < RQD < 100$ for $35 > J_V > 4.5$).			
2. The parameter J_n representing the number of joint sets will often be affected by foliation, schistosity, slaty cleavage or bedding etc. If strongly developed, these parallel 'joints' should obviously be counted as a complete joint set. However, if there are few 'joints' visible, or if only occasional breaks in the core are due to these features, then it will be more appropriate to count them as 'random' joints when evaluating J_n .			
3. The parameters J_r and J_a (representing shear strength) should be relevant to the weakest significant joint set or clay filled discontinuity in the given zone. However, if the joint set or discontinuity with the minimum value of J_r/J_a is favourably oriented for stability, then a second, less favourably oriented joint set or discontinuity may sometimes be more significant, and its higher value of J_r/J_a should be used when evaluating Q. The value of J_r/J_a should in fact relate to the surface most likely to allow failure to initiate.			
4. When a rock mass contains clay, the factor SRF appropriate to loosening loads should be evaluated. In such cases the strength of the intact rock is of little interest. However, when jointing is minimal and clay is completely absent, the strength of the intact rock may become the weakest link, and the stability will then depend on the ratio rock-stress/rock-strength. A strongly anisotropic stress field is unfavourable for stability and is roughly accounted for as in note 2 in the table for stress reduction factor evaluation.			
5. The compressive and tensile strengths (σ_c and σ_t) of the intact rock should be evaluated in the saturated condition if this is appropriate to the present and future in situ conditions. A very conservative estimate of the strength should be made for those rocks that deteriorate when exposed to moist or saturated conditions.			

Figure A.4 (cont'd) Classification of Individual Parameters used in Q-system (Barton *et al.*, 1974)


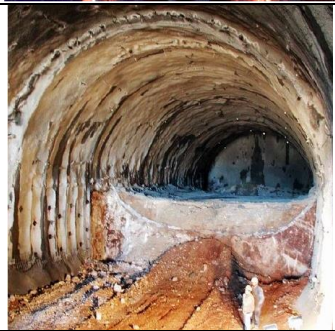



Appearance of rock mass	Description of rock mass	Suggested value of D
	<p>Excellent quality controlled blasting or excavation by Tunnel Boring Machine results in minimal disturbance to be confined rock mass surrounding a tunnel</p>	<p>D=0</p>
	<p>Mechanical or hand excavation in poor quality rock masses (no blasting) results in minimal disturbance to the surrounding rock mass.</p> <p>Where squeezing problems result in significant floor heave, disturbance can be severe unless a temporary invert, as shown in the photograph, is placed</p>	<p>D=0</p> <p>D=0.5 No invert</p>
	<p>Very poor quality blasting in a hard rock tunnel results in severe local damage, extending 2 or 3 m, in the surrounding rock mass.</p>	<p>D=0.8</p>
	<p>Small scale blasting in civil engineering slopes results in modest rock mass damage, particularly if controlled blasting is used as shown on the left hand side of the photograph. However, stress relief results in some disturbance.</p>	<p>D=0.7 Good blasting</p> <p>D=1.0 Poor blasting</p>
	<p>Very large open pit mine slopes suffer significant disturbance due to heavy production blasting and also due to stress relief from overburden removal.</p> <p>In some softer rocks excavation can be carried out by ripping and dozing and the degree of damage to the slopes is less.</p>	<p>D=1.0 Production blasting</p> <p>D=0.7 Mechanical excavation</p>

Figure A.5 Guidelines for Estimating Disturbance Factor D